

Simulating the Influence of Shifts in Snow Redistribution on Semi-Arid Upland Vegetation
in a Warming Climate

A Dissertation

Presented in Partial Fulfillment of the Requirements for the
Degree of Doctorate of Philosophy

with a

Major in Natural Resources

in the

College of Graduate Studies

University of Idaho

by

Benjamin S. Soderquist

Major Professor: Kathleen Kavanagh, Ph.D.

Committee Members: Timothy Link, Ph.D.; Eva Strand, Ph.D.; Mark Seyfried, Ph.D.

Department Administrator: Randall Brooks, Ph.D.

August 2017

Authorization to Submit Dissertation

This dissertation of Benjamin S. Soderquist, submitted for the degree of Doctor of Philosophy (Ph.D.) with a Major in Natural Resources and titled “Simulating the Influence of Shifts in Snow Redistribution on Semi-Arid Upland Vegetation in a Warming Climate,” has been reviewed in final form. Permission, as indicated by the signatures and dates below, is now granted to submit final copies to the College of Graduate Studies for approval.

Major Professor: _____ Date: _____
Kathleen Kavanagh, Ph.D.

Committee Members: _____ Date: _____
Timothy Link, Ph.D.

_____ Date: _____
Eva Strand, Ph.D.

_____ Date: _____
Mark Seyfried, Ph.D.

Department Administrator: _____ Date: _____
Randall Brooks, Ph.D.

Abstract

In mountainous regions of the western United States, snow is a primary control on ecohydrological processes. In these environments, complex terrain results in steep temperature and precipitation gradients, leading to the heterogeneous distribution of snow water resources across the landscape. At local scales, the spatial distribution of water resources can be further shaped through the wind driven transport and deposition of snow. In snow dominated, semi-arid environments, melt water generated from snowdrifts may provide critical soil moisture subsidies to upland plant communities. Under warming temperatures, snow dominated precipitation regimes will become increasing rain dominated. In plant communities that are closely coupled with drifting snow, decreases in redistributed precipitation along with longer and drier growing seasons could reduce soil moisture availability and increase drought stress. A process model coupled with historic and future climate was used to assess the impacts of shifts in climate and precipitation phase on upland vegetation. Specifically, the response of three widespread rangeland species and plant functional types found in drift zones at three sites in a snow-dominated semi-arid watershed were simulated. After accounting for redistributed precipitation, biogeochemical simulations indicate that snowdrifts have historically provided supplemental soil moisture to aspen (*Populus tremuloides*), growing at dry mid-elevation sites. Under future conditions, warmer temperatures increased the average growing season length of aspen approximately two weeks. However, at mid-elevation sites, increased spring aspen productivity was offset by carbon losses incurred from increasingly severe summer drought. The response of co-located mountain big sage (*Artimisia tridentata ssp. vaseyana*) and C3 grasses varied under mid-21st century conditions. Across all sites, increased growing season length led to increased productivity for mountain big sage. However, despite longer growing seasons, mid-21st century productivity rates for C3 grasses remained relatively unchanged from historical conditions. These results indicate that shifts in precipitation phase and growing season conditions can differentially impact individual species that currently comprise upland plant communities. Future management of rangelands for vulnerable species, wildlife habitat, and carbon sequestration should consider the implications of temperature induced shifts in winter precipitation phase.

Acknowledgements

This dissertation would not have been possible without the guidance and support of others. First, I would like to acknowledge my major advisor Katy Kavanagh for giving me the opportunity to learn the research process. Since I first moved to Moscow I have grown so much under her mentorship and can't thank her enough for her patience and insight. Second, my committee members Tim Link, Eva Strand, and Mark Seyfried have been wonderful people to work with. Through all the ups and downs associated with a Ph.D. program, my committee has always been available to both encourage and challenge me as a scientist. Lastly, this experience was so rewarding largely because of my peers at the University of Idaho. It's been great to meet such a diverse group of people, all of whom have a passion for science and the environment. Thanks to them for all the good conversations, adventures, and bird hunts on the Palouse that kept me grounded.

I am forever grateful to my parents who taught me to love the wildlands we have in Idaho and gave me the independence to explore and study them. I also thank my brothers, Graham and Travis. Those years we spent together in Moscow were some of my favorites. I also thank my grandparents, who supported and encouraged my educational decisions from the very beginning. If it wasn't for this program I would have never met my partner Chloe. She has been with me from the first semester and has always been there to encourage me.

It has been a humbling experience to join the long line of researchers who have worked in Reynolds Creek. This place is an invaluable scientific resource and logistical support from folks like Mark Murdock, Steve Van Vactor, Zane Cram, and Barry Caldwell are what make research happen. Thank you for maintaining the datasets, roads, and watershed vehicles. I couldn't have done this without the work you do. Here's to another 50+ years of data.

Finally, this work wouldn't have been possible without federal research funding. Financial support for this research was provided by the McIntire-Stennis cooperative forestry research program (PL87-788), the Department of the Interior Northwest Climate Science Center (NW CSC) through a cooperative agreement no. G14AP00153 from the United States Geological Survey (USGS), and the USGS Northwest Climate Science Center/McCall Outdoor Science School Fellowship in Climate Science Communication. These programs have been so important to me and countless other early career scientists.

Table of Contents

Authorization to Submit.....	ii
Abstract	iii
Acknowledgements.....	iv
Table of Contents	v
List of Tables	vii
List of Figures	viii
Chapter 1: Dissertation Introduction.....	1
References.....	5
Figure	7
Chapter 2: Simulating the Dependence of Aspen (<i>Populus tremuloides</i>) on Redistributed Snow in a Semi-Arid Watershed.....	8
Abstract	8
2.1 Introduction.....	9
2.2 Methods.....	11
2.3 Results.....	18
2.4 Discussion	22
2.5 Conclusions.....	28
References.....	29
Tables.....	34
Figures.....	35
Chapter 3. Growing Season Conditions Mediate the Dependence of Aspen on Redistributed Snow Under Climate Change.....	41
Abstract	41
3.1 Introduction.....	42
3.2 Methods.....	45
3.3 Results.....	51

3.4 Discussion	56
3.5 Conclusions	59
References	61
Tables	66
Figures.....	68

Chapter 4. Warming Temperatures and Reductions in Redistributed Snow

Differentially Impact the Simulated Productivity of Sagebrush Steppe Vegetation. 77

Abstract	77
4.1 Introduction	78
4.2 Methods.....	81
4.3 Results	87
4.4 Discussion	93
4.5 Conclusions	97
References	99
Tables	105
Figures.....	107

Appendices..... 114

Appendix 1: Supporting information for Chapter 2.....	114
Appendix 2: Supporting information for Chapter 3.....	118
Appendix 3: Supporting information for Chapter 4.....	125

List of Tables

Table 2.1. Site description and leaf area index (LAI) for Reynolds Mountain East (RME), Johnston Draw (JDW), and Sheep Creek (SC). Standard deviations are indicated in parentheses when applicable.....	34
Table 3.1. Site description and leaf area index (LAI) for Reynolds Mountain East (RME), Johnston Draw (JDW), and Sheep Creek (SC). Standard deviations are indicated in parentheses (n=20 simulation years at SC and RME, 13 simulation years at JDW).....	66
Table 3.2. Changes in precipitation, snow residence, growing season days, net primary production (NPP), net ecosystem production (NEP) from historical to mid- 21 st century conditions. Standard deviations are indicated in parentheses (n= 20 total simulation years at SC and RME, 13 simulation years at JDW). Growing season length is the period of initial leaf flush to complete leaf senescence simulated by Biome-BGC MuSo.	67
Table 4.1. Site description and climate at Sheep creek (SC), Reynolds Mountain east (RME), and Johnston Draw (JDW) under historic and mid-21 st century climate scenarios. Effective precipitation represents increased drift zone precipitation resulting from the redistribution of snow based on drift factors applied to uniform precipitation. Standard deviations are included in parentheses (20 simulation years at SC and RME, 13 simulation years at JDW).....	105
Table 4.2. Average shifts in growing season length, net primary productivity (NPP), and net ecosystem productivity (NEP) for aspen, sagebrush, and C3 grasses at Sheep creek (SC), Reynolds Mountain east (RME), and Johnston Draw (JDW) under historic and mid-21 st century climate scenarios. Total number of simulation years varies by length of meteorological datasets at each site.	106

List of Figures

- Figure 1.1.** Key ecohydrological processes and feedbacks..... 7
- Figure 2.1.** Locations of aspen stands used for this study within the Reynolds Creek Experimental Watershed and Critical Zone observatory. Johnston Draw (JDW) and Sheep Creek (SC) are mid-elevation sites. Reynolds Mountain East (RME) is the highest elevation site receiving the highest annual precipitation..... 35
- Figure 2.2.** Simulated and measured root zone soil moisture storage ($S_{rootzone}$, mm) at each site for 2014, a year where redistributed snow prolonged available soil moisture at Sheep Creek (SC) (b). Root zone depths are 120 cm for RME (a) and JDW (c), and 110 cm for SC (b). Simulations accounting for snow drifts are depicted in blue, while simulations assuming a uniform precipitation layer are red..... 36
- Figure 2.3.** Average pre-dawn leaf water potentials ($\Psi_{pre-dawn}$) taken from three plots at each site across the 2012-2015 growing seasons. Standard deviations are indicated by error bars. Higher precipitation sites Johnston Draw (JDW) and Reynolds Mountain East (RME) typically experience increased growing season $\Psi_{pre-dawn}$ relative to the dry, mid-elevation site Sheep Creek (SC)..... 37
- Figure 2.4.** Last day of snowpack presence simulated by both Biome-BGC and ISNOBAL. Distribution along the 1:1 line indicates variation between the two models ($R^2=0.76$, $y=1.1148x-15.921$). Sheep Creek (SC) and Johnston Draw (JDW) are mid-elevations sites. Reynolds Mountain East (RME) is the highest elevation site. 38
- Figure 2.5.** Annual precipitation (panels a,b,c) and net primary production (NPP, panels e,d,f) and values for RME and SC from 1985-2015 and JDW from 2003-2015. Precipitation accounting for redistributed snow was determined by applying drift factors to measured precipitation occurring below 0°C. Rates of increase in total annual precipitation indicate variations in the timing and magnitude of precipitation falling as snow..... 39

Figure 2.6. Response of snowpack, VWC (θ_v), and net primary productivity (NPP) to redistributed precipitation at Sheep Creek (SC) for 1995 (a,b,c), 2007 (d,e,f), and 2015 (g,h,i). Biome-BGC simulated snow water, VWC, and NPP are shown for both uniform and redistributed precipitation treatments. Measured precipitation events are shown in gray bars (panels a,d,g). Despite large drift formation in 1995, cooler temperatures and spring rains supplemented soil moisture in the absence of a drift. Unlike 1995 and 2015, drift presence was far more important during 2007, a year with above average temperatures and increased growing season evaporative demand. After accounting for the redistribution of snow, NPP remained positive nearly 40 days longer during 2007..... 40

Figure 3.1. Aspen stand locations in the Reynolds Creek Critical Zone observatory (RCEW). Johnston Draw (JDW) and Sheep Creek (SC) are warmer, mid-elevation sites, whereas Reynolds Mountain East (RME) is a cooler, high elevation site..... 68

Figure 3.2. Average monthly temperature increases (error bars denote one standard deviation, $n=20$) from historic (1985-2005) and mid-century (2046-2065) projections obtained from 20 GCMs used in the Multivariate Adaptive Constructed Analog (MACA) downscaling method. Average monthly temperature increases were applied to measured T_{max} and T_{min} at each site to create warming scenarios representative of mid-century conditions... .. 69

Figure 3.3. Average annual effective precipitation and temperature for each site under historical and mid-century conditions. Effective precipitation is the total amount of annual precipitation after accounting for the redistribution of snow. Error bars represent one standard deviation ($n= 20, 20,$ and 13 years for SC, RME, and JDW respectively). Rising temperatures decreases the amount of precipitation falling as snow resulting in decreased redistribution and lower effective precipitation by mid-century. Decreases in redistributed precipitation are largest at the driest site with the largest drift, Sheep Creek (SC), whereas Reynolds Mountain East (RME) and Johnston Draw (JDW) are sites with smaller drifts that experience smaller changes in redistributed precipitation with warming..... 70

Figure 3.4. Measured and simulated soil storage in the top meter of soil during 2014-2015 at Sheep Creek (SC), Reynolds Mountain East (RME), and Johnston Draw (JDW). Probe failure prevented storage calculations at JDW from July 2015 to January 2016. Across sites, simulated soil moisture storage followed measured growing season trends. However, rates of soil water recharge in the fall and early winter typically were overestimated by Biome-BGC MuSo..... 71

Figure 3.5. Simulated leaf area index (LAI) during 2012 and its associated mid-century year (2062). Warming induced shifts in spring green up increase synchrony between periods of growth with incoming precipitation. However, extended growing season length leads to reductions in maximum LAI at warmer, mid-elevation sites (JDW and SC)..... 72

Figure 3.6. Annual net primary productivity (NPP) for historic and mid-century simulations at each site. Simulations span a 20-year period for SC and RME, and a 13-year period for JDW. 73

Figure 3.7. Daily simulations of snow water, average daytime vapor pressure deficit (VPD), and net primary production (NPP) for each site during 2012 and its associated mid-century year 2062. Blue lines represent historic conditions, while red lines represent warmer, mid-century conditions. Shifts in phenology with warming temperature are depicted by the onset of positive NPP rates in the spring..... 74

Figure 3.8. Daily simulations of snow water, average daytime vapor pressure deficit (VPD), and net primary production (NPP) for each site during 2015 and its associated mid-century year 2065. Blue lines represent historic conditions, while red lines represent warmer, mid-century conditions..... 75

Figure 3.9. Annual simulated net ecosystem productivity (NEP) for each site. Biome-BGC simulations indicate that all sites largely maintain positive rates of ecosystem productivity and remain carbon sinks into the mid 21st century. At SC, historical years with large carbon sinks were typically cooler than average with prolonged snow pack presence..... 76

Figure 4.1. Proportion of measured monthly precipitation falling below average daily temperatures of 0°C for historical and mid-21st century conditions. For discussion of shifts in precipitation phase, precipitation occurring below this temperature threshold is assumed to fall as snow. Error bars indicate standard deviations (n= 20 simulation years at SC and RME, n= 13 simulation years at JDW)..... 107

Figure 4.2. Average monthly redistributed snow water held in the drift at each site under historical and mid-21st century conditions. Error bars indicate standard deviations (n= 20 simulation years at SC and RME, n= 13 simulation years at JDW). Drift size at each site is a function of topography, temperature, and total precipitation. Variations in calculated drift factors led to similar snow redistribution patterns at the dry mid-elevation site (SC) and wet high-elevation site (RME) while the wetter mid-elevation (JDW) experienced less snow accumulation..... 108

Figure 4.3. Simulated annual NPP rates for each species under historical and mid-21st century conditions. At mid-elevation sites (SC and JDW) aspen experienced decreased NPP under mid-21st century conditions. However, NPP of mountain big sagebrush experienced increased at all sites with warming temperatures. NPP of C3 grasses remained relatively unchanged across historical and mid-21st climate scenarios..... 109

Figure 4.4. Cumulative NPP for aspen, mountain big sagebrush, and C3 grasses at each site under historical (1996-2015) and mid-21st century conditions (2046-2065). Note that simulation periods for JDW are only 13 years compared to those of SC and RME (20 years) resulting in lower cumulative NPP. Under both climate scenarios, aspen accumulated the most carbon relative to mountain big sagebrush or C3 grasses. However, mountain big sagebrush experienced the largest proportional increase in total NPP relative to aspen or C3 grasses with warming..... 110

Figure 4.5. Average daily NPP (red and blue lines) for aspen, mountain big sagebrush, and C3 grasses at Sheep Creek (SC) across all simulation years (n=20 at RME and SC, 13 at JDW). Shaded bands indicate maximum and minimum simulation ranges. For shorter statured mountain big sagebrush and C3 grasses, several cool years with prolonged snow drift presence delayed spring growth under historical conditions. Under mid-21st century conditions, increased evaporative demand significantly reduced aspen and C3 grass NPP during the mid/late summer. 111

Figure 4.6. Daily NPP for each species at Sheep Creek (SC) during 2014 (blue) and the corresponding mid-21st century year 2064 (red). This simulation year experienced above average temperatures and below average total precipitation. Total annual NPP for aspen and C3 grasses was reduced under warmer and drier conditions, whereas mountain big sagebrush NPP remained similar under both historical and mid-21st century conditions..... 112

Figure 4.7. Proportion of years with acting as a net carbon sink (i.e. positive rates of net ecosystem production (NEP)) for each species under historical (1996-2015) and mid-21st century conditions (2046-2065). Under warmer and drier conditions, aspen and mountain big sagebrush maintain positive NEP rates across a majority of historical and future simulation years, although the magnitude of NEP for individual years can be reduced relative to historical conditions. Annual NEP of C3 grasses consistently alternated between positive and negative rates under both historical and mid-21st century climate scenarios. . 113

Chapter 1: Dissertation Introduction

In arid and semi-arid environments, the distribution and productivity of plant communities is largely driven by a combination of soil moisture availability and the need to minimize drought stress by closing stomata (Caylor et al., 2009). Thus, carbon assimilation by vegetation is tightly coupled with the availability of water needed to sustain photosynthesis. The distribution of productive upland semi-arid plant communities is typically in heterogeneous patches, with the location of these patches being driven by abiotic processes including preferential water flow or wind (Aguilar and Sala, 1999). Although they often represent a small proportion of the landscape, these productive communities are ecologically important and are often characterized by increased productivity (Breshears, 2006), rapid nutrient cycling and turnover of organic material (Belnap et al., 2005), diverse habitat structure (Fuhlendorf and Engle, 2001), and increased rates of biodiversity. Future shifts in temperature and precipitation may have significant ecohydrological impacts on these small, albeit important, ecosystem components.

The structure and spatial extent of productive vegetation patches across the landscape provides additional insight into the coupled ecological and hydrological processes and feedbacks that shape arid and semi-arid ecosystems (Thompson et al., 2011). Critical hydrological fluxes including evapotranspiration, infiltration, and streamflow are all influenced by vegetation. As a result, changes in vegetation or community structure can, in turn, influence hydrological fluxes across a range of temporal and spatial scales. However, the complex ecohydrological interactions in semi-arid environments continue to limit our ability to predict both ecological and hydrological responses under changing conditions. Productive semi-arid plant communities are often comprised of numerous species that may differ in their response to changes in temperature or precipitation. As a result, interdisciplinary approaches that link ecological and hydrological processes will become increasingly important when predicting the response of water-limited systems under future environmental change (Newman et al., 2006).

In mountainous regions of the western United States specifically, rising temperatures will likely alter the hydrology and ecology of many ecosystems with snow-dominated precipitation regimes. Where snowpack is particularly sensitive to fluctuations in temperature, warming will likely lead to decreases in the proportion of winter precipitation

falling as snow (Klos et al., 2014). Shifts in precipitation phase (e.g. rain or snow) can alter numerous hydrological processes including the timing of surface water input (Seyfried et al., 2009), canopy interception (Niemeyer et al., 2016), timing of snow residence (Luce et al., 2014), and streamflow (Nayak et al., 2010) all of which in turn influence the vegetation structure and productivity. In mountainous areas where topography and orographic effects create strong temperature and precipitation gradients, the spatial distribution of snow water resources can be highly variable. The redistribution of snow by wind is of particular importance and results in a heterogeneous distribution of precipitation across the landscape. Future decreases in the amount of precipitation falling as snow in complex terrain will result in a more spatially uniform distribution of precipitation. This will most heavily impact patchy and heterogeneously distributed plant communities that were reliant on soil moisture subsidies associated with drifting snow.

Since incoming precipitation in snow-dominated precipitation regimes has largely been asynchronous with periods of seasonal plant growth and soil moisture use, increased soil moisture inputs generated from pockets of redistributed snow (i.e. snowdrifts) may be an important control on the amount and duration of plant available water. Plant communities that are likely to experience particularly significant shifts in environmental conditions and a loss of resources with warming are those located within drift zones, where the accumulation of redistributed snow has historically been a primary source of growing season soil moisture. However, the impacts of future changes in precipitation phase (e.g. rain or snow) on vegetation in complex terrain remain uncertain. The response of plant communities to changes in precipitation phase is additionally influenced by variations in plant physiology, site characteristics (e.g. soils, aspect, slope), species composition, and atmospheric conditions (e.g. vapor pressure deficit). Understanding how vegetation will respond to changes in climate requires an ecohydrological perspective since shifts in vegetation can lead to feedbacks that alter key hydrological and biophysical processes such as precipitation interception, soil water infiltration, runoff, transpiration, soil temperature, and radiative fluxes (Ludwig et al., 2005, Breshears, 2006, Vose et al., 2016).

Hydrological and ecological processes are closely linked in upland plant communities established in drift zones (Figure 1.1). In these systems, the magnitude of redistributed snow is a function of total incoming precipitation, precipitation phase, and the

topographical characteristics of a site. Once snow is redistributed by wind, soil moisture available to plants is further constrained by additional site and soil characteristics including total soil moisture storage capacity and texture (hydrological controls, Figure 1.1). These plant communities are additionally comprised of numerous species with diverse physiological traits, rooting depths, and plant water use strategies. Differences in vegetation structure and characteristics can play a key role in the use and relative importance of soil water inputs generated from redistributed snow (ecological controls, Figure 1.1). As a result, ecological shifts such as mortality events or changes in species composition can influence hydrological processes. Likewise, hydrological changes such as shifts in precipitation phase can alter ecological processes. Under a future, altered state where temperatures are warmer, decreases in the snow:rain ratio can potentially have cascading effects across every aspect of the system. Changes in precipitation phase will ultimately shift the spatial patterns of precipitation distribution in complex terrain. However, the extent to which these impacts will influence ecohydrological processes is less certain. With these cascading effects in mind, predicting the response of drift zone vegetation to shifts in climate requires an integrated approach where both hydrological and ecophysiological controls on plant function are considered.

Dissertation scope and objectives

The scope of this dissertation centers on upland plant communities closely associated with snow drifts in a semi-arid watershed with a winter dominated precipitation regime. The following chapters primarily focus on the ecological responses to changing precipitation regimes (e.g. ecological controls, Figure 1.1). Since CO₂ uptake and transpiration are intimately linked, simulation models based on first-degree principles of carbon and water balance present a mechanistic approach towards understanding how shifts in water availability will impact whole plant function under a wide range of environmental conditions (Newman et al., 2006). In this dissertation, I use field measurements to inform a biogeochemical process model run using detailed climate datasets to determine how changes in precipitation phase will impact drift zone plant communities. To assess the dependence of vegetation on redistributed precipitation and response to warming temperatures, we simulated several ecosystem processes for three wide ranging species encountered in sagebrush steppe ecosystems under recent historical conditions and warmer mid-21st century

conditions. Each of the following three chapters are structured as a stand-alone paper to be submitted and published in peer-reviewed journals.

Chapter two assesses the dependence of aspen (*Populus tremuloides*), a highly productive drift zone species, on redistributed snow under historical conditions assuming both a uniform and redistributed precipitation spatial distribution. In this study, the response of aspen to redistributed snow is solely the result of topographical complexity. Simulations indicate, that under historical temperature regimes, snowdrifts have been an important source of growing season soil moisture at aspen stands receiving low amounts of total precipitation.

Chapter three builds on the results of chapter two by linking aspen productivity and redistributed snow to temperature changes projected under future climate change conditions. For this study, we applied projected temperature increases to measured historical datasets to represent conditions predicted by the mid-21st century. We then assessed how both reductions in snow:rain and changes in growing season conditions influence aspen productivity. Results from this study show that, under warmer temperatures, aspen can benefit from increased productivity during prolonged and more favorable spring growing conditions. However, increased drought severity later in the summer can offset spring carbon gains leading to a net loss in productivity at warmer and drier sites only.

Chapter four extends the results of chapter three to incorporate the response of two additional co-located species and plant functional types found in drift zone plant communities. The goal of this study was to determine how plants with differing growth forms, phenology, and ecophysiological traits might respond to shifts in climate and precipitation redistribution. The results of this paper provide a more comprehensive overview into the potential implications for species vulnerability, carbon cycling and sequestration in snow-dominated sagebrush steppe ecosystems. Simulations from this chapter suggest that, while all species remain productive, future conditions favor evergreen species like mountain big sage compared to deciduous aspen or C3 grasses.

References:

- Aguiar, M.R. and Sala, O.E., 1999. Patch structure, dynamics and implications for the functioning of arid ecosystems. *Trends in Ecology & Evolution*. 14: 273-277.
- Belnap, J., Welter, J.R., Grimm, N.B., Barger, N. and Ludwig, J.A., 2005. Linkages between microbial and hydrologic processes in arid and semiarid watersheds. *Ecology*. 86: 298-307.
- Breshears, D.D., 2006. The grassland–forest continuum: trends in ecosystem properties for woody plant mosaics. *Frontiers in Ecology and the Environment*. 4: 96-104.
- Fuhlendorf, S.D. and Engle, D.M., 2001. Restoring Heterogeneity on Rangelands: Ecosystem Management Based on Evolutionary Grazing Patterns: We propose a paradigm that enhances heterogeneity instead of homogeneity to promote biological diversity and wildlife habitat on rangelands grazed by livestock. *BioScience*. 51: 625-632.
- Klos, P. Z., Link, T.E., & Abatzoglou, J.T. 2014. Extent of the rain-snow transition zone in the western U.S. under historic and projected climate. *Geophysical Research Letters*. 41: 4560-4568.
- Luce, C.H., Lopez-Burgos, V. and Holden, Z., 2014. Sensitivity of snowpack storage to precipitation and temperature using spatial and temporal analog models. *Water Resources Research*. 50: 9447-9462.
- Ludwig, J.A., Wilcox, B.P., Breshears, D.D., Tongway, D.J. and Imeson, A.C., 2005. Vegetation patches and runoff–erosion as interacting ecohydrological processes in semiarid landscapes. *Ecology*. 86: 288-297.
- Nayak, A., Marks, D., Chandler, D.G., Seyfried, M., 2010. Long-Term Snow, Climate, and Streamflow Trends at the Reynolds Creek Experimental Watershed, Owyhee Mountains, Idaho, United States. *Water Resources Research*. 46: 1-15.
- Newman, B.D., Wilcox, B.P., Archer, S.R., Breshears, D.D., Dahm, C.N., Duffy, C.J., McDowell, N.G., Phillips, F.M., Scanlon, B.R. and Vivoni, E.R., 2006. Ecohydrology of water-limited environments: A scientific vision. *Water Resources Research*. 42(6).
- Niemeyer, R. J., Link, T. E., Seyfried, M. S., & Flerchinger, G. N. 2016. Surface water input from snowmelt and rain throughfall in western juniper: potential impacts of climate change and shifts in semi-arid vegetation. *Hydrological Processes*. 30: 3046–3060.
- Seyfried, M. S., Grant, L. E., Marks, D., Winstral, A., & Mcnamara, J. 2009. Simulated soil water storage effects on streamflow generation in a mountainous snowmelt environment, Idaho, USA. *Vadose Zone*. 10: 858–873.

- Thompson, S.E., Harman, C.J., Troch, P.A., Brooks, P.D. and Sivapalan, M., 2011. Spatial scale dependence of ecohydrologically mediated water balance partitioning: A synthesis framework for catchment ecohydrology. *Water Resources Research*. 47(10).
- Vose, J.M., Miniati, C.F., Luce, C.H., Asbjornsen, H., Caldwell, P.V., Campbell, J.L., Grant, G.E., Isaak, D.J., Loheide, S.P. and Sun, G., 2016. Ecohydrological implications of drought for forests in the United States. *Forest Ecology and Management*. 380: 335-345.

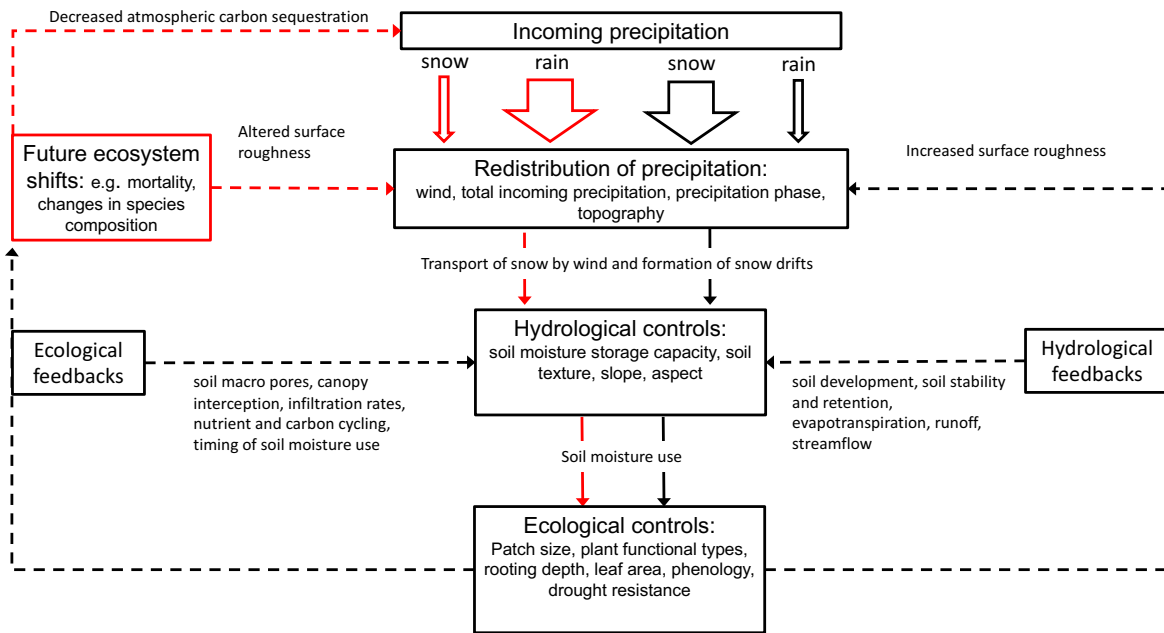


Figure 1.1. Interactions linking key ecological and hydrological processes in semi-arid upland plant communities growing in drift zones (modified from Ludwig et al., 2005). Hydrological and ecological controls are a function of both site and vegetation characteristics. Key processes are outlined by solid lines. Potential feedbacks are outlined by dashed lines. Conditions under historically snow-dominated precipitation regimes are outlined in black, warmer rain-dominated conditions are outlined in red (relative proportions of historical and future snow:rain are indicated by arrow size). Future climate and/or ecosystem shifts could potentially alter or reverse historical ecological and hydrological feedbacks.

Chapter 2: Simulating the Dependence of Aspen (*Populus tremuloides*) on Redistributed Snow in a Semi-Arid Watershed.

Soderquist B. S.¹, Kavanagh K. L.², Link T. E.¹, Seyfried M. S.³, Winstral, A. H.⁴

¹ Department of Forest, Rangeland, and Fire Sciences, University of Idaho, Moscow, ID, 83844, USA, ² Department of Ecosystem Science and Management, Texas A&M University, College Station, TX, 77843-2138, USA, ³ USDA Agricultural Research Service, 800 Park Blvd., Plaza IV, Suite 105, Boise, ID, 83712, USA. ⁴ Swiss Federal Research Institute for Snow and Avalanche Research WSL, Flüelastrasse 11, 7260 Davos Dorf, Switzerland.

Keywords: *Populus tremuloides*, net primary production, snowmelt, soil moisture, drought stress

Abstract

In semi-arid mountainous regions across the western USA, the distribution of upland aspen (*Populus tremuloides*) is often related to heterogeneous soil moisture subsidies resulting from redistributed snow. As temperatures increase, interactions between decreasing snowpack and future trends in the net primary productivity (NPP) of aspen forests remain uncertain. This study characterizes the importance of heterogeneous distribution of snow water to aspen communities in the Reynolds Creek Critical Zone Observatory located in southwestern Idaho, USA. NPP of three aspen stands was simulated at sites spanning elevational and precipitation gradients using the biogeochemical process model Biome-BGC and precipitation data adjusted to account for drifting snow. During drought years, simulations below the largest drifts that included wind-redistributed snow resulted in NPP values nearly 77% higher than simulations assuming uniform precipitation. Compared to a spatially homogeneous precipitation distribution, Biome-BGC simulations accounting for redistributed precipitation were in better agreement with previous simulations of snow accumulation and soil moisture field measurements. However, increased effective precipitation resulting from drifting snow did not have a significant role in aspen productivity at sites receiving higher annual precipitation, where soil moisture was non-limiting even in the absence of redistributed snow. At these sites, additional soil moisture inputs generated by snowdrifts often exceeded the storage capacity of the soil and contributed little to plant available water used later in the growing season.

2.1 Introduction

In mountainous ecosystems, interactions between hydrological and ecological processes can have profound impacts on the distribution and vigor of forests. Specifically, in regions of the intermountain west the redistribution of snow by wind can dramatically influence the amount and timing of water availability to vegetation and ecological communities (Litaor et al., 2008, Maurer and Bowling, 2014, Kormos et al., 2014, Vose et al., 2016). However, the dependence of plant productivity on these late season hydrological subsidies has not been adequately quantified. The relationship between redistribution of snow and the distribution of vegetation is particularly apparent in many semi-arid ecosystems of the Great Basin and intermountain western United States, where upland aspen (*Populus tremuloides*, hereby referred to as aspen) stands are frequently found in areas where snow drifting occurs (Burke et al., 1989, Sheppard et al., 2006). In many of these semi-arid regions, the availability of soil moisture is closely linked to the distribution of vegetation. In these small aspen communities, the presence of snow has a direct impact on both the timing of available soil moisture and vegetation productivity. Future shifts in the amount of redistributed precipitation via increasing temperatures may alter ecosystem function since upland aspen communities are highly productive relative to many other adjacent plant communities, characterized by increased understory biodiversity (Kuhn et al., 2011), and provide important, isolated habitats for many different avian and mammalian species (DeByle 1985, Griffis-Kyle and Beier, 2003).

Precipitation regimes are one of the principal drivers influencing forest net primary productivity (NPP), or the flux of carbon assimilated by vegetation minus autotrophic respiration (Van der Molen et al., 2011). Impacts associated with precipitation changes, such as reduced snowpack, decreased soil moisture availability, and increased evaporative demand have particularly affected aspen forests across much of North America (Allen et al., 2010, Worrall et al., 2013, Anderegg et al., 2013, Tai et al., 2016). In many parts of the western United States, precipitation occurs primarily in the winter, and through the processes of snowpack accumulation and melt, directly influences forest processes including phenology and aspen productivity (Barbour et al., 1991, Meier et al., 2015). However, since the mid 20th century, snowpacks across western North America have been declining (Mote et al., 2005, Knowles et al., 2006, Nayak et al., 2010 and 2012, Kapnick and Hall, 2012, Klos

et al., 2014). As temperatures have increased, numerous areas are experiencing an increase in the proportion of winter precipitation occurring in the form of rain (Nayak et al. 2010), reduced duration of snow cover, and a decline in the peak snow water equivalent (SWE) with no concomitant increase in annual precipitation.

In complex terrain, decreases in the proportion of precipitation falling as snow can also affect the spatial distribution of soil moisture. Snow can be transported across the landscape by wind creating scour and drift zones where effective precipitation inputs, defined here as the total amount of precipitation entering the soil profile, can be highly non-uniform across the landscape. Since heavier, denser water droplets are much less prone to topographically-induced depositional variations and are not subject to wind-driven redistribution after deposition as compared to ice crystals, warming-induced shifts in precipitation phase can produce more spatially uniform precipitation patterns. These changes in effective precipitation across the landscape may play a critical role in aspen productivity. Thus, interactions between the redistribution of snow and aspen productivity need be thoroughly assessed to determine how future shifts in winter precipitation phase and the loss of hydrologic storage in snow drifts may impact productive and ecologically important semi-arid species such as aspen.

The objective of this study is to understand the connections between changes in the annual proportion of snow and rain and the subsequent response in aspen NPP in semi-arid climates that characterize much of the western North America. We assess the relationship between water-contributing snow mass and aspen NPP at three stands using a biogeochemical process model run using long term meteorological datasets. Each of the selected aspen stands are located within a semiarid watershed that is transitioning from a snow- to a rain-dominated precipitation regime (Nayak et al., 2010). Field measurements of plant water status, soil moisture, and phenology indicate that aspen experience varying degrees of water stress depending on their location within the watershed's precipitation gradient. Within the watershed, the redistribution of snow has been simulated across a range of elevations and terrain. To assess the dependence of each stand on the redistribution of precipitation, model-forcing precipitation data at each site were adjusted to represent the snow drift that is located above each field-monitored aspen stand. Simulations of aspen NPP were then completed for two separate scenarios where uniform and redistributed

precipitation distributions were considered. Once a redistributed precipitation layer was accounted for, we hypothesized that: 1) simulated soil moisture availability will be prolonged later into the growing season, and 2) the resulting increase in soil moisture will lead to increased simulated aspen NPP relative to simulations assuming a uniform precipitation layer. Hypothesis 1 was tested by comparing soil moisture measured at each site to simulated soil moisture assuming both uniform and redistributed precipitation layers. Hypothesis 2 was tested by comparing simulated NPP for both uniform and redistributed precipitation layers across a wide-range of historic hydrometeorological conditions.

2.2 Methods

Using long-term meteorological datasets to simulate hydrological and ecological processes allows us to link historic inter-annual variability in snow redistribution to the resulting vegetation response which is additionally influenced by site and growing season conditions. We used a combination of field measurements and previous simulations of snow redistribution to inform a process based biogeochemical model to better understand the connections between redistributed precipitation and carbon fluxes in upland aspen ecosystems. To account for the presence of drifting snow, measured precipitation data were adjusted using drift factors calculated from previously validated simulations of snow redistribution. Final precipitation adjusted climate datasets spanned 13 to 31 years depending on the site and were used to simulate carbon fluxes and other ecosystem processes, including snowpack accumulation, soil moisture use, photosynthesis, and transpiration at a daily time step.

2.2.1 Site selection and description

Established in 1960 by the United States Department of Agriculture (USDA), the Reynolds Creek Experimental Watershed (RCEW) and Critical Zone Observatory (RCCZO) are collocated in the Owyhee Mountains of southwest Idaho (Figure 2.1). The RCEW encompasses an area of 239 km² and has been the location of extensive research focusing on long-term monitoring to advance the understanding of hydrologic processes in complex terrain and develop hydrological models (Marks et al., 2001). Since its creation, an extensive array of hydrological and meteorological instrumentation has been maintained throughout the watershed. Over the period of observation, the RCCZO has experienced an approximately 2°C increase in mean annual temperature leading to a shift in phase of winter

precipitation (Seyfried et al., 2011). Across the watershed, particularly at mid and low elevations, declines in snowpack and increases in rain on snow events have been documented over the past 50 years (Nayak et al., 2010).

The distribution and function of vegetation within the RCCZO is strongly controlled by terrain, precipitation, and soil moisture availability (Finzel et al., 2015). Across middle and upper elevations of the watershed, highly productive aspen stands are often distributed along leeward slopes and we hypothesize that they utilize water subsidies stemming from large snowdrifts that persist late into the spring months (Seyfried et al. 2011). Three sites located in the southern regions of the RCEW were used in this study: 1) in the Reynolds Mountain East (RME) drainage, 2) in the Sheep Creek (SC) drainage, and 3) in the upper Johnston Draw drainage (JDW) (Figure 2.1, Table 2.1). Each site consists of a small aspen stand with a snowdrift located immediately upslope. Site elevations span the current rain/snow transition zone, which is most susceptible to warming-induced changes in precipitation phase.

2.2.2. Plant water relations

Measurements of soil moisture (θ_v) and pre-dawn branch water potentials ($\Psi_{pre-dawn}$) were conducted during the 2012 -2015 growing seasons. Soil moisture was monitored at one to two soil moisture profiles in each stand. In the spring of 2012, soil moisture sensors were installed at RME. Soil moisture sensors (Decagon Devices, Pullman WA) were installed at depths of 10, 30, 60, and 120 cm at two profiles extending from the stand edge to stand interior. Measurements were recorded hourly and stored using data loggers (Models EM50 and EM50R, Decagon Devices, Pullman WA). Similar soil moisture transects were installed at SC in the spring of 2013, where two profiles extended from the stand edge to stand interior with soil moisture sensors at depths of 10, 30, 70, and 100 cm. Soils at RME and SC were fairly homogenous without distinct sand or clay layers. Due to the relative homogeneity of the soils, site specific calibrations of the sensors were not necessary (Kizito et al., 2008). The soil moisture at JDW was monitored by a single sensor profile (Stevens Water Monitoring Systems, Inc., Portland, OR) located in the center of the aspen stand with sensors at 5, 20, 50, 75, and 88 cm depths.

Volumetric water content (θ_v , $m^3 m^{-3}$) measured from installed probes was then used to calculate total root zone soil moisture storage ($S_{rootzone}$, mm) at each site. Simulated $S_{rootzone}$

was calculated from the simulated soil depth and daily θ_v values integrated across the single uniform soil layer parameterized in Biome-BGC (Table 2.1, described below). Using the same estimated soil depth, total measured $S_{rootzone}$ for a given site was calculated using the equation:

$$S_{root\ zone} = \sum_{i=1}^{i=number\ of\ layers} \theta_i * D_i \quad (1)$$

where θ_i is the measured volumetric water content of layer i , and D is the depth (mm) of layer i . Due to differences in effective root zone and soil moisture probe depths, site-specific storage equations were used to calculate $S_{rootzone}$ (Table S1, Appendix 1).

Monthly measurements of $\Psi_{pre-dawn}$ were made at most sites during the 2012-2015 growing seasons using a pressure chamber (PMS instruments, Corvallis, OR) and standard methods (Scholander, 1965). At each site, two branch samples were collected before sunrise from a dominant tree at three plots extending from stand edge to stand center. Sampled trees were chosen based on their proximity to the automated soil moisture profiles along each transect. Branches were taken from consistent heights (~1-2 m) from the same trees across the growing season. Based on porometer measurements (SC-1 leaf porometer, Decagon Devices, Pullman, WA), nighttime transpiration was negligible (data not shown) and $\Psi_{pre-dawn}$ was assumed to be in equilibrium with Ψ_{soil} , which therefore provided information about the timing and magnitude of soil moisture limitation experienced by aspens at each site.

2.2.3. Phenology

Timing of aspen phenology was measured at each site during the 2013-growing season using daily time-lapse imagery spanning spring leaf flush to leaf senescence. Images were taken with a time-lapse camera (Wingscapes, Ebsco Industries, Birmingham, AL) once a day from a fixed location. Changes in phenology were estimated using the 2G_RBi difference index (Richardson et al., 2007) calculated from red, green, and blue color channels extracted from one to two points located within the canopy of each stand. Buffer zones were defined for each point in the canopy and were set to maximize the area of continuous canopy. If a stand contained more than one measured location in the canopy, the 2G_RBi difference indices were averaged to produce a single value representing the whole stand.

2.2.4. Simulations of snow redistribution.

Simulations of snow redistribution were used to determine the amount of water held in snowdrifts above or neighboring the aspen stands simulated using Biome-BGC. Each simulated stand (described below) lies within or borders where snow drifting and ablation dynamics were simulated using iSnobal. iSnobal (Marks et al., 1999) is a spatially adapted version of the physically based, mass- and energy-balance snow model SNOBAL that produces grid based simulations of snow states and energetics based on climate variables modulated by vegetation and topography (Winstral and Marks, 2002, Reba et al., 2011, Winstral et al., 2013). The model simulates a two-layer snowpack consisting of a thinner, more dynamic surface layer that interacts directly with the atmosphere and a second deeper layer affected only by the overlying snow layer and underlying soil. Meteorological drivers are air and soil temperature, vapor pressure, downwelling longwave radiation, net shortwave radiation, wind speed, and precipitation. The snowpack is distributed over a grid based on a digital elevation model (DEM) allowing for snowpack variations driven by topographic complexity to be effectively represented. Additionally, canopy cover inputs incorporate the effects of vegetation on snow accumulation and distribution. The model computes snow states including snow water equivalent (SWE, mm), depth (m), density (kg m^{-3}), layer temperatures, and average liquid-water content (%) (Marks et al., 2001). This model has been applied to watersheds of various sizes across the Pacific Northwest and has been extensively tested and validated within the RCEW (Marks and Winstral, 2001, Seyfried et al., 2009, Reba et al., 2011, Nayak et al., 2012). iSnobal has been further developed within the RCEW to account for the redistribution of snow across a range of catchment scales (Winstral et al., 2013). The iSnobal simulations from Reba et al., 2011 (1984-2008 at RME) and Winstral et al., 2013 (2007-2008 at SC and 2006-2007 at JDW) were the primary sources used to adjust the precipitation forcing data applied in Biome-BGC.

Drift factors used to adjust precipitation data were calculated using values of iSnobal-simulated peak SWE from a point located in the center of drifts either directly upslope of stands simulated by Biome-BGC or from a representative drift nearby, as in the case of SC, where the stand lies just outside the modeled catchment. The annual drift factor (*DF*) was calculated as the ratio of peak SWE simulated by iSnobal to total measured snow

without drift effects, from the date of initial drift formation to the date of peak SWE simulated by iSnobal (here referred to as the drift accumulation period) using the equation:

$$DF = \frac{\text{Peak simulated SWE (mm)}}{\text{Total measured uniform snow (mm) across drift accumulation period}} \quad (2)$$

Drift factors were applied to all precipitation data occurring below freezing temperatures. Since Biome-BGC operates on a daily time step, the full drift factor was applied to total daily precipitation if average daytime temperature (T_{day}) and average nighttime temperature (T_{night}) were $\leq 0^{\circ}\text{C}$. If either T_{day} or T_{night} were $> 0^{\circ}\text{C}$, a drift factor with a rate of increase 50% less than the full drift factor was applied to total daily precipitation. This decreased drift factor application conservatively accounts for the occasional rain on snow event that cannot be captured by a daily time step. A drift factor was not applied to daily precipitation if both T_{day} and T_{night} were $> 0^{\circ}\text{C}$. If years simulated in Biome-BGC had been simulated by iSnobal, the calculated drift factor was applied. However, if years used in Biome-BGC simulations were not simulated by iSnobal, the average drift factor calculated from available iSnobal simulations was used (29 years at SC, 11 years at JDW, 7 years at RME).

2.2.5. Estimates of NPP

Estimates of NPP were obtained using Biome-BGC (version 4.2, Thornton et al., 2002) a biogeochemical process model that predicts forest productivity through the simulation of carbon, nitrogen, water, and energy fluxes. Carbon assimilation is simulated from above and below ground pools and fluxes describing photosynthetic growth and decomposition of organic matter. Vegetation simulated from these fluxes is characterized by a single, user defined, plant functional type. The model is run with daily meteorological inputs and parameterized with site and species-specific ecophysiological variables. Photosynthetic processes are divided into two layers within the canopy, where photosynthesis and canopy conductance are calculated separately for sunlit and shaded leaves. Soil hydrology is based on a single, uniform soil layer with a user-defined depth. Soil texture is characterized by percentages of sand, silt, and clay. Phenological processes are a combined function of both soil temperature and photoperiod. For leaf flush to occur, soil temperatures calculated from an 11-day running average of daily air temperatures must exceed critical temperature thresholds. Incoming solar radiation also limits vegetation growth and a critical day length of 10.9 hours contributes to both leaf flush and senescence

(White et al., 1997). Leaf senescence is triggered by both cooling soil temperatures and decreasing photoperiod.

2.2.6. Parameterization of BIOME-BGC v 4.2

Biome-BGC is a process based biogeochemical model that has been extensively validated and analyzed under a variety of forest ecosystems and conditions (Churkina et al., 2003, Boisvenue and Running, 2010). Biome-BGC is driven with inputs of maximum daily temperature (T_{max} , °C), minimum daily temperature (T_{min} , °C), average daylight temperature (T_{day} , °C), average daylight vapor pressure deficit (VPD, Pa), total daily precipitation (cm), daily average shortwave radiant flux density ($W\ m^{-2}$), and length of daylight period (s). Air temperature, relative humidity, and precipitation were measured at climate stations neighboring each site. T_{day} , daylight length, and average shortwave flux density were estimated using the point based microclimate model MTCLIM (version 4.3, Thornton et al., 2000). Average daylight VPD was calculated from hourly measurements of temperature and relative humidity. Complete climate data sets spanned 1985-2015 for RME and SC, and from 2003-2015 for JDW. Final simulations assumed both a uniform and redistributed precipitation layer accounting for the drifting of snow.

Biome-BGC simulations also require a set of ecophysiological parameters (White et al., 2000). In the case of a deciduous broadleaf forest (DBF) biome, model performance is most sensitive to seven ecophysiological parameters (specific leaf area (SLA), fine root carbon: nitrogen ($C:N_{root}$), and foliar carbon: nitrogen ($C:N_{leaf}$), maximum stomatal conductance ($g_{s,max}$), percent leaf nitrogen as Rubisco (PLNR), light extinction coefficient (k), and the water interception coefficient (W_{int})). We measured three of these seven parameters at each site: SLA, $C:N_{root}$, and $C:N_{leaf}$. $C:N_{leaf}$ was measured from sunlit, upper canopy leaves collected during the summers of 2012 and 2013. Leaves were sampled along a transect of three plots extending from stand edge to stand interior at each site. To minimize the effects of shading and competition, upper canopy branches were retrieved from a dominant, representative tree within each plot. At least seven large, sunlit leaves were selected from the branches taken from each plot and placed in sample bags containing moist paper and stored on ice in a cooler. Freshly sampled leaves were photographed next to an analog measurement scale for subsequent of leaf area. Leaves were oven dried at 65-70 °C for 48 hours and prepared for C:N analysis. Carbon masses from each sample were

additionally used for calculations of SLA, defined in Biome-BGC as $\text{m}^2 \text{kg leaf C}^{-1}$. Leaf area calculated using the image analysis software ImageJ (Schneider et al., 2012, available online: <http://rsb.info.nih.gov/ij/index.html>). The sampling strategy for fine roots was similar to that of leaves, and was completed during the same timeframe. Aspen roots $<5 \text{ mm}$ in diameter were sampled from three plots spanning stand edge to stand center at each site. Before analysis, sampled roots were gently washed with water to remove excess dirt and debris. Once cleaned, roots were oven dried at $65\text{-}70 \text{ }^\circ\text{C}$ for 48 hours and analyzed for C:N values. Differences in $C:N_{\text{leaf}}$, $C:N_{\text{root}}$, and SLA across sites were determined using a one way ANOVA.

The majority of the remaining ecophysiological parameters were obtained from previously published studies or adjusted based on field measurements. Estimates of the light extinction coefficient (k), water interception coefficient (W_{int}), and maximum stomatal conductance ($g_{s_{\text{max}}}$) were obtained from published values (Table S2, Appendix 1). PLNR was also decreased from default values based on estimates calculated from SLA, $C:N_{\text{leaf}}$, and maximum carboxylation rates ($V_{c_{\text{max}}}$) (White et al., 2000, Lenz et al., 2010). Due to covariation with other parameters like SLA and $C:N_{\text{leaf}}$, PLNR was allowed to vary within the standard deviation of the combined average of calculated values across all three sites (0.08, SD=0.02, see White et al. 2000 for calculation). Additional site-specific parameters including soil texture and soil depth were measured or estimated at soil profiles excavated at each site, where soil samples extending to 100-120 cm were collected at two plots located at stand edge and stand interior. Samples from sequential depths at each soil profile were sieved to 2 mm. Average percentages of sand, silt, and clay were measured by sedimentation tests, where soil texture is calculated based on the rate and volume of particle sedimentation in water. Values were used to parameterize soil texture for the uniform soil layer used by Biome-BGC simulations at each site (Table 2.1).

2.2.7. Model evaluation

For Biome-BGC, comparisons between simulated and observed leaf area index (LAI), soil moisture, snowmelt, and dates of leaf flush and senescence are useful assessments of model performance (Running and Waring, 2007). Maximum LAI was measured at each stand in the early summer of 2013 using a LP-80 ceptometer (Decagon Devices, Pullman, WA). Simulations of S_{rootzone} were compared to measured values from

2012 -2015. Timing of Biome-BGC snowmelt and total SWE were compared to available iSnobal output. Additionally, phenological measurements at each site were used to further inform and assess the accuracy of simulations.

2.3 Results

2.3.1. Measured soil moisture storage

Measured $S_{rootzone}$ across all sites tended to follow similar seasonal trends throughout the year, where peak soil moisture storage occurred during the late winter and early spring following peak snowmelt (Figure 2.2). From the onset of spring green up, measured $S_{rootzone}$ declined steadily across each growing season. From 2013-2015, the frequency and intensity of spring and summer precipitation events varied across the measurement period. While summer precipitation events occasionally replenished the upper 30 cm of soil, their influence was often short lived due to higher rates of evapotranspiration during the summer months (not shown). As soil moisture became increasingly limited in the region measured by soil moisture sensors, measured $S_{rootzone}$ began to plateau as either plant water use decreased or soil moisture was withdrawn at depths extending beyond the measured profile (Figure 2.2). Once the minimum $S_{rootzone}$ was reached, it remained relatively constant at each site until the occurrence of late summer and early fall precipitation events. Typically, the most significant rain events took place in the early fall, near the end of the growing season. However, the magnitude and frequency of rain events varied from year to year.

2.3.2. Indicators of Drought Stress

The timing and magnitude of drought stress varies by site. Measurements at RME and JDW, sites with higher annual precipitation, (Table 2.1) reflected adequate levels of soil moisture with $\Psi_{pre-dawn}$ remaining around -0.5 MPa across much of the 2012-2015 growing seasons (Figure 2.3). At these sites, $\Psi_{pre-dawn}$ values typically began to decrease in early to mid-September and reach minimum values in early October during leaf senescence. Conversely, SC $\Psi_{pre-dawn}$ declined earlier in the growing season, where minimum $\Psi_{pre-dawn}$ levels occasionally fell below -1.4 MPa, and could remain below -1.0 MPa for extended periods of time (e.g. 2013, 2015). Variations in $\Psi_{pre-dawn}$ across the measurement period suggest that changes in precipitation timing and phase may play an important role in drought stress experienced by aspen stands along this precipitation gradient.

2.3.3. Phenology

Growing seasons predicted by Biome-BGC varied in length with most variability occurring in the timing of spring leaf flush (mean date of onset, SC= Julian day 120 ± 15 , JDW= 121 ± 17 , RME= 126 ± 15 days). Across the entire simulation period, average growing season lengths were 182, 181, and 174 days long at SC, JDW, and RME, respectively. At all sites, modeled growing season onset was primarily a function of soil temperature calculated from an 11-day running average of daily temperatures. Since there is no correction in Biome BGC's phenology model for the insulating effects of snowpack on soil temperature, the annual growing season onset dates for a given year remained the same for simulations of uniform and redistributed precipitation (Figure 2.6 c, f, i). Simulated leaf senescence was governed almost entirely by photoperiod at each site, with complete canopy senescence occurring in late October.

Time-lapse photos from the 2013 growing season indicated reasonable agreement between simulated and observed spring phenology. Biome-BGC simulated leaf flush began on day of year 121, whereas measured green-up reached 50% of maximum on day of year 126. Complete leaf senescence was observed from days 295-298 compared to simulated senescence occurring on day 302. Averaged across all sites, 2013 simulated green-up occurred 6.7 days earlier than green-up predicted by the 2g_Rbi difference index (SD= 3.8, n=3, Richardson et al. 2007).

2.3.4. Redistribution of precipitation

Average drift factors also varied between sites. SC had the largest drift factor of (3.98, SD=1.61), followed by JDW (2.17, SD=1.00), and RME (1.45, SD= 0.24). After applying drift factors to measured precipitation data, effective annual precipitation was dramatically increased at SC (Figure 2.5b), whereas precipitation increases were more modest at JDW and RME where drifts above each stand tended to be smaller (Figure 2.5a, c). The magnitude of precipitation changes also varied from year to year at each site, indicating annual variability in the temperature during precipitation events, dominant precipitation phase, and timing of events.

2.3.5. Timing and accumulation of snowmelt

Initially, Biome-BGC simulations were unable to accurately depict snowmelt accumulation and melt dynamics of snowdrifts. For example, at mid-elevation sites, the

snowpack was often transitory during the winter, whereas validated iSnobal simulations predicted the continuous presence of snow in the drift zone throughout the winter months (December through March). To address rapid melt rates in Biome BGC, the daily temperature threshold to initiate snow melt was calibrated based on the well-validated physically-based snow simulations. The threshold was therefore lowered from $T_{\text{avg}} > 0^{\circ}\text{C}$ to $T_{\text{min}} > 2^{\circ}\text{C}$ at SC and JDW and $T_{\text{min}} > 0^{\circ}\text{C}$ at RME. After adjustments to melt initiation temperatures, snowmelt timing in simulations accounting for redistributed snow by Biome-BGC improved and remained unbiased ($R^2=0.76$, $y=1.1148x-15.921$, Figure 2.4). At RME, JDW, and SC, final melt out day for years that had both iSnobal and precipitation-adjusted Biome-BGC simulations occurred within an average of 7 (SD=6, n=24), 13 (SD=7, n=2), and 24 (SD=9, n=2) days of iSnobal simulations, respectively.

2.3.6. Parameterization of Biome-BGC

As determined by a one way ANOVA, measured values of $C:N_{\text{root}}$, $C:N_{\text{leaf}}$, and SLA were significantly different across sites (all p values < 0.001, $\alpha=0.05$, Table S2, Appendix 1). Simulations were subsequently run using site-specific averages. Average soil textures for each site varied slightly in sand content but fell into the general classification of silt loam. Soils at all sites had very low rock contents (<5%). Final estimated soil depths varied between sites with RME and JDW having the deepest effective soil depths of 1.2 m and SC having a slightly lower effective soil depth of 1.1 m due to a restrictive layer at ~1 m (Table 2.1).

2.3.7. Biome-BGC simulated soil moisture

Although the simulated S_{rootzone} was more accurate after accounting for the redistribution of snow, reductions in the simulated S_{rootzone} tended to occur more rapidly in Biome-BGC compared to measured values (Figure 2.2). While the rate of soil moisture use was greater than observed, the growing season S_{rootzone} in simulations accounting for the redistribution of snow tracked measured values more closely than simulations assuming a uniform precipitation layer. At SC in particular, the S_{rootzone} simulated using uniform precipitation inputs frequently fell to levels lower than those measured and remained limiting across longer periods of the growing season until the onset of replenishment from late summer and fall precipitation (Figure 2.2).

Seasonal fluctuations in simulated θ_v were similar to trends in $S_{rootzone}$, where θ_v increased to field capacity during snowmelt at all sites after accounting for the redistribution of snow (Figure 2.6). At the driest site, SC, simulations assuming a uniform precipitation layer often had a substantial soil moisture deficit which persisted through the spring months following complete snowcover ablation. During dry years (e.g. 2007) at SC, vegetation in simulations assuming a uniform precipitation layer experienced pre-leaf flush θ_v values approximately $0.15 \text{ m}^3\text{m}^{-3}$ lower than simulations accounting for redistributed precipitation (Figure 2.6e). At all sites, simulated soil moisture use patterns were similar to those observed, where simulated soil moisture was gradually reduced after spring leaf flush as transpiration continued throughout the growing season.

Timing of soil moisture limitation was determined when simulated declining soil moisture levels plateaued and NPP rates became negative. Biome-BGC simulations only indicated prolonged periods of limiting soil moisture for SC whereas differences between uniform and adjusted simulations for JDW and RME were negligible. Years similar to 2007, with low levels of measured precipitation and pronounced summer drought experienced the greatest relative increases in plant available soil moisture from snow redistribution. During these years, plant available soil moisture between simulations assuming uniform and redistributed precipitation could be extended by as much as 35 days for dry years (Figure 2.6f).

2.3.8. Simulated NPP

Across the entire simulation period, NPP assuming a uniform precipitation layer varied across sites, averaging 418, 447, and 333 $\text{g C m}^{-2} \text{ yr}^{-1}$ at RME, JDW, and SC, respectively. Large increases in aspen NPP after precipitation redistribution adjustments were only observed at SC (Figure 2.5e), where average annual NPP across the 31-year simulation period increased just over 18% to 396 $\text{g C m}^{-2} \text{ yr}^{-1}$. RME and JDW experienced little to no change in NPP across the entire simulation period (Figure 2.5d, f). For dry years, where growing season precipitation was minimal (i.e. 2007), NPP at SC was dramatically affected by the addition of redistributed snow (Figure 2.6f). Specifically, 2007 was a drier than average year with 303 mm of annual uniform precipitation. After accounting for redistributed snow, precipitation was increased to 670 mm. Total annual NPP assuming a uniform precipitation layer was 200 kg C m^{-2} , whereas total annual NPP accounting for

redistributed snow was 354 kg C m^{-2} , an increase of over 75% (Figure 2.6f). Additionally, NPP remained positive nearly 40 days longer when redistributed snow was considered.

While dry years were most likely to experience a response, redistribution of snow did not always result in increased NPP. At SC, differences between uniform and redistributed simulations were inconsistent across the simulation period and were occasionally negligible during certain years (e.g. 1995, 2015, Figures 2.5, 2.6c, i). For example, 1995 (Figure 2.6) was a relatively cool year with nearly the same amount of measured precipitation as 2007. However, cooler temperatures in 1995 delayed snowmelt while spring rains decreased both the soil moisture deficit and evaporative demand early in the growing season (Figure 2.6a). Together, these factors helped alleviate drought stress and subsequently offset the benefits of redistributed snow, and hence resulted in annual NPP values that were effectively the same across redistributed and homogeneous precipitation treatments (Figure 2.6c).

Simulations also indicate that above average temperatures and decreased snowpack don't always result in large differences between uniform and redistributed precipitation cases. Compared to 2007, which was a warm year with a continuous snowpack, 2015 had increased winter and spring temperatures that significantly reduced precipitation occurring as snow leading to a small, transitory snowpack (Figure 2.6g). Even with a redistributed precipitation layer, little drift formation occurred and relatively early ablation during the winter and spring reduced the late season soil moisture subsidy to the point where annual NPP was similar for both uniform and redistributed simulations (Figure 2.6i). During the 2015 growing season, the loss of this soil moisture subsidy was supplemented by larger and more frequent spring and summer rains (Figure 2.6f, g). Despite above average temperatures and a transitory snowpack, 2015 was a year with some of the highest NPP rates across all sites (Figure 2.5d, e, f), indicating that the redistribution of precipitation is only one of numerous factors that can lead to increased annual productivity.

2.4 Discussion

2.4.1. Soil moisture availability

Increased late season soil moisture with the incorporation of redistributed snow was only observed at the SC aspen stand where topographical conditions facilitate the formation of a particularly large drift (as reflected by the calculated drift factor). At that site,

simulations of $S_{rootzone}$ and θ_v showed prolonged periods of limited plant available soil moisture, particularly during years with low annual precipitation and a high soil moisture deficit under the uniform precipitation case (Figures 2.2, 2.6). In contrast, smaller drifts at RME and JDW failed to prolong plant available water, indicating an adequate supply of soil moisture even in the absence of redistributed precipitation. Based on the results of this study, aspen stands most likely to benefit from redistributed snow are those receiving less than about 500 mm of average annual uniform precipitation. Simulations also suggest that, in the absence of large soil moisture storage capacities, a large portion of snow water may exit the system early in the growing season, limiting its availability later in the growing season. Studies conducted in similar semi-arid watersheds have found that soil water storage capacities can be a limiting factor in snow water uptake by vegetation (Smith et al., 2011) and that snow water can pass through upper soil layers relatively quickly regardless of maximum snow depth (Grant et al., 2004).

While the redistribution of snow was reasonably incorporated into Biome-BGC, incorporating additional detail into the simulation of hydrological processes spanning the soil, plant, atmosphere continuum (SPAC) will strengthen our understanding of the interactions between snowpack and vegetation function (Vose et al., 2016). The overestimated rates of soil moisture depletion simulated by Biome-BGC (Figure 2.2) may be the result of several factors including the generalized representation of stomatal control, soil depth, and soil profile structure in Biome-BGC, or sensitivities in the parameterization of the site parameters such as average uniform soil texture and effective soil depth. Since soil moisture probes used a single calibration curve, calculations of $S_{rootzone}$ may have increased error due to textural differences across soil layers. However, factory testing and experiments from Kizito et al. (2008) indicate that the sensors used in this study produce accurate measurements of θ_v across a broad range of soil textures using a single calibration curve.

Soil moisture dynamics are further complicated when plant water uptake is considered in addition to snowmelt timing and seasonal variability in evaporative demand. Previous research examining the water balance of the upper SC catchment has shown that spring precipitation doesn't usually contribute much to streamflow but can play an important role in reducing evaporative demand and soil moisture deficits that occur later in the

growing season (Chauvin et al., 2011). These findings, in addition to the simulations in this study, indicate that soil moisture availability and use can be largely influenced by not only the amount of snow water availability, but also by spring growing conditions when transpiration and vegetation growth rates are typically high.

2.4.2. Aspen productivity and response

While comparable NPP data specific to western, semi-arid aspen forests are limited, simulated annual NPP rates of $420 \text{ g C m}^{-2} \text{ yr}^{-1}$ were within the range of values published for aspen in many parts of North America. Previous modeling studies of boreal aspen forests indicate that simulated mean NPP rates range widely from 332 to $804 \text{ g C m}^{-2} \text{ yr}^{-1}$ and can vary substantially depending on soil type and plant water availability (Huang et al., 2013). Similarly, measured NPP values in similar boreal regions report NPP values between 416 to $440 \text{ g C m}^{-2} \text{ yr}^{-1}$ (Gower et al., 1997) with the most productive sites reaching $795 \text{ g C m}^{-2} \text{ yr}^{-1}$ in Alaska (Gower et al., 2001).

As seen with simulations of soil moisture, increased NPP was only observed at SC after accounting for the redistribution of snow, contrary to the hypothesis that all sites would experience increased productivity due to snow drifting. This trend may be partially the result of the site's relative location within the local precipitation gradient. SC currently experiences half of the annual precipitation relative to RME and exists in an area of larger drift formation than the other two study sites. The effect of the snow subsidy is reduced at sites receiving more precipitation, where productivity of aspen stands may be less sensitive since soil moisture is non-limiting at these wetter sites, especially when combined with lower growing season VPDs, and adequate soil storage capabilities.

While simulated phenology agreed well with observations of leaf flush and senescence during the 2013 growing season, the phenological sub routine in Biome-BGC could be improved. Although the model accounts for both temperature and radiation controls on plant phenology, corrections for snowpack have not been implemented in this version of Biome-BGC. For these simulations specifically, this simplification could have potential implications for total growing season length. The impact on growing season is twofold. Reductions in snow pack may result in earlier spring leaf flush while prolonged snowpack presence could also delay leaf flush leading to shorter overall growing seasons. For simulations accounting for the redistribution of precipitation, snowpack usually melts before

leaf flush. However, cooler years with high amounts of snow water can have periods where spring photosynthesis overlaps snowpack presence. Since snowpack does not delay leaf flush in the model, this may result in overestimates of growing season length during cooler years. This bias is most prominent at RME, the coolest site where snowpack presence is often the most persistent. For 2013, BGC predicts leaf flush occurring 11 days earlier than observed. This larger error relative to warmer sites like SC and JDW (simulated leaf flush occurred 4 days earlier than measured), is likely due to the model's oversimplification of the insulating properties of the snowpack and subsequent effects on soil temperature and plant phenology.

As depicted in the simulations, aspen growth and senescence are closely linked to changes in soil temperature and photoperiod (Fracheboud et al., 2009). However, *Populus* phenology has also shown sensitivity to shifts in temperature during both early and late season phenological events (Rohde et al., 2011). These interactions are not represented in the Biome-BGC phenology model, and may not fully capture the range of vegetation response to continued warming spring and fall temperatures and decreased snow pack and that will result with further climate change. While phenological processes were necessarily simplified in Biome-BGC, our simulations capture the primary environmental controls determining growing season length and are in relative agreement with observations.

The combination of factors, including precipitation timing, elevation, and site characteristics, results in complex interactions which vary across relatively small scales within the RCEW. For instance, while SC was the only site to experience significant increases in NPP, the response varied by year, indicating the presence of other factors linking vegetation productivity to precipitation phase and timing. Sheep Creek NPP tended to have the largest response to redistribution of snow on years when uniform precipitation (rain) was low (e.g. 2007, Figure 2.6d). However, for years where uniform precipitation was high, the magnitude of increase in NPP was much smaller. Although the response showed a large degree of variability, the overall year to year trend in annual NPP from 1985 to 2015 was stabilized after accounting for redistributed snow (Figure 2.5e), indicating that a snow water subsidy from drifts may provide an important buffering effect during extreme drought or low snow years.

Unlike 2007, where there was a pronounced period of summer drought, simulation years with cool summer temperatures and frequent spring precipitation often showed little response to the redistribution of precipitation. For instance, although 1995 was a year where snowpack presence was significantly reduced in the absence of a drift, cooler temperatures and frequent spring rains helped reduce the spring soil moisture deficit (Figure 2.6a). Growing season rain events were also more frequent during the spring and summer of 1995 (Figure 2.6a) and provided brief pulses in available soil moisture in addition to reducing transpiration rates. While summer precipitation did occur during 2007, the events were fewer and smaller ultimately having little impact on long term soil moisture availability, VPD reduction, or increased mid-summer NPP (Figure 2.6).

While these results indicate that a decrease in snow water inputs from redistributed snow can have important ecological implications, vegetation leaf area can exert additional controls on soil moisture availability. This was most apparent during 2015, a year with above average temperatures and approximately average annual precipitation. Daily simulations of NPP and θ_v for SC (Figure 2.6) show how canopy development can influence seasonal trends in soil moisture use. For 2015, differences in maximum LAI between uniform (LAI= $1.3 \text{ m}^2 \text{ m}^{-2}$) and redistributed simulations (LAI= $1.6 \text{ m}^2 \text{ m}^{-2}$) led to differing rates of soil moisture depletion across the growing season (Figure 2.6h). The higher LAI occurring in the redistributed precipitation simulations resulted in higher rates of NPP in the spring followed by periods of soil moisture limitation later in the summer. Conversely, uniform precipitation simulations had a lower LAI, leading to slightly lower daily NPP rates during the spring. Ultimately, decreased LAI and spring NPP rates for uniform precipitation simulations led to more conservative soil moisture use later in the growing season (Figure 2.6h). While trends in daily NPP differed between precipitation cases, total annual NPP for uniform and redistributed precipitation simulations were similar for 2015. Overall, these simulation years highlight the variety of vegetation responses to changes in snowpack. However, it is important to note that while subsequent years of ample soil moisture and low evaporative demand may allow some recovery in vegetation productivity, severe drought years can have significant legacy effects and may ultimately exert sufficient stress to limit complete recovery or result in stand death (Anderegg et al., 2013, Vose et al., 2016).

These results show the responses of soil moisture and NPP to redistributed precipitation can differ by year and between sites in relatively close proximity. While certain soils in the RCEW may be limited by their storage potential, these simulations suggest that larger drifts in areas with higher seasonal soil moisture deficits are much more likely to subsidize plant available soil moisture relative to minor drifts where the majority of snowmelt exits the system before the onset of drought stress. The results in this study also indicate that interactions between soil moisture, evaporative demand, and precipitation thresholds must be considered together to understand the importance of redistributed precipitation on vegetation productivity.

As climate change continues to alter water resource and energy availability in semi-arid ecosystems, understanding the response of vegetation communities to shifting hydroclimatic regimes is essential for developing effective long term management plans for vulnerable species, habitat conservation, and landscape carbon sequestration. We show that the reduction in seasonal hydrological storage in the form of redistributed snow may negatively impact drought sensitive species like aspen. It is also important to note that an increase in temperature has not been incorporated into this study. Thus, the shifts in NPP presented here are simply the result of the presence or absence of a snow water subsidy stemming from redistributed snow accumulated because of the interactions of wind fields with complex topography. While future increases in temperature are not considered in this study, solely considering the redistribution of snow suggests that drifts have historically been an important source of soil moisture to aspen stands located in areas with relatively low precipitation. Nevertheless, it is essential to assess the importance of water resources and soil moisture availability in the context of climate change. While rising temperatures will likely increase the importance of snow water subsidies, growing seasons are also expected to lengthen with increased evaporative demand during the summer months, thereby exacerbating drought conditions. In addition to changes in growing season conditions, future shifts in the amount of incoming precipitation should also be considered. Increases in total precipitation under climate change could potentially buffer spring soil moisture deficits caused by reductions in redistributed precipitation. For example, spring rains during years like 1995 and 2015 were sufficient to offset the loss of snow water subsidies experienced under a homogenous precipitation layer. Currently, the response of vegetation communities

to ongoing shifts in precipitation and in particular, redistributed precipitation regimes, phenology, and increased drought severity remains an important area of uncertainty in semi-arid ecosystems.

2.5 Conclusions

While no significant changes in the amount of total precipitation have been documented within the RCEW over the past decades (Nayak et al, 2010, Seyfried et al., 2011) the ratio of total annual snow to rain is expected to continue to decrease. Although the total amount of precipitation may remain consistent, any shifts in the timing and phase of precipitation could have profound impacts on vegetation communities depending on their location along a shifting precipitation phase gradient. The results presented here indicate that the redistribution of precipitation only prolongs soil moisture availability at sites that both receive 500 mm or less annual precipitation and have high soil moisture storage capacity. Unlike the driest site, increased soil moisture inputs resulting from drifting had little effect on growing season soil moisture availability at sites receiving higher annual precipitation amounts. Considering the heterogeneous distribution of available resources is essential when assessing the vulnerability of ecosystems to climate change. Studies not accounting for the presence of heterogeneous soil moisture subsidies or soil characteristics may underestimate carbon fluxes in landscapes where the distribution of water resources is complex and shapes the distribution of key vegetation communities. This is an important consideration to make when identifying sensitive species or regions that may be susceptible to changes in temperature and precipitation. Therefore, future management of vulnerable aspen communities should consider climate change induced shifts in precipitation phase and the role hydrological refugia plays in maintaining ecosystem resilience.

Acknowledgments

We thank the Reynolds Creek Critical Zone Observatory staff for assistance in the field. Financial support for this research was provided by the McIntire-Stennis cooperative forestry research program (PL87-788) and by the Department of the Interior Northwest Climate Science Center (NW CSC) through a cooperative agreement no. G14AP00153 from the United States Geological Survey (USGS).

References:

- Allen, C. D., Macalady, A. K., Chenchouni, H., Bachelet, D., McDowell, N., Vennetier, M., Kitsberger, T., Rigling, A., Breshears, D.D., Hogg, E.H., et al. 2010. A global overview of drought and heat-induced tree mortality reveals emerging climate change risks for forests. *Forest Ecology and Management*. 259: 660–684.
- Anderegg, L. D. L., Anderegg, W. R. L., Abatzoglou, J., Hausladen, A. M., & Berry, J. A. 2013. Drought characteristics' role in widespread aspen forest mortality across Colorado, USA. *Global Change Biology*. 19: 1526-1537.
- Barbour, M.G., Berg, N.H., Kittel T.G., Kunz, M.E. 1991. Snowpack and the Distribution of a Major Vegetation Ecotone in the Sierra Nevada of California. *Journal of Biogeography*. 18: 141-149.
- Blankinship, J. C., Meadows, M. W., Lucas, R. G., Hart, S. C. 2014. Snowmelt timing alters shallow but not deep soil moisture in the Sierra Nevada. *Water Resources Research*. 50: 2108–2123.
- Boisvenue, C., & Running, S. W. 2010. Simulations show decreasing carbon stocks and potential for carbon emissions in Rocky Mountain forests over the next century. *Ecological Applications*. 20: 1302–1319.
- Burke, I.C., Reiners, W.A. and Olson, R.K. 1989. Topographic control of vegetation in a mountain big sagebrush steppe. *Plant Ecology*. 84: 77-86.
- Chauvin, G. M., Flerchinger, G. N., Link, T. E., Marks, D., Winstral, A. H., & Seyfried, M. S. 2011. Long-term water balance and conceptual model of a semi-arid mountainous catchment. *Journal of Hydrology*. 400: 133–143.
- Churkina, G., Tenhunen, J., Thornton, P., Falge, E. M., Elbers, J. a., Erhard, M., et al. 2003. Analyzing the Ecosystem Carbon Dynamics of Four European Coniferous Forests Using a Biogeochemistry Model. *Ecosystems*. 6: 168–184.
- Clifford, M. J., Royer, P. D., Cobb, N. S., Breshears, D. D., & Ford, P. L. 2013. Precipitation thresholds and drought-induced tree die-off: insights from patterns of *Pinus edulis* mortality along an environmental stress gradient. *The New Phytologist*. 200: 413–421.
- DeByle, N.,B. 1985. Wildlife. In: DeByle NV, Winokur RP (eds) Aspen: ecology and management in the western United States. General Technical Report RM-119. USDA Forest Service, Rocky Mountain Forest and Range Experiment Station, Fort Collins. 135–152.
- Donovan, L. A., Linton, M. J., & Richards, J. H. 2001. Predawn plant water potential does not necessarily equilibrate with soil water potential under well-watered conditions. *Oecologia*. 129: 328–335.

- Ewers, B. E., Oren, R., Johnsen, K. H., & Landsberg, J. J. 2001. Estimating maximum mean canopy stomatal conductance for use in models. *Canadian Journal of Forest Research*. 31: 198–207.
- Finzel, J.A., Seyfried, M.S., Wertz, M.A., & Launchbaugh, K.L. 2015. Simulation of long-term soil water dynamics at Reynolds Creek, Idaho: implications for rangeland productivity. *Ecohydrology*. 9: 673-687.
- Flerchinger, G.N., Cooley, C.L., Hanson, C.L., & Seyfried, M.S. 1998. A uniform versus an aggregated water balance of a semi-arid watershed. *Hydrological Processes*. 12:331-342.
- Flerchinger, G.N. and Cooley, K.R. 2000. A ten-year water balance of a mountainous semi-arid watershed. *Journal of Hydrology*. 237: 86-89.
- Fracheboud, Y., Luquez, V., Björkén, L., Sjödin, A., Tuominen, H., & Jansson, S. 2009. The control of autumn senescence in European aspen. *Plant Physiology*, 149: 1982–1991.
- Gower, S. T., Vogel, J. G., Norman, M., Kucharik, C. J., & Steele, S. J. 1997. Carbon distribution and aboveground net primary production in aspen, jack pine, and black spruce stands in Saskatchewan and Manitoba, Canada. *Journal of Geophysical Research*. 102: 29–41.
- Gower, S. T., Krankina, O., Olson, R. J., Apps, M., & Linder, S. 2001. Net primary production and carbon allocation patterns of boreal forest ecosystems. *Ecological Applications*. 11: 1395–1411.
- Griffis-Kyle, K.L. and Beier, P. 2003. Small isolated aspen stands enrich bird communities in southwestern ponderosa pine forests. *Biological Conservation*. 100: 375-385.
- Huang, M., Barbour, S. L., Elshorbagy, A., Zettl, J., & Si, B. C. 2013. Effects of Variably Layered Coarse Textured Soils on Plant Available Water and Forest Productivity. *Procedia Environmental Sciences*. 19: 148–157.
- Kapnick, S., & Hall, A. 2011. Causes of recent changes in western North American snowpack. *Climate Dynamics*. 38: 1885–1899.
- Keyser, A.R., Kimball, J.S., Nemani, R.R., and Running, S.W. 2000. Simulating the effects of climate change on the carbon balance of high-latitude forests. *Global Change Biology*. 6: 185-195.
- Kizito, F., Campbell, C. S., Campbell, G. S., Cobos, D. R., Teare, B. L., Carter, B., & Hopmans, J. W. 2008. Frequency, electrical conductivity and temperature analysis of a low-cost capacitance soil moisture sensor. *Journal of Hydrology*. 352: 367-378.

- Kuhn, T.J., Safford, H.D., Jones, B.E. and Tate, K.W. 2011. Aspen (*Populus tremuloides*) stands and their contribution to plant diversity in a semiarid coniferous landscape. *Plant Ecology*. 212: 1451-1463.
- Klos, P. Z., Link, T.E., & Abatzoglou, J.T. 2014. Extent of the rain-snow transition zone in the western U.S. under historic and projected climate. *Geophysical Research Letters*. 41: 4560-4568.
- Kormos, P. R., Marks, D., McNamara, J. P., Marshall, H. P., Winstral, A., & Flores, A. N. 2014. Snow distribution, melt and surface water inputs to the soil in the mountain rain-snow transition zone. *Journal of Hydrology*. 519: 190–204.
- Knowles, N., Dettinger, M.D., Cayan, D.R. 2006. Trends in Snowfall versus Rainfall in the Western United States. *Journal of Climate*. 19: 4545-4559.
- Lenz, K. E., Host, G.E., Roskoski, K., Noormets, A., Sober, A., Karnosky, D.F. 2010. Analysis of a Farquhar-von Caemmerer-Berry leaf-level photosynthetic rate model for *Populus tremuloides* in the context of modeling and measurement limitations. *Environmental pollution*. 158:1015-1022.
- Marks, D., Domingo, J., Susong, D., Link, T., & Garen, D. 1999. A spatially distributed energy balance snowmelt model for application in mountain basins. *Hydrological Processes*. 13: 1935-1959.
- Marks, D. and Winstral, A., 2001. Comparison of snow deposition, the snow cover energy balance, and snowmelt at two sites in a semiarid mountain basin. *Journal of Hydrometeorology*. 2: 213-227.
- Maurer, G. E. and Bowling, D.R. 2014. Seasonal snowpack characteristics influence soil temperature and water content at multiple scales in interior western U.S. mountain ecosystems. *Water Resources Research*. 50: 5216-5234.
- Meier, G. A., Brown, J. F., Eveltizer, R. J., Vogelmann, J. E. 2015. Phenology and climate relationships in aspen (*Populus tremuloides* Michx.) forest and woodland communities of southwestern Colorado. *Ecological Indicators*. 48: 189–197.
- Millar, C. I., Stephenson, N. L., & Stephens, S. L. 2007. Climate change and forests of the future: managing in the face of uncertainty. *Ecological applications*. 17: 2145-2151.
- Mote, P.W., Hamlet, A.F., Clark, M.P., & Lettenmaier, D.P. 2005. Declining Mountain Snowpack in Western North America. *Bulletin of the American Meteorological Society*. 86: 39–49.
- Nayak, A., Marks, D., Chandler, D.G., Seyfried, M., 2010. Long-Term Snow, Climate, and Streamflow Trends at the Reynolds Creek Experimental Watershed, Owyhee Mountains, Idaho, United States. *Water Resources Research*. 46:1-15.

- Nayak, A., Marks, D., Chandler, D., Winstral, A., 2012. Modelling Interannual Variability in Snow-Cover Development and Melt for a Semiarid Mountain Catchment. *Journal of Hydrologic Engineering*. 17:74-84.
- Reba, M., Marks, D., Winstral, A., Link, A., Kumar, M. 2011. Sensitivity of the snowcover energetics in a mountain basin to variations in climate. *Hydrological Processes*. 25: 3312-3321.
- Rohde, A., Bastien, C., & Boerjan, W. 2011. Temperature signals contribute to the timing of photoperiodic growth cessation and bud set in poplar. *Tree physiology*. 31: 472-482.
- Richardson, A. D., Jenkins, J. P., Braswell, B. H., Hollinger, D. Y., Ollinger, S. V., & Smith, M.L. 2007. Use of digital webcam images to track spring green-up in a deciduous broadleaf forest. *Oecologia*. 152:332-334.
- Schneider, C.A., Rasband, W.S., Eliceiri, K.W. 2012. NIH Image to ImageJ: 25 years of image analysis. *Nature Methods*. 9: 671-675.
- Scholander, P. F., Bradstreet, E. D., Hemmingsen, E. A., & Hammel, H. T. 1965. Sap pressure in vascular plants negative hydrostatic pressure can be measured in plants. *Science*. 148: 339-346.
- Seyfried, M. S., Grant, L. E., Marks, D., Winstral, A., & McNamara, J. 2009. Simulated soil water storage effects on streamflow generation in a mountainous snowmelt environment, Idaho, USA. *Vadose Zone*. 10: 858-873.
- Seyfried, M. S., Chandler, D., Marks, D. 2011. Long-Term Soil Moisture Trends Across a 1000-m Elevational Gradient. *Vadose Zone Journal*. 10: 1276-1286.
- Shepperd, W.D., Rogers, P.C., Burton, D., Bartos, D.L., 2006. Ecology, biodiversity, management, and restoration of aspen in the Sierra Nevada, General Technical Report RMRS-GTR-178. Rocky Mountain Research Station, USDA Forest Service, Fort Collins, Colorado, 122 p.
- Smith, T. J., McNamara, J. P., Flores, a. N., Gribb, M. M., Aishlin, P. S., & Benner, S. G. 2011. Small soil storage capacity limits benefit of winter snowpack to upland vegetation. *Hydrological Processes*. 25: 3858-3865.
- Strukelj, M., Brais, S., Quideau, S. A., Angers, V. A., Kebli, H., Drapeau, P., & Oh, S. W. 2013. Chemical transformations in downed logs and snags of mixed boreal species during decomposition. *Canadian Journal of Forest Research*. 43: 785-798.
- Tai, X., Mackay, D.S., Anderegg, W.R., Sperry, J.S. and Brooks, P.D., 2016. Plant hydraulics improves and topography mediates prediction of aspen mortality in southwestern USA. *New Phytologist*. 213: 113-127.

- Thornton, P. E., Hasenauer, H., & White, M. A. 2000. Simultaneous estimation of daily solar radiation and humidity from observed temperature and precipitation: an application over complex terrain in Austria. *Agricultural and Forest Meteorology*. 104: 255-271.
- Thornton, P.E., Law, B.E., Gholz, H.L., Clark, K.L., Falge, E., Ellsworth, D.S., Goldstein, A.H., Monson, R.K., Hollinger, D., Falk, M. and Chen, J., 2002. Modeling and measuring the effects of disturbance history and climate on carbon and water budgets in evergreen needleleaf forests. *Agricultural and forest meteorology*. 113:185-222.
- Van der Molen, M. K., Dolman, a. J., Ciais, P., Eglin, T., Gobron, N., Law, B. E., ... Wang, G. 2011. Drought and ecosystem carbon cycling. *Agricultural and Forest Meteorology*. 151: 765–773.
- Vose, J.M., Miniati, C.F., Luce, C.H., Asbjornsen, H., Caldwell, P.V., Campbell, J.L., Grant, G.E., Isaak, D.J., Loheide, S.P. and Sun, G., 2016. Ecohydrological implications of drought for forests in the United States. *Forest Ecology and Management*. In press.
- Waring R.H., and Running S.W. 2007 *Forest Ecosystems: Analysis at Multiple Scales* 3rd Ed. Elsevier/Academic Press, Amsterdam, Boston.
- White, M. A., P. E. Thornton, and S. W. Running. 1997. A continental phenology model for monitoring vegetation responses to interannual climatic variability, *Global Biogeochemical Cycles*. 11: 217–234.
- White, M. A., Thornton, P. E., Running, S. W., & Nemani, R. R. 2000. Parameterization and Sensitivity Analysis of the BIOME–BGC Terrestrial Ecosystem Model: Net Primary Production Controls. *Earth Interactions*. 4: 1–85.
- Winstral, A. and Marks, D. 2002. Simulating wind fields and snow redistribution using terrain based parameters to model snow accumulation and melt over a semi-arid mountain catchment. *Hydrological Processes*. 16: 3585-3603.
- Winstral, A., Marks, D., & Gurney, R. 2013. Simulating wind-affected snow accumulations at catchment to basin scales. *Advances in Water Resources*. 55: 64–79.
- Worrall, J. J., Rehfeldt, G. E., Hamann, A., Hogg, E. H., Marchetti, S. B., Michaelian, M., & Gray, L. K. 2013. Recent declines of *Populus tremuloides* in North America linked to climate. *Forest Ecology and Management*. 299: 35–51.

Tables:**Table 2.1.** Site description and leaf area index (LAI) for Reynolds Mountain East (RME), Johnston Draw (JDW), and Sheep Creek (SC). Standard deviations are indicated in parentheses when applicable.

Parameter	RME	JDW	SC	Method
Elevation (m)	2038	1782	1817	---
Mean annual air temperature (°C)	5.3 (0.7)	8.3 (0.8)	7.1 (0.7)	Simulation period mean
Mean annual uniform precipitation (mm)	947 (176)	665 (99)	422 (115)	Simulation period mean
Sand, silt, clay (%)	25, 70, 5	36, 59, 5	31, 58, 11	Measured
Biome-BGC simulated soil depth (m)	1.2	1.2	1.1	Adjusted
Observed LAI (m ² m ⁻²)	0.9 (0.7)	1.7(1.1)	1.4 (0.9)	Measured
Biome-BGC LAI (m ² m ⁻²)	1.4	1.5	1.6	Simulation period mean

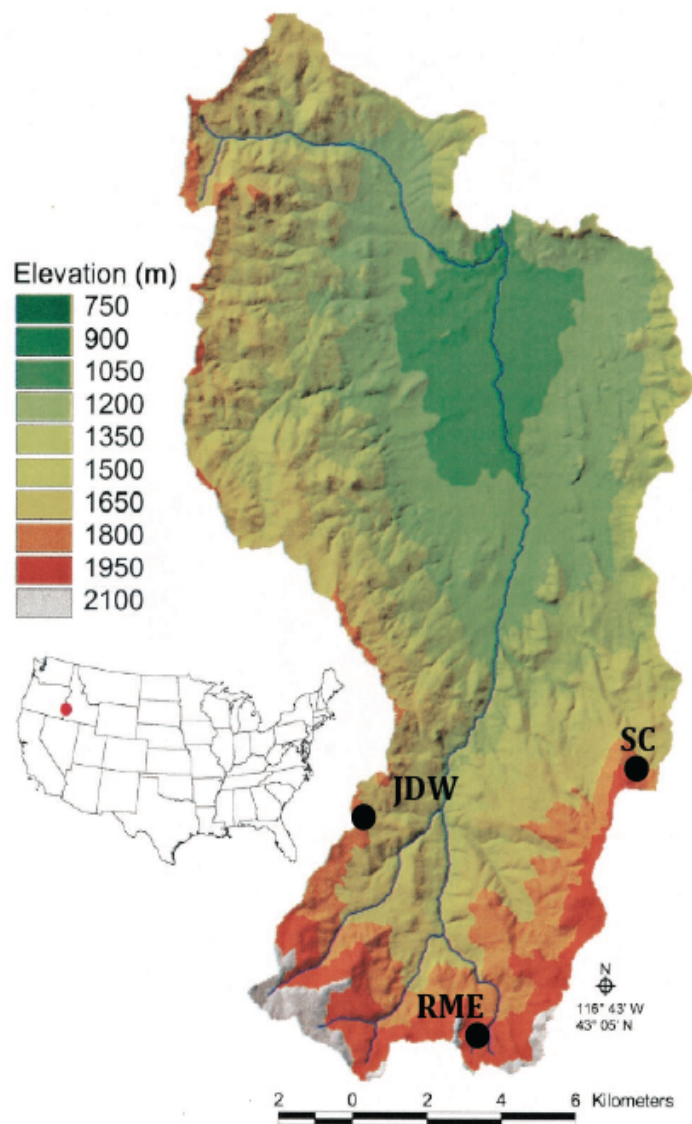
Figures:

Figure 2.1. Locations of aspen stands used for this study within the Reynolds Creek Experimental Watershed and Critical Zone observatory. Johnston Draw (JDW) and Sheep Creek (SC) are mid-elevation sites. Reynolds Mountain East (RME) is the highest elevation site receiving the highest annual precipitation.

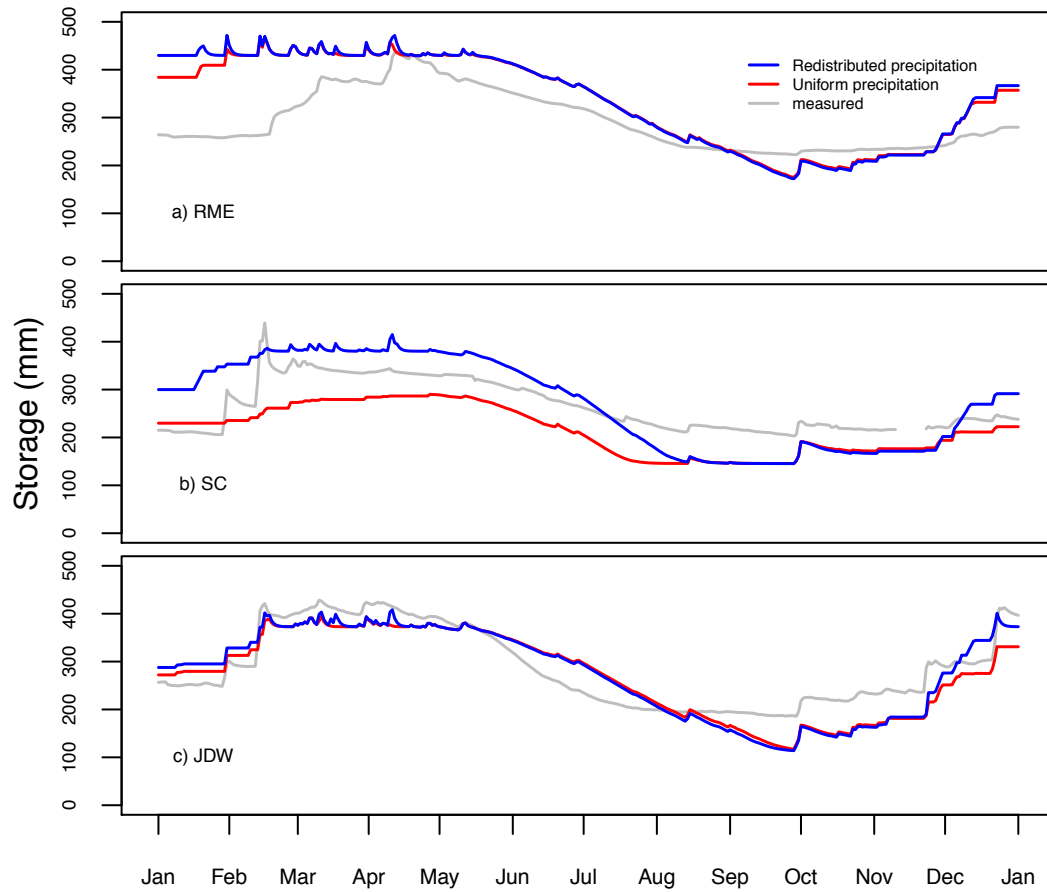


Figure 2.2. Simulated and measured root zone soil moisture storage ($S_{root\,zone}$, mm) at each site for 2014, a year where redistributed snow prolonged available soil moisture at Sheep Creek (SC) (b). Root zone depths are 120 cm for RME (a) and JDW (c), and 110 cm for SC (b). Simulations accounting for snow drifts are depicted in blue, while simulations assuming a uniform precipitation layer are red.

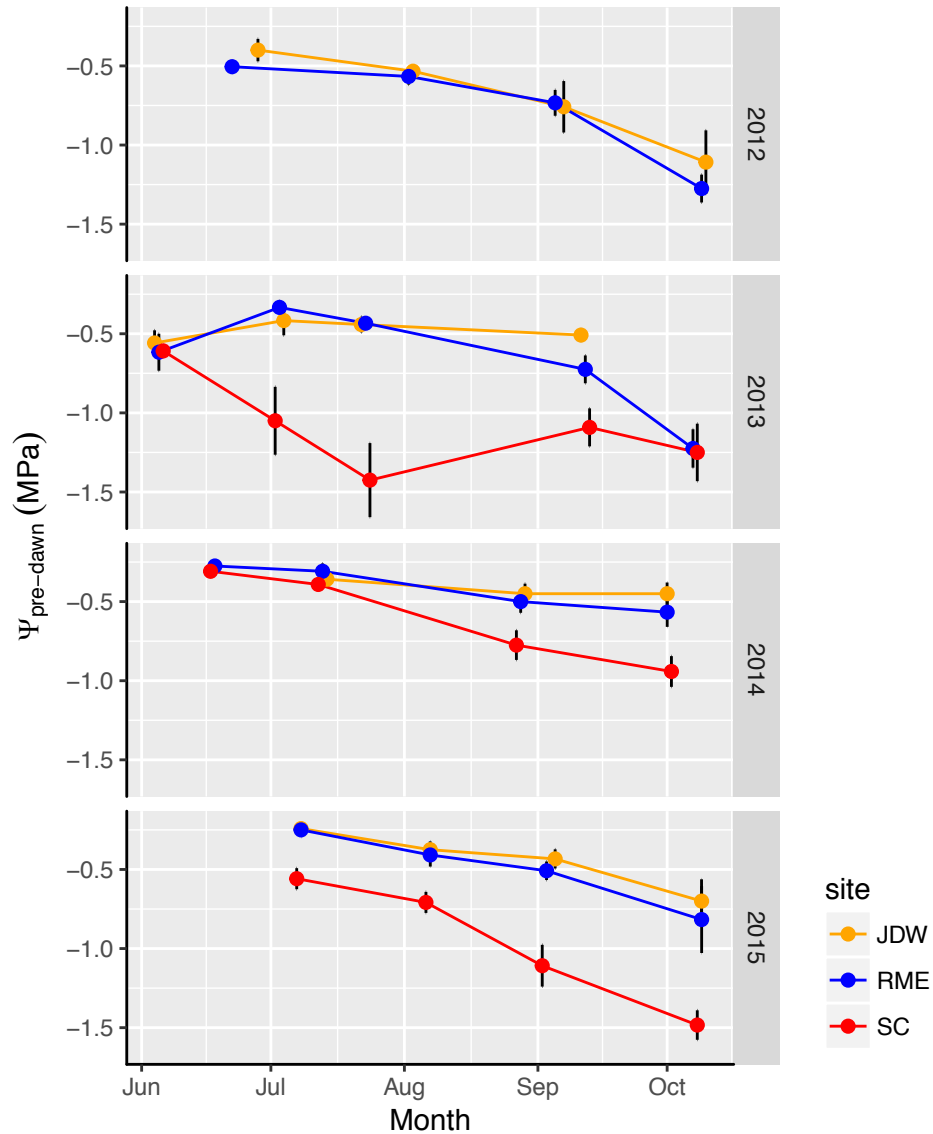


Figure 2.3. Average pre-dawn leaf water potentials ($\Psi_{\text{pre-dawn}}$) taken from three plots at each site across the 2012-2015 growing seasons. Standard deviations are indicated by error bars. Higher precipitation sites Johnston Draw (JDW) and Reynolds Mountain East (RME) typically experience increased growing season $\Psi_{\text{pre-dawn}}$ relative to the dry, mid-elevation site Sheep Creek (SC).

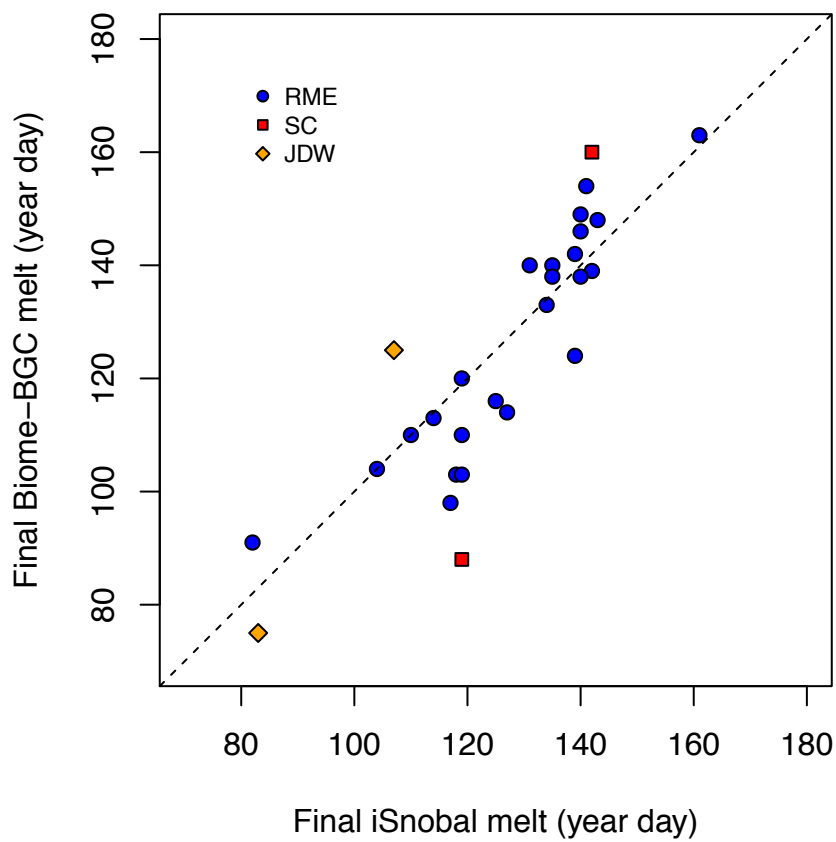


Figure 2.4. Last day of snowpack presence simulated by both Biome-BGC and ISNOBAL. Distribution along the 1:1 line indicates variation between the two models ($R^2=0.76$, $y=1.1148x-15.921$). Sheep Creek (SC) and Johnston Draw (JDW) are mid-elevations sites. Reynolds Mountain East (RME) is the highest elevation site.

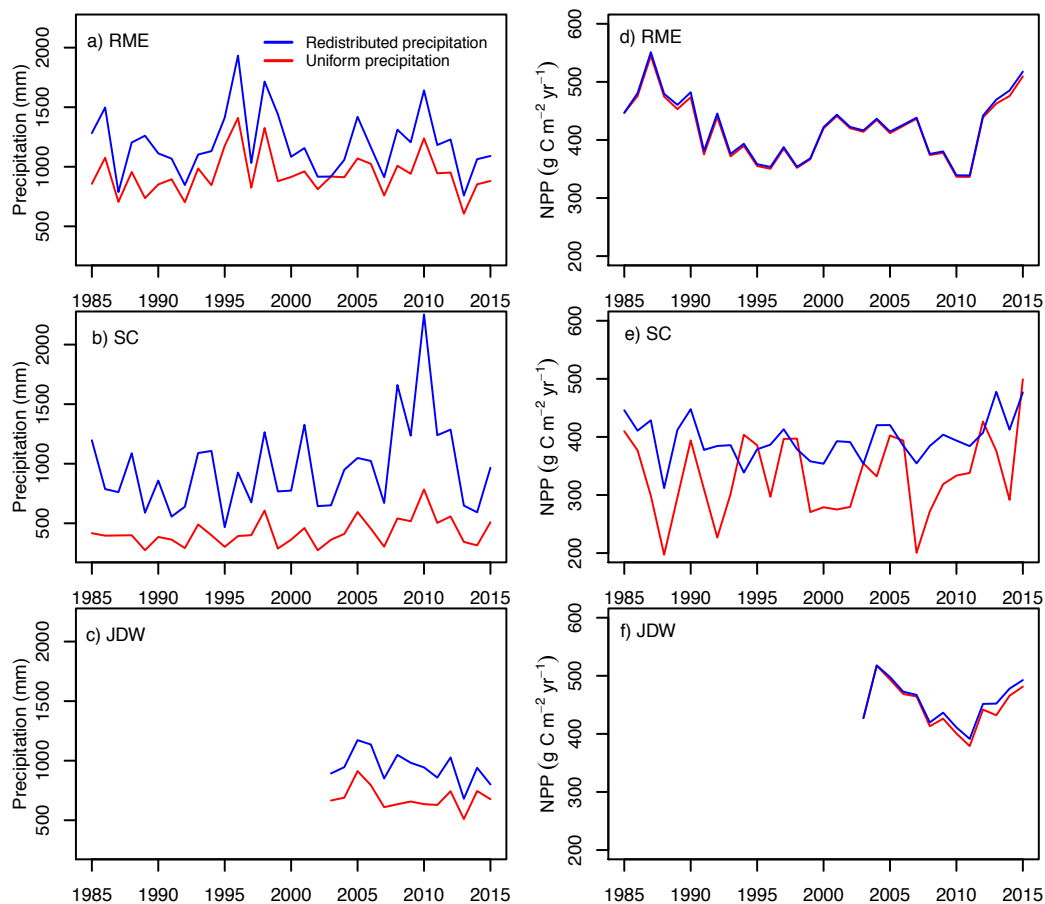


Figure 2.5. Annual precipitation (panels a,b,c) and net primary production (NPP, panels e,d,f) and values for RME and SC from 1985-2015 and JDW from 2003-2015. Precipitation accounting for redistributed snow was determined by applying drift factors to measured precipitation occurring below 0°C . Rates of increase in total annual precipitation indicate variations in the timing and magnitude of precipitation falling as snow.

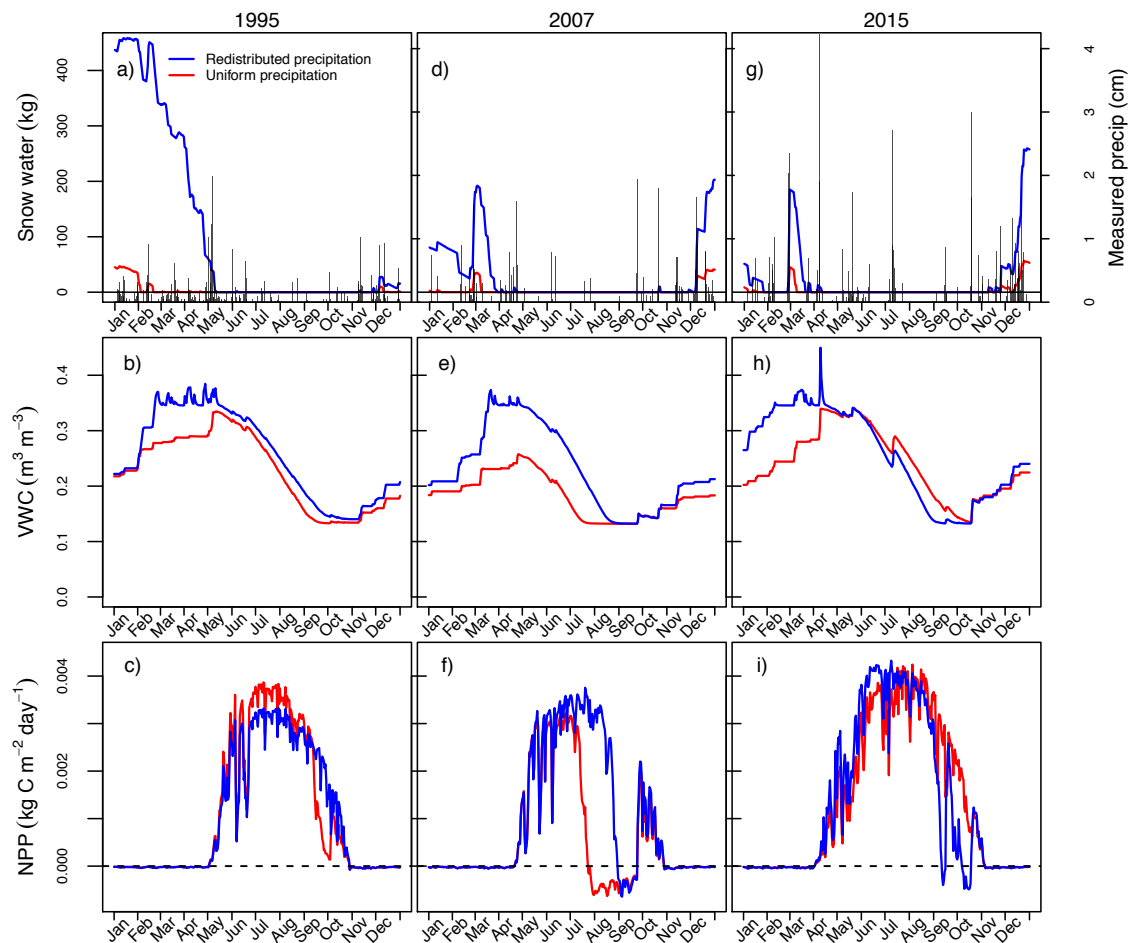


Figure 2.6. Response of snowpack, VWC (θ_v), and net primary productivity (NPP) to redistributed precipitation at Sheep Creek (SC) for 1995 (a,b,c), 2007 (d,e,f), and 2015 (g,h,i). Biome-BGC simulated snow water, VWC, and NPP are shown for both uniform and redistributed precipitation treatments. Measured precipitation events are shown in gray bars (panels a,d,g). Despite large drift formation in 1995, cooler temperatures and spring rains supplemented soil moisture in the absence of a drift. Unlike 1995 and 2015, drift presence was far more important during 2007, a year with above average temperatures and increased growing season evaporative demand. After accounting for the redistribution of snow, NPP remained positive nearly 40 days longer during 2007.

Chapter 3. Growing Season Conditions Mediate the Dependence of Aspen on Redistributed Snow Under Climate Change.

Soderquist B. S.¹, Kavanagh K. L.², Link T. E.¹, Seyfried M. S.³, Strand, E. K.¹

¹ Department of Forest, Rangeland, and Fire Sciences, University of Idaho, Moscow, ID, 83844, USA, ² Department of Ecosystem Science and Management, Texas A&M University, College Station, TX, 77843-2138, USA, ³ USDA Agricultural Research Service, 800 Park Blvd., Plaza IV, Suite 105, Boise, ID, 83712, USA.

Keywords: *Populus tremuloides*, phenology, precipitation, vapor pressure deficit, drought, climate change

Abstract

Precipitation regimes in many snow-dominated semi-arid ecosystems are becoming increasingly dominated by winter rainfall because of climate change. Across these regions, snowpack plays a vital role in the distribution and timing of soil moisture availability. In areas affected by the redistribution of snow, rising temperatures will result in a more spatially uniform distribution of soil moisture, shifts in the timing of soil moisture inputs, advanced spring phenology, and altered growing seasons. Productive and wide ranging tree species like aspen, *Populus tremuloides*, may experience increased vulnerability to drought and mortality resulting from both reduced snowpack and increased evaporative demand during the growing season. To assess the response of aspen to shifts in redistributed snow and warming temperatures we simulated the net primary production (NPP) of aspen stands spanning the rain/snow transition zone in a semi-arid watershed in southwest Idaho, USA. Within the study area, the total amount of precipitation has remained unchanged over the past 50 years, however the percentage of the precipitation falling as snow has declined by approximately 4% per decade at mid-elevation sites. The biogeochemical process model Biome-BGC MuSo was used to simulate aspen NPP at three stands located directly below snowdrifts that provide melt water late into the spring. After adjusting precipitation inputs to account for the redistribution of snow, we assessed climate change impacts on future aspen productivity. Mid-century (RCP 8.5) aspen NPP was simulated using temperature projections from a multi-model average using the Multivariate Adaptive Constructed Analogs (MACA) data set. While climate change simulations indicated a ~25% decrease in

annual NPP for some years, NPP rates for other mid-century years remained relatively unchanged or increased due to intra-annual variations in growing season conditions. During years that experienced large decreases in NPP, the onset of drought stress occurred earlier due to earlier spring soil moisture use and prolonged periods of high summer vapor pressure deficits. These results indicate that vegetation response to decreased snowpack can result in increased drought stress and decreased NPP, although temperature-induced phenological shifts that increase the synchrony of leaf production and incoming precipitation ameliorate this response in some years.

3.1 Introduction

Precipitation regimes, specifically the timing of precipitation, play a key role in the cycling of carbon by vegetation across the landscape (van der Molen et al., 2011). In many arid and semi-arid ecosystems found across the inter-mountain United States, the timing of precipitation is often asynchronous with the timing of peak vegetation growth, transpiration, and subsequent soil moisture use (Lauenroth et al., 2014). The resulting asynchrony between vegetation productivity and incoming precipitation results from a combination of limiting climatological conditions including temperature, incoming radiation, and atmospheric evaporative demand (Boisvenue and Running, 2010). However, precipitation timing and subsequent soil water availability remain one of the primary drivers of vegetation distribution and ecosystem function in many semi-arid systems (Polley et al., 2013, Loik et al., 2014.).

In the interior Pacific Northwest, especially at mid to high elevations, most precipitation occurs as snow during the late fall, winter and early spring. Unlike rain, which is relatively uniformly distributed over the landscape, snow may be preferentially deposited and/or redistributed by wind. This leads to accumulations in snow drifts or losses from scour zones especially in complex terrain. The redistribution of frozen precipitation ultimately influences the spatiotemporal distribution of soil moisture available to vegetation during the growing season when temperature and incoming radiation are less limiting. Following spring snowmelt, growing plants typically experience pronounced periods of drought with little incoming precipitation and high vapor pressure deficits (VPD). These climatological constraints, combined with the heterogeneous distribution of soil moisture across the landscape, play a large role in the current distribution and structure of semi-arid

plant communities across semiarid temperate regions similar to the western United States where soil moisture availability is a primary limiting resource.

In many forested ecosystems, increasing temperatures are altering the climate that has historically played a large role in the current distribution and function of vegetation (Allen et al., 2013). Regions where water availability is the primary control on vegetation productivity may be particularly vulnerable to climate change-induced shifts in temperature and precipitation (Kelly and Goulden, 2008). *Populus tremuloides*, or aspen, is the most widespread tree species in North America (Worrall et al., 2013), with a range encompassing large areas with snow-dominated precipitation regimes. In upland semi-arid ecosystems, aspen frequently inhabit leeward hill slopes where snow drifts form during the winter (Shepperd et al., 2006). These aspen communities may be particularly sensitive to changes in precipitation phase, since snow drifts provide soil water subsidies relative to the more spatially uniform soil water inputs that occur when precipitation occurs as rain.

Recent widespread decline in aspen forests resulting from drought suggest that future changes in precipitation and drought severity will lead to increased aspen vulnerability under continued climate change (Rehfeldt et al., 2009, Anderegg et al., 2013, Worrall et al., 2013). While the timing of precipitation will largely remain concentrated during the winter and early spring across much of aspen's range in the intermountain west, rising temperatures will directly impact precipitation phase (e.g., rain or snow). Shifts in precipitation phase have been documented since the mid- 20th century in numerous areas historically characterized by snow-dominated precipitation regimes (Mote et al., 2005, Nayak et al., 2010). As climate change progresses, the rain/snow transition zone, defined here as the elevation where the winter precipitation phases are mixed, is projected to continue to increase in elevation. This will result in extensive areas throughout the western U.S. shifting from previously snow-dominated precipitation regimes to mixed snow/rain, or rain-dominated precipitation regimes (Klos et al., 2014). In complex terrain, increases in the proportion of rain will directly impact the redistribution of precipitation across the landscape, resulting in a more spatially uniform distribution of precipitation and a reduction in snow drifts. Shifts in precipitation phase will subsequently influence the timing and spatial distribution of surface water input (SWI), or the amount of rain or snow melt entering

the soil profile where it either exits as drainage below the rooting zone or is stored and used by vegetation later in the growing season.

Semi-arid upland aspen communities associated with snow drifts are often highly productive relative to the surrounding, low statured sage brush steppe vegetation growing under drier conditions. However, the response of upland aspen communities to rising temperatures remains uncertain, since shifts in phenology may facilitate increased productivity during periods that were previously temperature limited. Previous studies indicate that aspen stands can benefit from snow water stemming from large snow drifts that form in the winter and persist late into the spring (Chauvin et al., 2011, Soderquist et al., in review). Soderquist et al. (in review) found aspen stands most likely to benefit from the redistribution of precipitation were those growing in areas with higher average annual temperatures ($> \sim 7^{\circ}\text{C}$) and low average annual precipitation ($< \sim 500\text{mm}$). These results indicate that large snow drifts in areas with adequate soil moisture storage allow aspen stands to maintain positive rates of productivity during periods of peak drought. While the previous study (Soderquist et al., in review) indicated that snow drifts are a historically important sources of soil moisture, it only accounts for the presence or absence of a drift resulting from topographic variability and does not address future ecosystem dynamics driven by climate change. However, a more comprehensive understanding of how upland aspen communities will respond to co-occurring shifts in precipitation phase, phenology, and growing season conditions is needed.

Since aspen are a wide ranging and potentially drought sensitive species (Anderegg et al. 2013, Worrall et al., 2013), future shifts in carbon assimilation are useful indicators of both species and ecosystem resilience under changing conditions. This study focuses on two carbon fluxes, net primary and net ecosystem productivity, to assess aspen vulnerability under climate change. Net primary productivity (NPP) is a measure of the total vegetation carbon assimilated after accounting for autotrophic respiration. During periods of prolonged soil moisture limitation or high evaporative demand, respiration costs can exceed photosynthetic gains resulting in lower rates of NPP. Reductions in NPP are useful indicators of increased sensitivity to drought stress, vulnerability to carbon starvation, and declining physiological capacity. For this study, decreased aspen NPP at a given site would suggest reduced aspen viability under future conditions. Alternatively, net ecosystem

production (NEP) is the total ecosystem carbon flux including both autotrophic and heterotrophic respiration. Simulations indicating positive NEP rates describes an ecosystem acting as a carbon sink, whereas negative NEP rates indicate the ecosystem is functioning as a carbon source. In semi-arid ecosystems, both NPP and NEP are closely linked to available soil moisture, precipitation, and drought intensity (Poulter et al., 2014, Ahlstrom et al., 2015, Biederman et al., 2016).

In this study, we incorporate the combined effects of climate change on the redistribution of snow and changes in growing season conditions into simulations of snow drift dependent semi-arid aspen ecosystems. Using the biogeochemical process model Biome-BGC MuSo (Hidy et al., 2016), we simulated snow redistribution, NPP, and NEP at three aspen stands spanning the current rain:snow transition zone under both historical and mid-21st century conditions, where temperature increases are predicted to occur. Under warmer mid-century conditions, we predict that:

- 1) warmer spring temperatures and decreases in redistributed snow will lead to earlier spring leaf flush and increased spring NPP.
- 2) prolonged periods of drought under warmer and drier conditions will lead to reduced total NPP relative to historical conditions.

3.2 Methods

To assess the response of aspen and ecosystem productivity to reductions in redistributed precipitation, we applied historical and mid-21st century hydrometeorological data sets spanning 13-20 years to simulate aspen productivity using Biome BGC Muso (Hidy et al. 2016) at sites currently spanning the snow/rain transition zone where decreases in the proportion of winter precipitation falling as snow are predicted to continue with warming temperatures.

3.2.1. Site description

Simulations were run at three aspen stands spanning middle and high elevations in the Reynolds Creek Critical Zone Observatory and Experimental Watershed (RCEW) located in the Owyhee mountains of southwest ID, USA (Figure 3.1). The climate and precipitation regime of the RCEW is representative of many semi-arid ecosystems in the great basin and interior northwest USA (Nayak et al., 2010) where most precipitation occurs during the winter months, and is snow dominated at middle and high elevations. Winter and

early spring months are typically followed by a growing season characterized by periods where precipitation events are sporadic and average daytime vapor pressure deficits can frequently exceed 3 kPa. Over the period of instrumentation, no significant changes in total annual precipitation have been documented in the RCEW. However, since the monitoring was initiated in 1961, air temperatures in the watershed increased by approximately 2°C, resulting in a decrease in the proportion of snow across the watershed, particularly at lower and middle elevations (Nayak et al. 2010).

Within the RCEW, aspen stands currently span the rain: snow transition zone where the average total annual precipitation ranges from 420 to >950mm. The three sites selected for simulations span this temperature and precipitation phase gradient and include two mid-elevation stands, Sheep Creek (SC) and Johnston Draw (JDW), and a high elevation site, Reynolds Mountain East (RME) (Table 3.1). Each upland aspen stand is located on leeward hillslopes below a single snow drift where redistributed snow supplies soil moisture into the summer months (described in Soderquist et al., in review). Due to complex topography, drifts, and therefore moisture subsidies at each site vary in size. For example, while SC is the site with the lowest average annual precipitation, the interactions of the topography and wind field produces the largest drift (Table 3.2). Study sites at JDW and RME, despite receiving higher amounts of total precipitation, consist of stands located below smaller drifts. Soils at each site are classified as silt and sand loams and extend at least 1m in depth.

3.2.2. *Historical climate*

Historic climatic conditions used for simulations were based on measurements made at meteorological stations neighboring each site. For this study, we used historical climate records spanning 1996-2015 at RME and SC, and 2003-2015 at JDW. These datasets provided daily values of maximum daily temperatures (T_{max}), minimum daily temperatures (T_{min}), relative humidity (RH), and incoming precipitation that were used to develop climate datasets required to run Biome-BGC MuSo (discussed below).

3.2.3. *Climate change projections*

To represent climate change conditions predicted for the mid 21st century, projected temperature increases and changes in relative humidity were applied to historical climate datasets. Downscaled monthly T_{max} and T_{min} for both historic (1985-2005) and mid-century conditions (2046-2065) were obtained from a 20-model ensemble mean of CMIP5 global

climate models (Taylor et al., 2012) using the Multivariate Adaptive Constructed Analogs (MACA) downscaling method (Abatzoglou and Brown, 2012). Monthly temperatures were downscaled to 4 km grid cells based on a continued high CO₂ emissions scenario (RCP 8.5). Changes in T_{max} and T_{min} at each site were determined by the difference between monthly downscaled historic temperatures and projected mid-century temperatures obtained from the MACA data portal. Average monthly T_{max} and T_{min} increases were then applied to measured daily temperatures for the years 1996-2015 at RME and SC and 2003-2015 at JDW. Across much of the western United States, RH is projected to decrease slightly with warming temperatures (Ficklin and Novik, 2017). To account for future decreases in RH, we applied the average annual decrease in RH between downscaled historic (1985-2005) and mid-century projections (2046-2065) predicted by 18 GCMS in the MACA data portal to measured values.

By using identical precipitation inputs before accounting for the redistribution of frozen precipitation, we assume that historical trends in total annual precipitation and inter-annual variability will continue into the mid-21st century. Future shifts in precipitation phase resulting from warming temperatures are projected with much more confidence, whereas changes in regional precipitation amount, intensity, and timing remain more uncertain (IPCC, 2014, Maloney et al., 2014). Once temperature increases were applied to daily climate records, precipitation data for climate change simulations were adjusted to account for the redistribution of frozen precipitation under warmer, mid-century conditions.

3.2.4. Precipitation adjustments

As described in Soderquist et al. (in review), the redistribution of snow is represented in our climate datasets through the application of drift factors calculated from iSnobal simulations of snow redistribution to measured precipitation data. iSnobal is a spatially adapted version of the physically-based, mass- and energy-balance model Snobal that produces spatially-distributed simulations of snow states and fluxes based on climate forcings, vegetation, and topography (Winstral and Marks, 2002, Reba et al., 2011, Winstral et al., 2013). The iSnobal simulations from Reba et al., 2011 (1984-2008 at RME) and Winstral et al., 2013 (2007-2008 at SC and 2006-2007 at JDW) were the primary sources used to adjust the precipitation forcing data applied in Biome-BGC. Each aspen stand simulated by Biome-BGC MuSo lies within or borders iSnobal-simulated catchments.

Simulations of daily snow water equivalent (SWE) from the spatial snow model, (Reba et al., 2011, Winstral et al., 2012), were used along with precipitation measurements to calculate drift factors (DF) using the equation:

$$DF = \frac{\text{Peak simulated SWE (mm)}}{\text{Total measured uniform snow (mm) across drift accumulation period}} \quad (1)$$

where peak simulated SWE is the seasonal maximum SWE extracted from a point in the center of each iSnobal-simulated drift and the drift accumulation period is defined as the period from initial drift formation to peak SWE simulated by iSnobal. For both historical and simulations of future climate projections, the average historic drift factor at each site was used across all simulation years. Annual drift factors were applied to all measured precipitation data occurring below freezing temperatures. For both historic and mid-century simulations, the full drift factor was applied to total daily precipitation if average daytime temperature (T_{daytime}) and average nightly temperature (T_{night}) were $\leq 0^{\circ}\text{C}$. If only T_{daytime} or T_{night} were $\leq 0^{\circ}\text{C}$, a drift factor with a rate of increase 50% less than the full drift factor was applied to total daily precipitation.

3.2.5. Soil moisture storage

Soil moisture was monitored at one to two soil moisture profiles in each stand. In the spring of 2012, soil moisture sensors were installed at RME. Soil moisture sensors (Decagon Devices, Pullman WA) were placed at depths of 10, 30, 60, and 120 cm at two profiles extending from the stand edge to stand interior. Similar soil moisture transects were installed at SC in the spring of 2013, where two profiles extended from the stand edge to stand interior with soil moisture sensors at depths of 10, 30, 70, and 100 cm. Soil moisture at JDW was monitored by a single hydra probe profile (Stevens Water Monitoring Systems, Inc., Portland, OR) located in the center of the aspen stand with sensors at 5, 20, 50, 75, and 88 cm depths.

Volumetric water content (θ , m^3m^{-3}) measured from installed probes was used to calculate soil moisture storage (S , mm) at each site. Total soil storage for the top 100 cm of soil was calculated using the equation:

$$S_{100} = \sum_{i=1}^{i=\text{number of layers}} \theta_i * D_i \quad (2)$$

where θ_i is the volumetric water content of layer i , and D is the depth (mm) of layer i . Due to differences in probe depths, site-specific storage equations were used to calculate S_{100} (Table S2, Appendix 2). Like measured S_{100} , S_{100} simulated by Biome-BGC MuSo was calculated from θ simulated at four depths in the top meter of soil.

3.2.6. *Biome-BGC MuSo model description and parameterization*

Biome-BGC MuSo v 4.0 (where MuSo stands for multilayer soil module, Hidy et al., 2016) is an extended version of the one-dimensional biogeochemical process model Biome-BGC (v4.2, Thornton et al., 2002) that simulates ecosystem processes through daily fluxes of energy, water, carbon, and nitrogen. While Biome-BGC MuSo is still a one-dimensional model, simulations of soil hydrology, plant water uptake, and plant response to drought have been significantly restructured. Among these improvements, changes in the soil sub-routine and calculations of soil moisture limitation are the most significant and relevant for this study. We briefly introduce these changes below, but for a more comprehensive overview of the theoretical basis behind all model modifications see Hidy et al., 2016.

In Biome-BGC v 4.2, soil depth and plant available soil water is constrained by a uniform, single layer soil profile. Biome-BGC MuSo expands this module to include seven, fixed depth soil layers where soil texture is user defined and can vary by layer. These changes provide the basis for a more realistic representation of soil structure, soil hydrology, and plant water uptake in model simulations. Water from rainfall or snowmelt initially infiltrates into the soil, redistributes to the various soil layers, and is either stored within the soil or exits as outflow. Within the soil profile, soil moisture available to plants is constrained by the maximum rooting depth and an empirical root distribution parameter. Soil moisture uptake by roots can be constrained by either decreases in soil water potential or changes in relative soil water content. For this study, changes in soil water content (SWC, m^3m^{-3}) were used to limit plant water uptake. First, to simulate soil moisture availability in an individual soil layer, critical points along the soil water characteristic curve such as saturation (*sat*), field capacity (*fc*), and wilting point (*wp*) are either user-defined or internally calculated using soil texture parameters. Changes in simulated SWC are then used to calculate the normalized soil water content (NSWC) using the equation:

$$NSWC = \frac{SWC - SWC_{wp}}{SWC_{sat} - SWC_{wp}}, \text{ if } SWC_{wp} < SWC$$

$$NSWC = 0, \text{ if } SWC_{wp} \geq SWC$$
(3)

The NSWC is then used to determine the soil moisture stress index (SMSI) for a given layer, a dimensionless value that falls between 0 (maximum drought stress) and 1 (minimum drought stress). Changes in the SMSI across the root zone are subsequently used in calculations of stomatal conductance, soil water transpiration, and drought-related senescence.

For this study, we maintain the original phenology subroutine in Biome-BGC 4.2 where leaf flush and senescence for deciduous vegetation is governed by a combination of soil temperature and photoperiod thresholds. For aspen, differences in phenological simulations between sites and across historical and mid-21st century climate scenarios are driven entirely by changes in air temperature. Onset of spring growth, or leaf flush, is initiated when day length exceeds 10.9 hours and soil temperatures calculated from an eleven-day running average of daily air temperatures exceed critical thresholds. At the end of the growing season, leaf senescence is triggered when either soil temperatures or day length fall below critical thresholds.

Like Biome-BGC 4.2, Biome-BGC MuSo operates on a daily time step and is driven by daily inputs of maximum (T_{max}) and minimum temperature (T_{min}), average daytime temperature ($T_{daytime}$) and vapor pressure deficit (VPD), incoming solar radiation ($W\ m^{-2}$), and day length (s). Historical and adjusted mid-century meteorological datasets (described earlier) provided T_{max} , T_{min} , and average daytime VPD calculated from temperature and relative humidity. To account for the influence of aspect on incoming radiation and day length at each site, day length, $T_{daytime}$, and incoming shortwave radiation were simulated for both historical and mid-21st century climate scenarios using the microclimate model MTCLIM (v. 4.3, Thornton et al., 2000). Biome-BGC MuSo also requires annual inputs of atmospheric CO₂ concentrations for simulations of photosynthesis and gas exchange. Since temperature increases in this study follow RCP 8.5, annual atmospheric CO₂ concentrations (ppm) recommended by the coupled model intercomparison project (CMIP5) for RCP 8.5

were used for both historical (1996-2015) and mid-century (2046-2065) simulations (Meinshausen et al., 2011).

Soil textures were measured at approximately 10cm, 30 cm, 70 cm, and 100cm depths at each site. Average measured values of sand, silt, and clay for each depth were then used to parameterize the seven-layer soil profile defined in Biome-BGC MuSo. Biome-BGC MuSo simulates ecosystem processes for a deciduous broadleaf plant functional type (PFT) specifically parameterized for aspen using ecophysiological data both derived from the literature and measured at each site (Table S1, Appendix 2 but see Soderquist et al., in review for a full description of parameterization methods). Ecophysiological parameter values calculated from field data (i.e. percent leaf nitrogen in Rubisco) were allowed to vary within one standard deviation of the total mean of all sites. Soil moisture uptake parameters were also adjusted by site based on observed soil moisture trends (Table S1, Appendix 2). For this study, site and ecophysiological parameters are assumed to remain constant for both historical and mid-century simulations.

3.2.7. Simulation and analysis

Historical simulations of S_{100} and LAI were compared to field observations, measured at each site. To assess the response of aspen to warming temperatures and reduced snowpack, simulation outputs at both annual and daily time steps were analyzed. Trends in snowpack, growing season length, NPP, and NEP were compared between historical and mid-century scenarios to determine the impact of increased temperatures on fluxes of plant and ecosystem carbon. Periods of snow residence were defined by the number of days where simulated snowpack was present. Shifts in phenology were determined by dates of spring leaf flush and senescence given by daily simulations of leaf area index (LAI). Drought impacts on carbon uptake were determined by shifts in simulated annual and daily NPP and annual NEP. For this study, the impacts of disturbances such as fire or harvest on ecosystem carbon are not considered.

3.3 Results

3.3.1. Temperature increases

Due to the relatively close proximity of the sites, average monthly increases between downscaled historical and projected mid-century temperatures were nearly identical. Average monthly increases in T_{max} and T_{min} across all 20 GCMs varied, with average monthly

temperatures increases ranging from 2.5°C to 3.7°C with the largest increases occurring during the summer months (Figure 3.2). Similar to the findings of Ficklin and Novik (2017), decreases in average annual relative humidity were modest, and a small, absolute decrease (3.0%) was applied to historic measurements to represent slightly drier mid-century conditions.

Since incoming precipitation was unchanged between historic and mid-century datasets, precipitation timing and periods of peak evaporative demand maintained the same inter-annual variability across all simulated cases. However, after applying mid-century changes in temperature and relative humidity, average day time VPD increased at all sites, with the largest increases occurring in the summer months during periods of high temperature and low relative humidity (Figs. S1, S2, Appendix 2). During warmer than average years (e.g. 2015), historical average daytime VPD occasionally exceeded 3.0 kPa at all sites. However, mid-century daytime VPD often exceeded 3.5 kPa and remained above 2.5 kPa for extended periods of time. Warmer, mid-elevation sites continued to have higher growing season VPD relative to RME, however all sites experienced VPD levels where stomatal conductance is increasingly limited (i.e. where VPD limitation ranges from 1.0 to 4.2 kPa, as parameterized for aspen, Table S1, Appendix 2).

3.3.2. Precipitation shifts

Since drift factors, annual uniform precipitation, and precipitation frequency are assumed constant between historic and mid-century simulations, temperature shifts were the sole driver of changing snowpack and precipitation redistribution. Under warmer mid-century conditions, there was less precipitation falling as snow, therefore there was less snow to redistribute and precipitation was more spatially uniform (Table 3.2, Figure 3.3). Reductions in effective precipitation inputs at aspen stands after accounting for the redistribution of snow were the smallest at the high elevation site, RME, where average annual redistributed precipitation was reduced from 1200mm to 1100mm (8%). Reductions were larger at mid-elevation sites, where average annual redistributed precipitation (effective precipitation) was reduced from 944 to 810 mm at JDW (14%) and 1030 to 757mm at SC (27%). Since these shifts in annual precipitation include both rain and snow during the cold season and precipitation occurring across the entire year, large changes in winter precipitation phase can be somewhat masked by annual precipitation averages. For

example, the maximum amount of snow water held in drifts could be severely reduced at all sites, such as the years where maximum SWE decreased by as much 85, 91, and 80% at SC, JDW, and RME, respectively.

Shifts in precipitation redistribution by mid-century are a function of both drift factors and increasing temperatures. By mid-century, historically stable snowdrifts at mid-elevation sites were reduced in size and became increasingly transitory (Figures 3.7, 3.8). Due to fewer snow events, average snow residence time across the winter and spring months was reduced by 63 days at RME, 73 days at SC, and 80 days at JDW under mid-century conditions (Table 3.2). While the accumulation of snow became increasingly temperature sensitive, drift size also played a role in seasonal snowpack. By mid-century, sites with larger drifts (SC), still experienced increasingly transitory snowpacks with larger melt rates, however precipitation accumulation occurring below freezing temperatures remained larger than that of RME and JDW where drifts were smaller.

3.3.3. Soil moisture storage

Simulated and measured spring S_{100} during 2014 and 2015 peaked between 350- 400 mm (Figure 3.4). Following spring leaf flush, storage was reduced across the growing season to an annual minimum of ~200mm. Simulated growing season S_{100} was slightly overestimated at wetter sites like JDW and RME, however simulations of peak and growing season S_{100} were in close agreement at SC. Following leaf senescence in October, simulated S_{100} increased faster than measured rates, and fall rains and winter snowfall recharged soil moisture more quickly in Biome-BGC MuSo simulations. Overestimates of soil recharge rates were most prominent at SC and RME (Figure 3.4). The more rapid simulated recharge rates are likely the result of the spatially heterogeneous soil wetting that occurs with snow redistribution and is not accounted for with the way snow drifts are simulated in Biome-BGC MuSo.

3.3.4. Phenology and growing season shifts

Compared to RME, where historic growing season length averaged 172 days (SD= 14.6, n=20 simulation years), growing season lengths were slightly longer at mid-elevation sites, averaging 178 (SD= 16.0, n= 20 simulation years) and 182 days (SD= 18.5, n=13 simulation years) at SC and JDW, respectively. Average maximum LAI simulated by Biome-BGC MuSo across the simulation period fell within the measured range at each site

(Table 3.1). Warmer, mid-21st century conditions resulted in longer growing seasons where average growing season length increased approximately two weeks at all sites (Table 3.2). Growing season shifts were primarily the result of warmer spring conditions and advanced dates of spring leaf flush. Increases in growing season length, as measured by simulated LAI, indicate that warming temperatures can lead to increasing synchrony between periods of leaf production and incoming precipitation (Figure 3.5). Leaf senescence remained unchanged by warming soil temperatures and continued to be controlled by decreasing photoperiod length that typically results in complete leaf senescence by late October (Figures 3.5, 3.7, 3.8).

3.3.5. Carbon fluxes: Net primary production (NPP)

At warmer, mid-elevation sites, average annual NPP rates across simulation treatments decreased under mid-century conditions (15 and 12% at SC and JDW, respectively, Figure 3.6, Table 3.2). Compared to JDW, where NPP was consistently lower by mid-century, the response of NPP to warming at SC showed more variability. At SC, mid-century NPP rates either matched those under historical conditions or decreased by over 25% for certain years (Figure 3.6). Unlike the warmer and drier mid-elevation sites, RME showed the opposite response, where mid-century NPP tended to remain at or above historic levels for most simulated years (average of 4.5 % increase across simulation period, Figure 3.6, Table 3.2).

At all sites, warming-induced shifts in daily NPP were highly sensitive to increased evaporative demand. However, the interactions between decreased snow pack and fluctuations in growing season conditions were most pronounced at SC, where fluctuations in annual NPP are driven by sub-annual interactions between spring productivity, growing season VPD, and precipitation. At SC, years with low growing season precipitation (e.g. 2012) didn't necessarily have the largest reductions in NPP under warming conditions. For 2012 specifically, historical spring NPP was limited by temperature but continued to maintain stable rates across the driest portions of the growing season until temperature and day-length became limiting, ultimately resulting in leaf senescence (Figure 3.7). Under mid-century conditions, earlier leaf flush led to significantly increased spring NPP and LAI relative to historic conditions, however increased evaporative demand and stomata closure later in the summer (~ late June) forces LAI development and NPP to fall below historic

rates that continue at reduced levels for most of the growing season (Figures 3.5a, 3.7). Despite warming, drought induced reductions in LAI and stomatal conductance under mid-century conditions result in reduced soil moisture use, ultimately leading to similar trends in root zone soil water content between climate scenarios.

Under mid-century conditions, increased summer precipitation does little to counteract the impacts of limiting evaporative demand on NPP. For example, 2015 was the warmest year of historical and mid-21st century simulations, however, more precipitation fell during the summer months compared to 2012 (Figures S1, S2, Appendix 2). 2015 had the highest NPP rates under historical conditions (Figure 3.6) even though mid-elevation sites experienced a severely reduced snowpack followed by a growing season where average daytime VPD exceeded 3.0 kPa (Figure 3.8). Following mid-century temperature increases, both mid-elevation sites experienced earlier spring leaf flush. However, mid-century spring NPP rates at SC and JDW sites were only slightly higher compared to those experienced under historical conditions (Figure 3.8). By mid-July, increased evaporative demand led to rapid reductions in stomatal conductance and NPP that persisted across the remainder of the growing season. In total, annual NPP at SC during 2015 was reduced by 27% under mid-21st century conditions indicating that warmer spring conditions and growing season precipitation are not always sufficient to compensate for drought induced reductions in productivity occurring later in the growing season.

3.3.6. Carbon fluxes: Net ecosystem production (NEP)

Despite warming temperatures, increased evaporative demand, and variations in vegetation response, simulations across all sites indicate that aspen stands will remain carbon sinks under mid-21st century conditions (Figure 3.9, Table 3.2). However, trends varied by site, where average NEP rates across historic and mid-21st century simulation periods decreased at RME (27.0 to 19.4 g C m⁻² yr⁻¹), increased at SC (-1.1 to 21.7 g C m⁻² yr⁻¹), and remained unchanged at JDW (31.9 to 33.1 g C m⁻² yr⁻¹). Like NPP, the largest shifts in NEP were observed at SC, where historical years characterized by cool temperatures and large amounts of snow accumulation (e.g 2008-2011) were often strong carbon sources (Figure 3.9). Under mid-21st century conditions, NEP for these years was much closer to being carbon neutral. Under mid-21st century conditions, warming did lead to reduced NEP for certain years. However, even with significant reductions in snow pack and

increases in VPD by mid-century (e.g. 2015/2065), NEP remained positive indicating some resilience in the carbon sink, even at mid-elevation sites.

3.4 Discussion

3.4.1. Temperature and snowpack

The temperature increases projected in this study represent a scenario where atmospheric CO₂ concentrations continue to increase at unmitigated rates. While these projections are relatively short term, even with immediate reductions in CO₂ emissions, we expect temperatures to continue increasing at their current rate in the coming decades (IPCC, 2014). Across the intermountain United States, semi-arid ecosystems spanning the rain/snow transition zone will very likely experience significant decreases in the amount of precipitation falling as snow by the mid 21st century. In areas where rising temperatures lead to increased winter rain and preclude the redistribution of precipitation, continued asynchrony between incoming precipitation and periods of vegetation growth may intensify periods of drought stress and ecosystem vulnerability.

Future decreases in winter precipitation falling as snow will likely result in an increasingly uniform spatial distribution of precipitation, hence changing the spatial and temporal distribution and timing of surface water input (SWI) across the landscape. In areas where precipitation regimes are dominated by snow, drifts that have historically held large amounts of SWE long into the growing season will become more sensitive to warming winter and spring temperatures, ultimately leading to increased melt rates and decreased snow residence time. While no sites in this study became 100% rain dominated by the mid-21st century, any soil moisture subsidies stemming specifically from the redistribution of snow were greatly reduced. Although we assume that drift factors calculated based on historic conditions will remain the same by mid-21st century, future changes in temperature, energy balance, or precipitation may influence the redistribution of precipitation in ways not considered in this analysis. However, studies simulating snowpack decreases at other sites within RCEW project similar declines under the same warming scenarios considered in this study (Niemeyer et al., 2016).

3.4.2. Phenological shifts

Advances in the timing of spring leaf flush resulting from warmer spring temperatures are expected since aspen phenology can be particularly sensitive to warming

temperatures and decreased snowpack (Meier et al., 2015). These results indicate that the average growing season for aspen in the RCEW may be increased by nearly two weeks by the middle of the 21st century. Our simulations additionally suggest that, at least in the case of aspen, phenological plasticity can play an important role in resilience to climate change, where warming temperatures allow vegetation to shift periods of productivity to align with more favorable conditions with more frequent precipitation and reduced evaporative demand. Similar increases in ecosystem productivity with increasing spring temperatures and longer growing seasons have been documented in boreal aspen stands (Kljun et al., 2006). However, it is important to note that, in this study we assume the relationships between phenological processes, chilling requirements, soil temperature, and radiation described by Biome-BGC MuSo will remain constant with warming temperatures. With these assumptions in mind, the results presented here conservatively depict phenological shifts where the physiological relationships between aspen phenology and temperature remain fixed between historic and mid-21st century conditions.

Warming and the subsequent shift of growing seasons earlier into the spring have two potential implications for ecosystem function. First, periods of vegetation productivity may become increasingly aligned with the timing of incoming precipitation (Figure 3.5). As periods of increased productivity and incoming precipitation become more synchronous, early season growth will likely become less limited by soil moisture and increased evaporative demand. However, advances in the timing of productivity must also be balanced with the second implication, where soil moisture or evaporative demand may limit aspen NPP later in the growing season (Richardson et al., 2010, Richardson et al., 2013). Increases in canopy development and carbon assimilation rates during the spring that outpace respiratory losses occurring later in the summer have been documented in temperate forests in the eastern United States where total growing season length is increasing with earlier springs and later autumns (Keenan et al., 2014). Our simulations suggest that, in semi-arid regions with winter dominated precipitation regimes, warming-induced phenological shifts earlier into the spring will become increasingly important to deciduous tree species like aspen, where periods of productivity have historically been largely asynchronous to periods of incoming precipitation and low evaporative demand.

3.4.3. *Aspen and ecosystem productivity*

At mid-elevation sites, earlier canopy development and increased NPP during the spring can play an important role in offsetting decreased productivity occurring during the driest periods of the growing season. However, at high elevations, where growing seasons have historically been limited by cooler temperatures and snowpack, aspen stands may experience increased NPP rates since higher total precipitation and lower evaporative demand buffer drought severity. While simulated NPP and NEP rates indicate that all sites continue to remain carbon sinks in the future, increasing sensitivity to evaporative demand and decreasing NPP at mid-elevation sites suggest that the ideal range of aspen in semi-arid Mediterranean climates where snow redistribution is an important hydrological process will contract as the climate continues to warm.

Although environmental conditions will become more limiting at lower elevations in the RCEW, the physiological and ecological mechanisms potentially driving future range shifts remain uncertain. Anderegg and HilleRisLambers (2016) show that species can utilize different strategies when avoiding drought stress along an aridity gradient. For aspen specifically, they show an increasing prevalence in morphological traits preventing hydraulic failure with increasing aridity. Aspen in the RCEW span a similar aridity gradient and may benefit from plasticity in traits controlling hydraulic function and water use. While hydraulic vulnerability is not considered in Biome-BGC MuSo, these simulations indicate that continued rates of carbon assimilation under mid-century conditions may allow aspen to maintain consistently positive NPP rates even under increasingly severe drought. Continued positive NPP rates indicate that aspen may have some flexibility to allocate resources that increase resilience against future mortality events resulting from limiting carbon resources.

Historically, aspen in RCEW have been able to remain consistently productive across a wide range of climatic conditions. When extended to mid-century climate conditions, these simulations indicate aspen ecosystems can continue to maintain relatively high rates of productivity. While previous studies have connected widespread aspen decline to prolonged periods of drought (Anderegg et al., 2013, Worrall et al., 2013), the results presented here suggest that aspen stands in this study currently exist in areas of locally increased hydrologic storage that are somewhat resilient to rising temperatures. Although the presence of snowdrifts has historically provided additional soil moisture to the driest

site, SC (Soderquist et al., in review), the capacity of both aspen to shift timing of growth and soils to store SWI stemming from winter and spring precipitation will play an increasingly important role in the ability of these stands to maintain current NPP rates during extremely warm years with little to no drift formation.

The simulations presented here provide insight into several of the ways upland aspen communities function under a changing climate. However, changes in precipitation phase and redistribution regimes are only a few of many factors that need to be considered when predicting the response of vegetation to climate change. When compared to simulations that only account for the presence or absence of snow drifts (Soderquist et al., in review), we see that shifts in the timing of spring growth and productivity under climate change can partially counter balance the impacts of an increasing spatial uniformity of precipitation. These results indicate that aspen's deciduous leaf habit may play an increasingly important role in their ability to utilize soil moisture across the growing season while at the same time moderating their exposure to prolonged periods of stress through leaf senescence and dormancy in the fall.

3.5 Conclusions

As temperatures and drought severity increase, so will the vulnerability of many semi-arid upland plant communities. Identifying and understanding the processes that enhance vegetation resilience is of utmost concern to managers with limited resources (Luce et al., 2016). For upland aspen stands growing below snow drifts, future decreases in redistributed precipitation and warmer growing season conditions resulted in decreased NPP at mid-elevation sites. Under mid-21st century conditions, simulations across the growing season generally showed that:

- 1) warmer spring conditions and increased synchrony with incoming precipitation led to earlier leaf flush and increased spring NPP rates in aspen stands

- 2) At drier sites, increased spring NPP under mid-century conditions was frequently outpaced by losses in productivity resulting from increasing VPD and drought severity later in the summer.

These results suggest that aspen stands spanning a shifting precipitation phase gradient have some capacity to adjust and remain productive under significant temperature and precipitation changes. While temperature directly influences both the precipitation phase and

intensity of evaporative demand, plants can utilize numerous strategies to adjust and moderate their function in the face of severe drought. Since the linkages between carbon flux and water dynamics are so strong in semi-arid environments like those encountered in the RCEW, future work should prioritize understanding how vegetation communities, comprised of species with diverse morphological and phenological traits, will respond to future changes in precipitation phase, drought intensity, and growing season length.

Acknowledgements

We thank the Reynolds Creek Critical Zone Observatory staff for assistance in the field. Financial support for this research was provided by the Department of the Interior Northwest Climate Science Center (NW CSC) through a cooperative agreement no. G14AP00153 from the United States Geological Survey (USGS).

References:

- Ahlström, A., Raupach, M.R., Schurgers, G., Smith, B., Arneeth, A., Jung, M., Reichstein, M., Canadell, J.G., Friedlingstein, P., Jain, A.K. and Kato, E. 2015. The dominant role of semi-arid ecosystems in the trend and variability of the land CO₂ sink. *Science*. 348: 895-899.
- Allen, C. D., Macalady, A. K., Chenchouni, H., Bachelet, D., McDowell, N., Vennetier, M., ... Cobb, N. 2010. A global overview of drought and heat-induced tree mortality reveals emerging climate change risks for forests. *Forest Ecology and Management*. 259: 660–684.
- Anderegg, L. D. L. and HilleRisLambers, J. 2016. Drought stress limits the geographic ranges of two tree species via different physiological mechanisms. *Global Change Biology*. 22: 1029–1045.
- Anderegg, W. R. L., Plavcová, L., Anderegg, L. D. L., Hacke, U. G., Berry, J. a, & Field, C. B. 2013. Drought's legacy: multiyear hydraulic deterioration underlies widespread aspen forest die-off and portends increased future risk. *Global Change Biology*. 19: 1188–96.
- Abatzoglou, J. T., & Brown, T. J. 2012. A comparison of statistical downscaling methods suited for wildfire applications. *International Journal of Climatology*. 32: 772–780.
- Biederman, J. A., Scott, R. L., Goulden, M. L., Vargas, R., Litvak, M. E., Kolb, T. E., Yepez, E. A., Oechel, W. C., Blanken, P. D., Bell, T. W., Garatuza-Payan, J., Maurer, G. E., Dore, S. & Burns, S. P. 2016. Terrestrial carbon balance in a drier world: the effects of water availability in southwestern North America. *Global Change Biology*. 22: 1867–1879.
- Berndt, H.W. and Gibbons, R.D. 1958. Root distribution of some native trees and understory plants growing on three sites within ponderosa pine watersheds in Colorado. Rocky Mountain Forest and Range Experiment Station.
- Boisvenue, C., & Running, S. W. 2010. Simulations show decreasing carbon stocks and potential for carbon emissions in Rocky Mountain forests over the next century. *Ecological Applications : A Publication of the Ecological Society of America*. 20: 1302–19.
- Chauvin, G. M., Flerchinger, G. N., Link, T. E., Marks, D., Winstral, a. H., & Seyfried, M. S. 2011. Long-term water balance and conceptual model of a semi-arid mountainous catchment. *Journal of Hydrology*. 400: 133–143.
- Ficklin, D. L., & Novick, K. A. 2017. Historic and projected changes in vapor pressure deficit suggest a continental-scale drying of the United States atmosphere. *Journal of Geophysical Research: Atmospheres*. In press.

- Hidy, D., Barcza, Z., Marjanovic, H., Sever, M.Z.O., Dobor, L., Gelybó, G., Fodor, N., Pintér, K., Churkina, G., Running, S. and Thornton, P. 2016. Terrestrial ecosystem process model Biome-BGCMuSo v4. 0: summary of improvements and new modeling possibilities. *Geoscientific Model Development*. 9: 4405-4437.
- Hidy, D., Barcza, Z., Haszpra, L., Churkina, G., Pintér, K. and Nagy, Z. 2012. Development of the Biome-BGC model for simulation of managed herbaceous ecosystems. *Ecological Modelling*. 226: 99-119.
- IPCC, 2014: Climate Change 2014: Synthesis Report. Contribution of Working Groups I, II and III to the Fifth Assessment Report of the Intergovernmental Panel on Climate Change [Core Writing Team, R.K. Pachauri and L.A. Meyer (eds.)]. IPCC, Geneva, Switzerland, 151 pp.
- Izaurrealde, R.C., Thomson, A.M., Morgan, J.A., Fay, P.A., Polley, H.W. and Hatfield, J.L., 2011. Climate impacts on agriculture: implications for forage and rangeland production. *Agronomy Journal*. 103: 371-381.
- Kang, S., Running, S. W., Kimball, J. S., Fagre, D. B., Michaelis, A., Peterson, D. L., ... Hong, S. 2014. Effects of spatial and temporal climatic variability on terrestrial carbon and water fluxes in the Pacific Northwest, USA. *Environmental Modelling & Software*. 51: 228–239.
- Keenan, T.F., Gray, J., Friedl, M.A., Toomey, M., Bohrer, G., Hollinger, D.Y., Munger, J.W., O’Keefe, J., Schmid, H.P., Wing, I.S. and Yang, B., 2014. Net carbon uptake has increased through warming-induced changes in temperate forest phenology. *Nature Climate Change*. 4: 598-604.
- Kelly, A.E. and Goulden, M.L. 2008. Rapid shifts in plant distribution with recent climate change. *Proceedings of the National Academy of Sciences*. 105: 11823-11826.
- Keyser, A.R., Kimball, J.S., Nemani, R.R., and Running, S.W. 2000. Simulating the effects of climate change on the carbon balance of high-latitude forests. *Global Change Biology*. 6: 185-195.
- Kljun, N., Black, T.A., Griffis, T.J., Barr, A.G., Gaumont-Guay, D., Morgenstern, K., McCaughey, J.H. and Nesic, Z., 2007. Response of net ecosystem productivity of three boreal forest stands to drought. *Ecosystems*. 10: 1039-1055.
- Klos, P. Z., Link, T.E., & Abatzoglou, J.T. 2014. Extent of the rain-snow transition zone in the western U.S. under historic and projected climate. *Geophysical Research Letters*. 41: 4560-4568.
- Lauenroth, W.K., Schlaepfer, D.R. and Bradford, J.B., 2014. Ecohydrology of dry regions: storage versus pulse soil water dynamics. *Ecosystems*. 17: 1469-1479.

- Loik, M.E., Breshears, D.D., Lauenroth, W.K. and Belnap, J. 2004. A multi-scale perspective of water pulses in dryland ecosystems: climatology and ecohydrology of the western USA. *Oecologia*. 141: 269-281.
- Luce, C. H., Vose, J. M., Pederson, N., Campbell, J., Millar, C., Kormos, P., & Woods, R. 2016. Contributing factors for drought in United States forest ecosystems under projected future climates and their uncertainty. *Forest Ecology and Management*. 380: 299–308.
- Maloney, E. D., Camargo, S. J., Chang, E., Colle, B., Fu, R., Geil, K. L., ... Zhao, M. 2014. North American climate in CMIP5 experiments: Part III: Assessment of twenty-first-century projections. *Journal of Climate*. 27: 2230–2270.
- Meier, G. a., Brown, J. F., Evelsizer, R. J., & Vogelmann, J. E. 2015. Phenology and climate relationships in aspen (*Populus tremuloides* Michx.) forest and woodland communities of southwestern Colorado. *Ecological Indicators*. 48: 189–197.
- Meinshausen, M., Smith, S. J., Calvin, K., Daniel, J. S., Kainuma, M. L. T., Lamarque, J. F., ... & Thomson, A. G. J. M. V. 2011. The RCP greenhouse gas concentrations and their extensions from 1765 to 2300. *Climatic change*. 109: 213-241.
- Mote, P. W., Hamlet, A. F., Clark, M. P., & Lettenmaier, D. P. 2005. Declining Mountain Snowpack in Western North America*. *Bulletin of the American Meteorological Society*. 86: 39–49.
- Nayak, A., Marks, D., Chandler, D.G., Seyfried, M. 2010. Long-Term Snow, Climate, and Streamflow Trends at the Reynolds Creek Experimental Watershed, Owyhee Mountains, Idaho, United States. *Water Resources Research*. 46:1-15.
- Niemeyer, R. J., Link, T. E., Seyfried, M. S., & Flerchinger, G. N. 2016. Surface water input from snowmelt and rain throughfall in western juniper: potential impacts of climate change and shifts in semi-arid vegetation. *Hydrological Processes*. 30: 3046–3060.
- Polley, H. W., Briske, D. D., Morgan, J. a., Wolter, K., Bailey, D. W., & Brown, J. R. 2013. Climate Change and North American Rangelands: Trends, Projections, and Implications. *Rangeland Ecology & Management*. 66: 493–511.
- Poulter, B., Frank, D., Ciais, P., Myneni, R.B., Andela, N., Bi, J., Broquet, G., Canadell, J.G., Chevallier, F., Liu, Y.Y. and Running, S.W., 2014. Contribution of semi-arid ecosystems to interannual variability of the global carbon cycle. *Nature*. 509: 600-603.
- Reba, M., Marks, D., Winstral, A., Link, A., Kumar, M. 2011. Sensitivity of the snowcover energetics in a mountain basin to variations in climate. *Hydrological Processes*. 25: 3312-3321.

- Rehfeldt, G. E., Ferguson, D. E., & Crookston, N. L. 2009. Aspen, climate, and sudden decline in western USA. *Forest Ecology and Management*. 258: 2353–2364.
- Richardson, A.D., Black, T.A., Ciais, P., Delbart, N., Friedl, M.A., Gobron, N., Hollinger, D.Y., Kutsch, W.L., Longdoz, B., Luysaert, S. and Migliavacca, M., 2010. Influence of spring and autumn phenological transitions on forest ecosystem productivity. *Philosophical Transactions of the Royal Society B: Biological Sciences*. 365: 3227-3246.
- Richardson, A.D., Keenan, T.F., Migliavacca, M., Ryu, Y., Sonnentag, O. and Toomey, M., 2013. Climate change, phenology, and phenological control of vegetation feedbacks to the climate system. *Agricultural and Forest Meteorology*, 169, pp.156-173.
- Shepperd, W.D., Rogers, P.C., Burton, D., Bartos, D.L., 2006. Ecology, biodiversity, management, and restoration of aspen in the Sierra Nevada, General Technical Report RMRS-GTR-178. Rocky Mountain Research Station, USDA Forest Service, Fort Collins, Colorado, 122 p.
- Strukelj, M., Brais, S., Quideau, S. A., Angers, V. A., Kebli, H., Drapeau, P., & Oh, S. W. 2013. Chemical transformations in downed logs and snags of mixed boreal species during decomposition. *Canadian Journal of Forest Research*. 43: 785-798.
- Sucoff, E. 1982. Water relations of the aspens. *University of Minnesota Agricultural Experiment Station. St. Paul*, (Technical Bulletin 338), p.4.
- Taylor, K. E., Stouffer, R. J., & Meehl, G. A. 2012. An overview of CMIP5 and the experiment design. *Bulletin of the American Meteorological Society*. 93: 485–498.
- Thornton, P. E., Hasenauer, H., & White, M. A. 2000. Simultaneous estimation of daily solar radiation and humidity from observed temperature and precipitation: an application over complex terrain in Austria. *Agricultural and Forest Meteorology*. 104: 255-271.
- Thornton, P.E., Law, B.E., Gholz, H.L., Clark, K.L., Falge, E., Ellsworth, D.S., Goldstein, A.H., Monson, R.K., Hollinger, D., Falk, M. and Chen, J. 2002. Modeling and measuring the effects of disturbance history and climate on carbon and water budgets in evergreen needleleaf forests. *Agricultural and forest meteorology*. 113:185-222.
- van der Molen, M. K., Dolman, a. J., Ciais, P., Eglin, T., Gobron, N., Law, B. E., ... Wang, G. 2011. Drought and ecosystem carbon cycling. *Agricultural and Forest Meteorology*. 151: 765–773.
- Winstral, A. and Marks, D. 2002. Simulating wind fields and snow redistribution using terrain based parameters to model snow accumulation and melt over a semi-arid mountain catchment. *Hydrological Processes*. 16: 3585-3603.

- Winstral, A., Marks, D., & Gurney, R. 2013. Simulating wind-affected snow accumulations at catchment to basin scales. *Advances in Water Resources*. 55: 64–79.
- White, M. A., Thornton, P. E., Running, S. W., & Nemani, R. R. 2000. Parameterization and Sensitivity Analysis of the BIOME–BGC Terrestrial Ecosystem Model: Net Primary Production Controls. *Earth Interactions*. 4: 1–85.
- White, M. A., P. E. Thornton, and S. W. Running. 1997. A continental phenology model for monitoring vegetation responses to interannual climatic variability, *Global Biogeochemical Cycles*. 11: 217–234.
- Worrall, J. J., Rehfeldt, G. E., Hamann, A., Hogg, E. H., Marchetti, S. B., Michaelian, M., & Gray, L. K. 2013. Recent declines of *Populus tremuloides* in North America linked to climate. *Forest Ecology and Management*. 299: 35–51.

Tables:**Table 3.1.** Site description and leaf area index (LAI) for Reynolds Mountain East (RME), Johnston Draw (JDW), and Sheep Creek (SC). Standard deviations are indicated in parentheses (n=20 simulation years at SC and RME, 13 simulation years at JDW).

Parameter	RME	JDW	SC	Method
Elevation (m)	2038	1782	1817	---
Mean annual air temperature (°C)	5.3 (0.6)	7.2 (0.8)	7.1 (0.7)	Historical mean
Biome-BGC MuSo maximum rooting depth (m)	1.5	1.5	1.15	Estimated in field
Observed LAI (m ² m ⁻²)	0.9 (0.7)	1.7(1.1)	1.4 (0.9)	Measured
Simulated LAI (m ² m ⁻²)	1.4	1.5	1.6	Historical mean

Table 3.2. Changes in precipitation, snow residence, growing season days, net primary production (NPP), net ecosystem production (NEP) from historical to mid- 21st century conditions. Standard deviations are indicated in parentheses (n= 20 total simulation years at SC and RME, 13 simulation years at JDW). Growing season length is the period of initial leaf flush to complete leaf senescence simulated by Biome-BGC MuSo.

Site	Measured uniform precip (mm)	Historical effective precip (mm)	Mid-century effective precip (mm)	Snow pack residence (days)	Growing season length (days)	NPP (g C m ⁻² yr ⁻¹) (% change)	Proportion C sink years (historical, mid-century)
Sheep Creek (SC)	446 (130)	1030 (412)	757 (321)	-73 (20)	+13 (6)	-15.3	0.50, 0.85
Reynolds Mountain East (RME)	962 (188)	1180 (242)	1109 (227)	-63 (20)	+14 (8)	+4.5	0.85, 0.85
Johnston Draw (JDW)	685 (99)	944 (134)	810 (99)	-80 (22)	+15 (6)	-11.9	0.92, 1.00

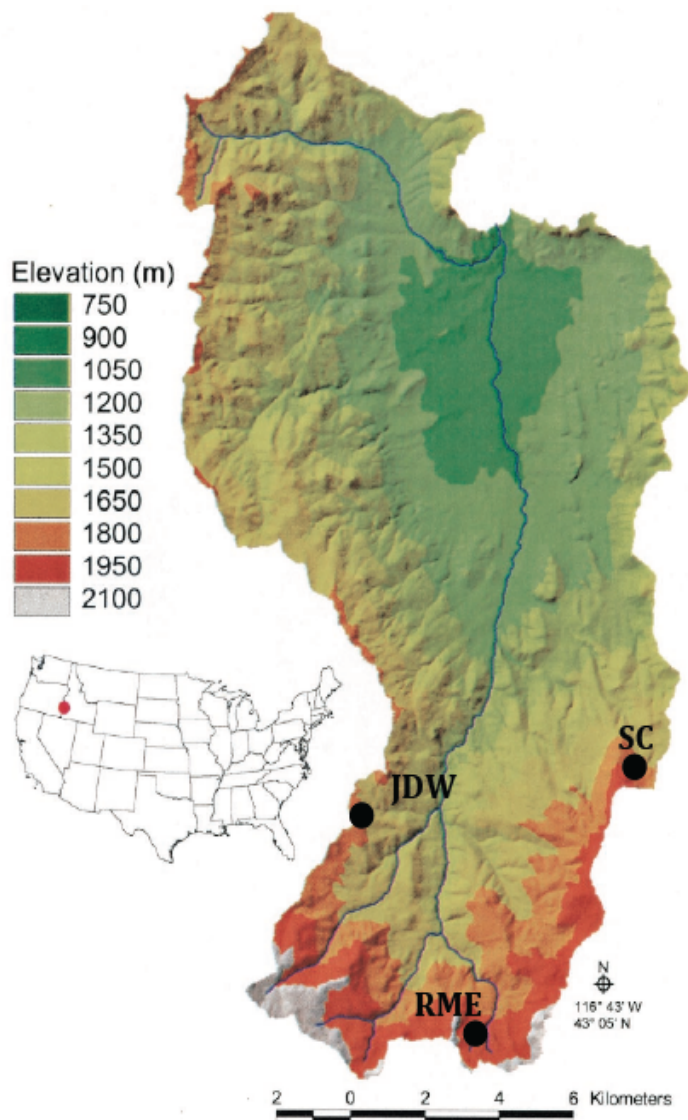
Figures:

Figure 3.1. Aspen stand locations in the Reynolds Creek Critical Zone observatory (RCEW). Johnston Draw (JDW) and Sheep Creek (SC) are warmer, mid-elevation sites, whereas Reynolds Mountain East (RME) is a cooler, high elevation site.

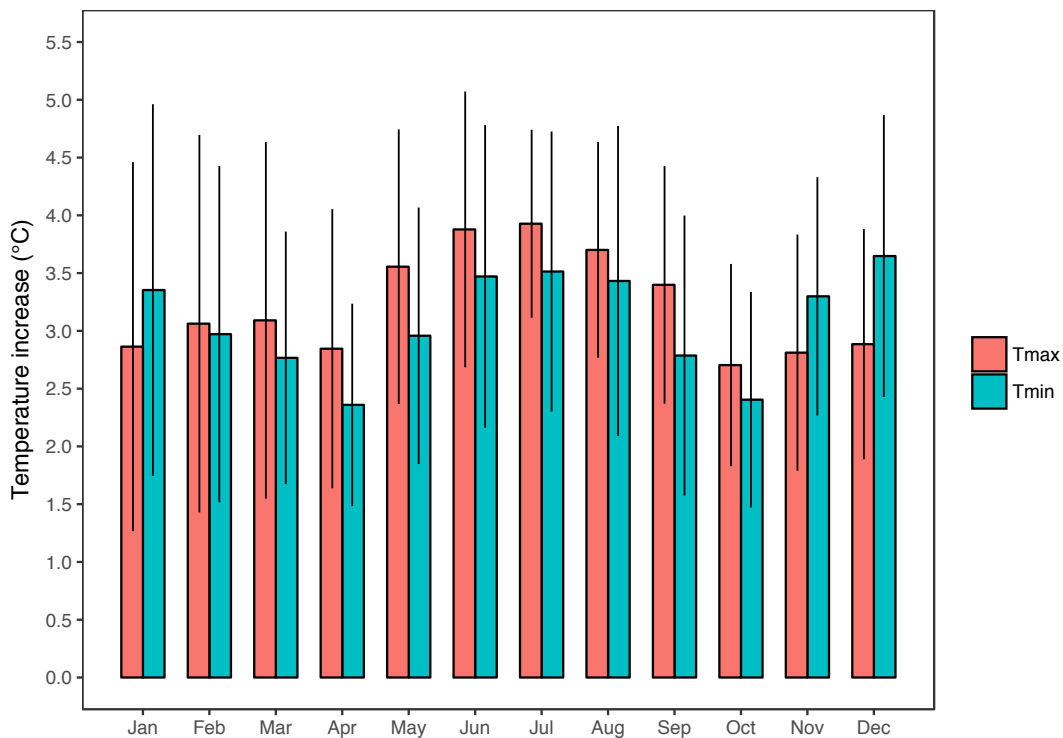


Figure 3.2. Average monthly temperature increases (error bars denote one standard deviation, $n=20$) from historic (1985-2005) and mid-century (2046-2065) projections obtained from 20 GCMs used in the Multivariate Adaptive Constructed Analog (MACA) downscaling method. Average monthly temperature increases were applied to measured T_{max} and T_{min} at each site to create warming scenarios representative of mid-century conditions.

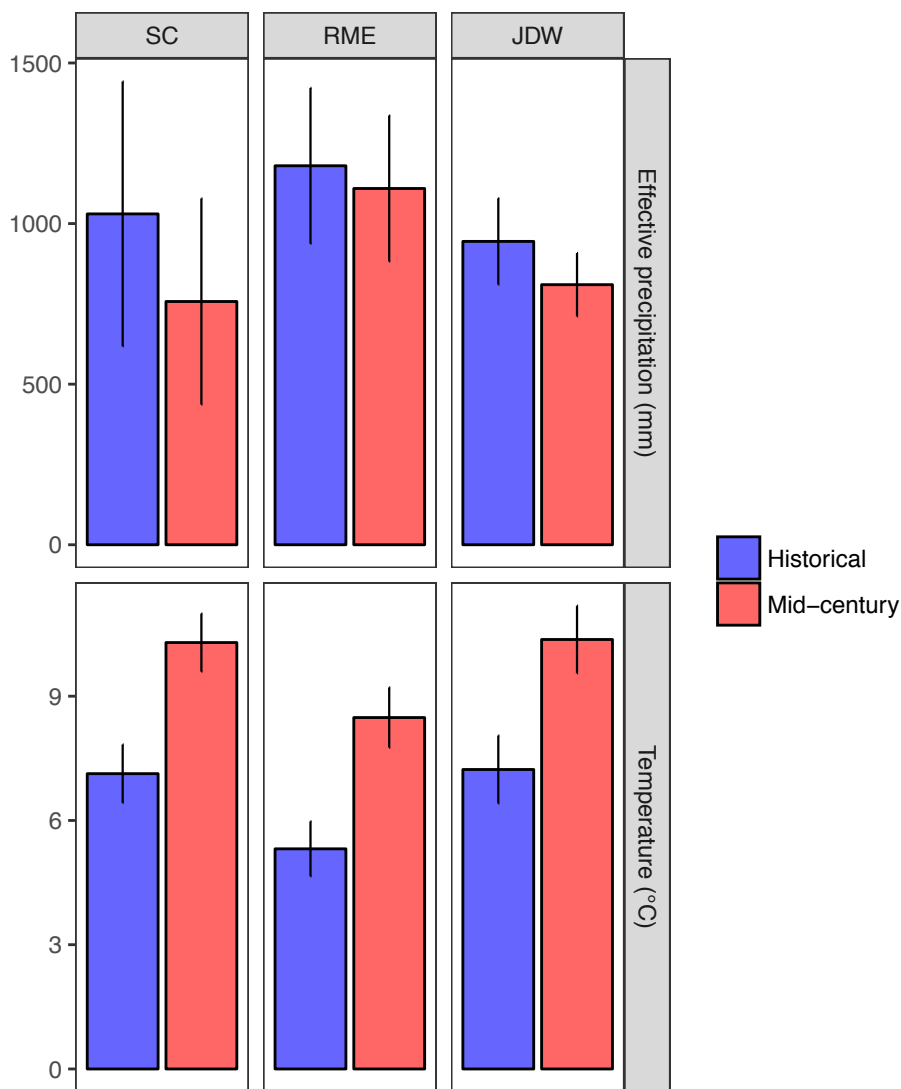


Figure 3.3. Average annual effective precipitation and temperature for each site under historical and mid-century conditions. Effective precipitation is the total amount of annual precipitation after accounting for the redistribution of snow. Error bars represent one standard deviation ($n=20, 20,$ and 13 years for SC, RME, and JDW respectively). Rising temperatures decreases the amount of precipitation falling as snow resulting in decreased redistribution and lower effective precipitation by mid-century. Decreases in redistributed precipitation are largest at the driest site with the largest drift, Sheep Creek (SC), whereas Reynolds Mountain East (RME) and Johnston Draw (JDW) are sites with smaller drifts that experience smaller changes in redistributed precipitation with warming.

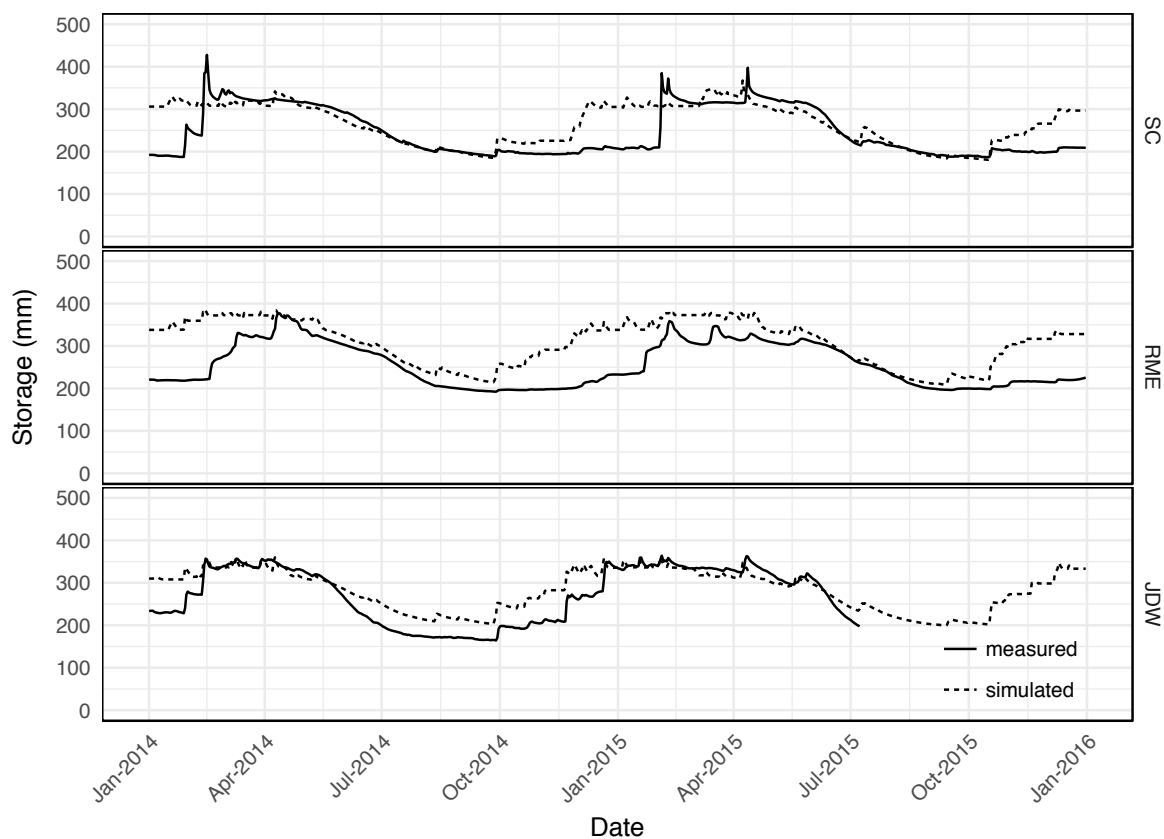


Figure 3.4. Measured and simulated soil storage in the top meter of soil during 2014-2015 at Sheep Creek (SC), Reynolds Mountain East (RME), and Johnston Draw (JDW). Probe failure prevented storage calculations at JDW from July 2015 to January 2016. Across sites, simulated soil moisture storage followed measured growing season trends. However, rates of soil water recharge in the fall and early winter typically were overestimated by Biome-BGC MuSo.

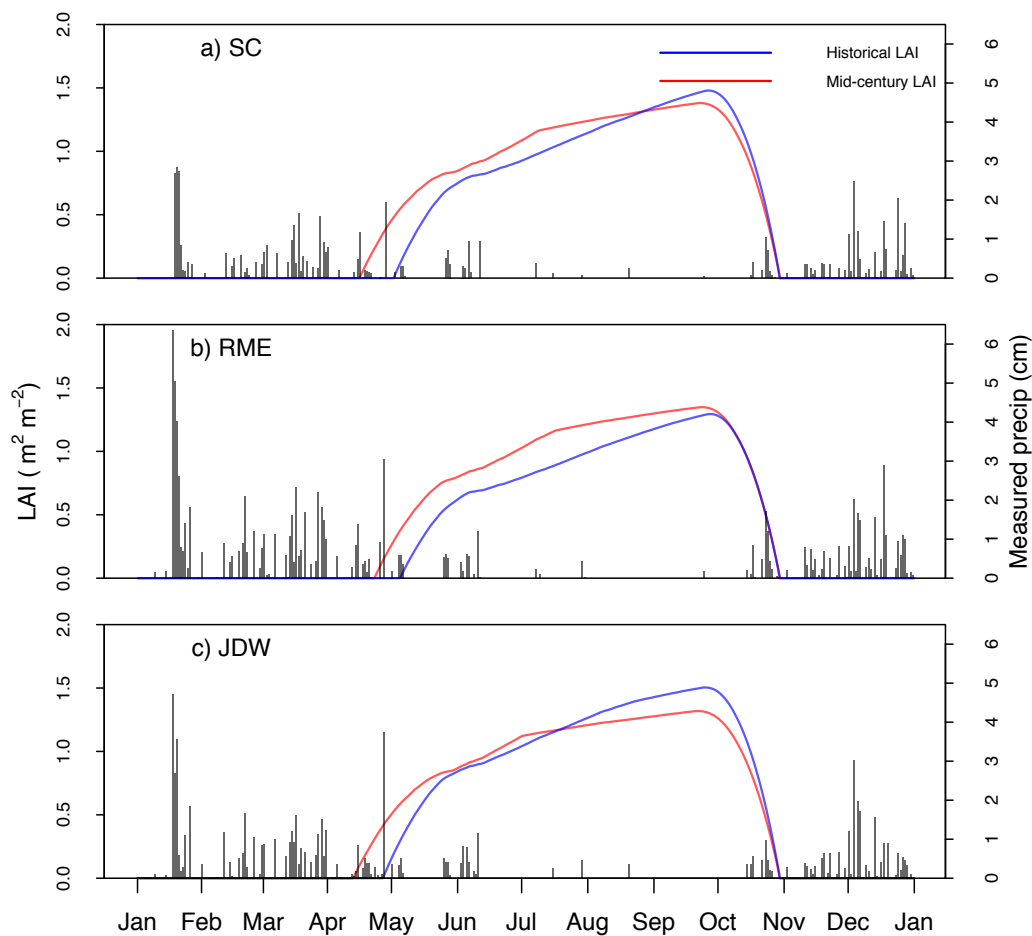


Figure 3.5. Simulated leaf area index (LAI) during 2012 and its associated mid-century year (2062). Warming induced shifts in spring green up increase synchrony between periods of growth with incoming precipitation. However, extended growing season length leads to reductions in maximum LAI at warmer, mid-elevation sites (JDW and SC).

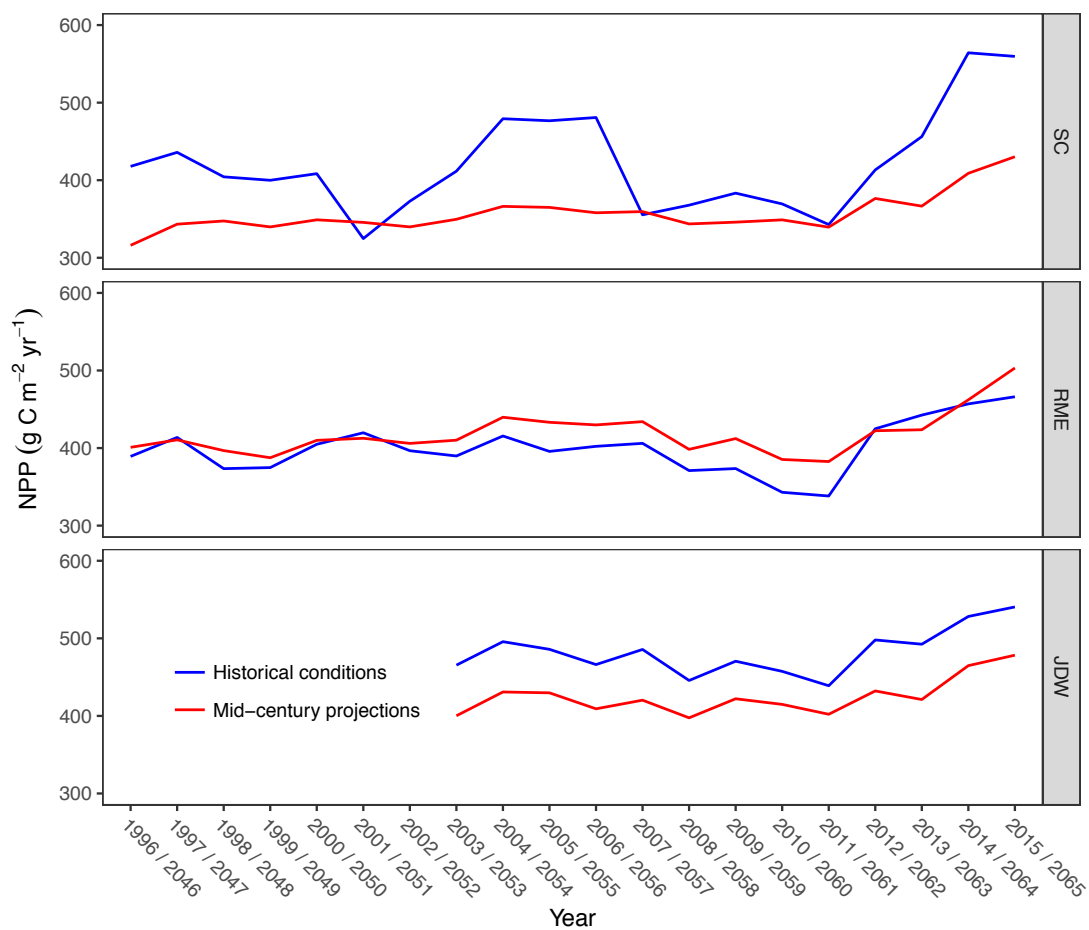


Figure 3.6. Annual net primary productivity (NPP) for historic and mid-century simulations at each site. Simulations span a 20-year period for SC and RME, and a 13-year period for JDW.

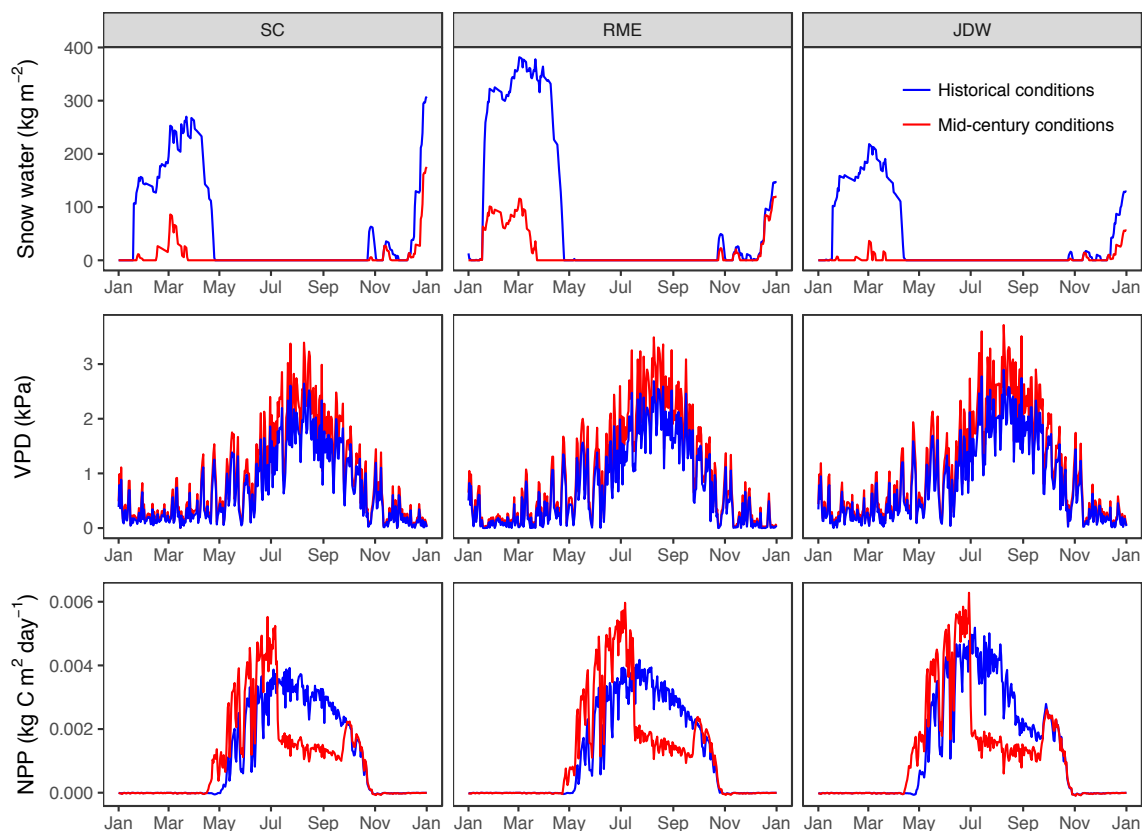


Figure 3.7. Daily simulations of snow water, average daytime vapor pressure deficit (VPD), and net primary production (NPP) for each site during 2012 and its associated mid-century year 2062. Blue lines represent historic conditions, while red lines represent warmer, mid-century conditions. Shifts in phenology with warming temperature are depicted by the onset of positive NPP rates in the spring.

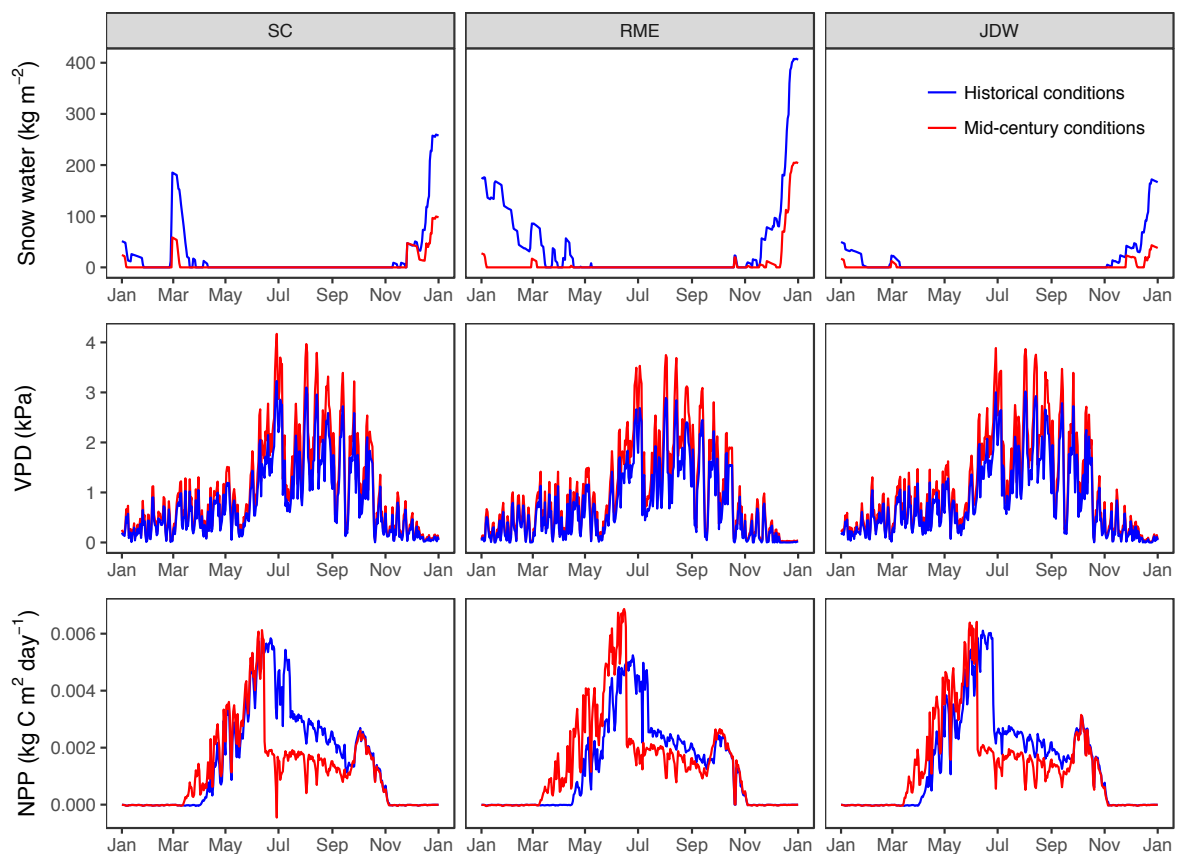


Figure 3.8. Daily simulations of snow water, average daytime vapor pressure deficit (VPD), and net primary production (NPP) for each site during 2015 and its associated mid-century year 2065. Blue lines represent historic conditions, while red lines represent warmer, mid-century conditions.

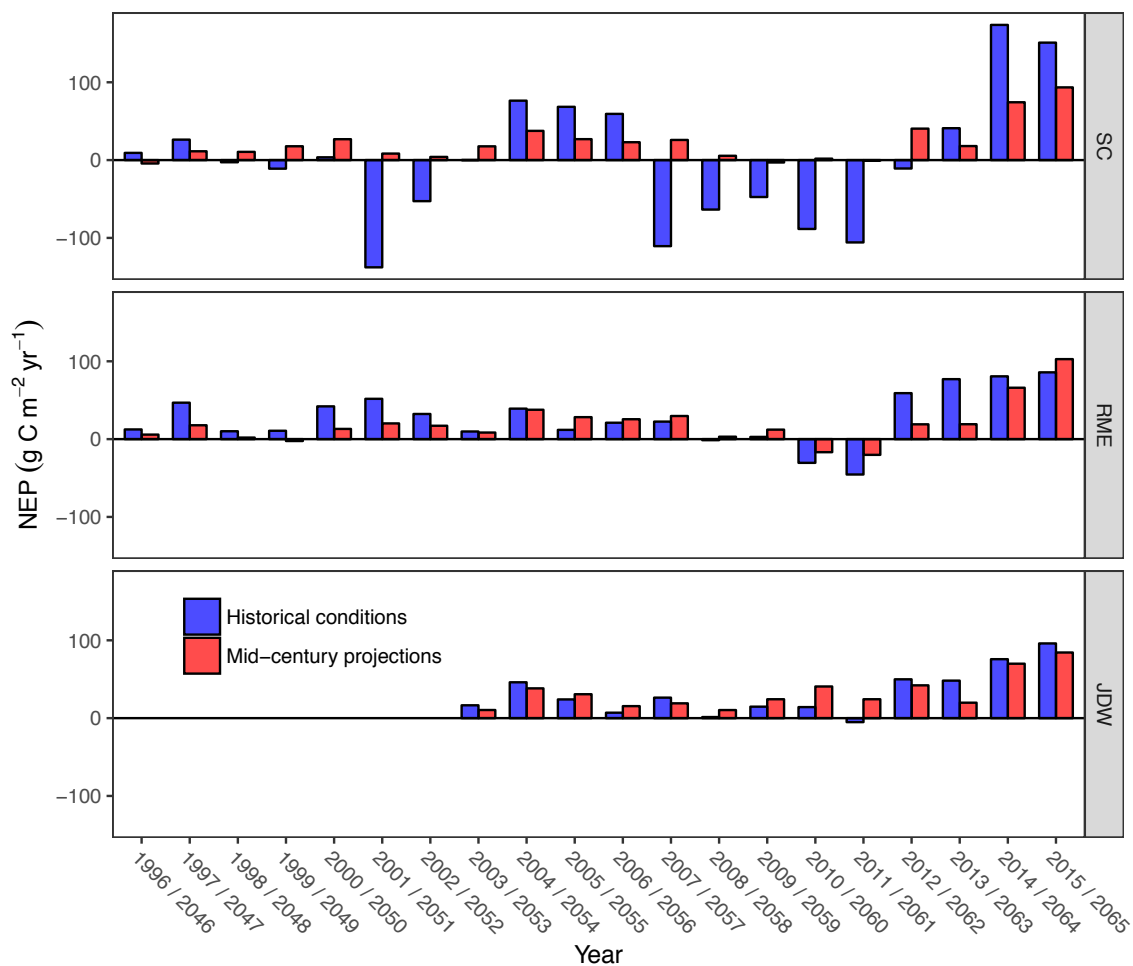


Figure 3.9. Annual simulated net ecosystem productivity (NEP) for each site. Biome-BGC simulations indicate that all sites largely maintain positive rates of ecosystem productivity and remain carbon sinks into the mid 21st century. At SC, historical years with large carbon sinks were typically cooler than average with prolonged snow pack presence.

Chapter 4. Warming temperatures and reductions in redistributed snow differentially impact the simulated productivity of sagebrush steppe vegetation.

Soderquist B. S.¹, Kavanagh K. L.², Strand, E. K.², Link T. E.¹, Seyfried M. S.³

¹ Department of Forest, Rangeland, and Fire Sciences, University of Idaho, Moscow, ID, 83844, USA, ² Department of Ecosystem Science and Management, Texas A&M University, College Station, TX, 77843-2138, USA, ³ USDA Agricultural Research Service, 800 Park Blvd., Plaza IV, Suite 105, Boise, ID, 83712, USA.

Keywords: rangelands, net primary production, snow pack, precipitation, drought stress, climate change

Abstract

Across many sagebrush steppe ecosystems with winter-dominated precipitation regimes, warming temperatures will reduce the proportion of winter precipitation falling as snow. In complex terrain, snow can be redistributed by wind creating snow drifts where effective precipitation and soil moisture can be significantly increased over relatively small spatial scales. Productive sagebrush steppe communities are closely tied to soil moisture availability and are frequently associated with drift zones where snow and deep soils accumulate and spring snowmelt replenishes soil moisture. Increasing temperatures and winter rainfall will simultaneously decrease the amount of redistributed snow and intensify drought experienced by plants currently established within drift zones. We simulated the net primary productivity (NPP) for three species that commonly comprise semi-arid drift zone communities. NPP of aspen (*Populus tremuloides*), mountain big sagebrush (*Artemisia tridentata ssp. vaseyana*), and C3 grasses was simulated at three sites under recent historical and mid-21st century climate scenarios in the Reynolds Creek Critical Zone Observatory and Experimental Watershed (RCEW) located in southwestern, ID, USA. Sites consisted of a single aspen stand and neighboring sagebrush steppe vegetation located within the area of drift formation. After adjusting historical precipitation data to account for both the reduction in the redistribution of precipitation and warmer and drier atmospheric conditions projected for the mid-21st century, simulations indicate that vegetation response to shifts in redistributed snow varies by plant functional type. With increasing temperatures and

reductions in snow cover, aspen stands are likely to experience up to a 25% reduction in annual NPP, while on average, mountain big sagebrush NPP was increased by 24% across all sites relative to historical simulations. Mid-21st century NPP of C3 grasses remained relatively unchanged relative to historical simulations. These results indicate that future shifts in the proportion of precipitation falling as snow vs rain and growing season conditions will differentially impact the suitability of drift zones for currently established vegetation. Future climate induced shifts in species composition in semi-arid drift zone communities may reduce site NPP and the ability of vegetation to sequester atmospheric carbon.

4.1 Introduction

Globally, semi-arid ecosystems significantly contribute to the inter-annual variability of terrestrial carbon fluxes and are highly responsive to the amount and timing of precipitation (Poulter et al., 2014, Ahlstrom et al., 2015). Across much of western North America, the seasonality of precipitation in many semi-arid regions is asynchronous with periods of peak vegetation productivity, where growing seasons are typified by low precipitation and pronounced drought conditions (Lauenroth et al., 2017). The asynchrony between incoming precipitation and plant growth is particularly distinct in many semi-arid sagebrush steppe ecosystems, the most widely distributed semi-arid vegetation type in North America (West, 1983). In these ecosystems, the distribution of vegetation communities is strongly coupled with topography and available soil moisture (Burke et al., 1989, Newman et al., 2006). In colder, mountainous regions, incoming precipitation predominately falls as snow where it can be preferentially deposited in leeward zones, or redistributed across complex terrain by wind (Lehning et al., 2008). The redistribution of snow results in the formation of drift zones behind leeward-facing slopes, around topographic depressions or patches of established vegetation that are sheltered from wind fields (Hiemstra et al., 2002, Winstral et al., 2013). The effective precipitation stored by the snowpack in these sheltered drift zones, defined here as the region occupied by snowdrifts, can be far greater than an otherwise uniform distribution of precipitation (Marks and Winstral, 2001). The heterogeneous distribution of frozen precipitation subsequently influences the surface water input and the spatial distribution of soil water available to vegetation that is exposed to prolonged drought conditions later in the growing season (Seyfried et al., 2009). Thus,

precipitation stored in drifts may act as important subsidy to vegetation communities established in an otherwise moisture limited climate.

Since the mid 20th century, rising temperatures have reduced the amount of precipitation falling as snow across large portions of the interior Pacific Northwest (Knowles et al., 2006, Kapnick and Hall, 2012). Along the rain/snow transition zones, or the elevations where the dominant winter precipitation phase is mixed, rising temperatures will very likely continue to reduce the redistribution of precipitation since future winter precipitation will become increasingly rain dominated (Barnett et al., 2005, Klos et al., 2014). Sagebrush steppe ecosystems are currently distributed across many of these elevations, and frequently span the rain/snow transition zone where precipitation phase (e.g. snow or rain) is highly sensitive to warming temperatures. As climate change continues to reduce the proportion of annual precipitation falling as snow, drift zone plant communities will experience simultaneous shifts in the spatial distribution of soil moisture along with changing growing season conditions. Historically, drift zones have been more mesic relative to exposed ridgetops or south facing slopes (Burke et al., 1989). Species assemblages associated with drifts are characterized by highly productive plant communities relative to the surrounding, water limited vegetation and are often dominated by deciduous tree species like trembling aspen (*Populus tremuloides*), evergreen and semi-evergreen shrub species like mountain big sagebrush (*Artemisia tridentata ssp. vaseyana*), and numerous cool season, perennial grasses utilizing the C3 photosynthetic pathway (e.g. *Calamagrostis rubescens*, *Festuca idahoensis*). Each of these plant functional types have diverse morphological and phenological traits and therefore may respond differently to reductions in redistributed precipitation as precipitation regimes shift from snow to rain dominated.

Since inter-annual precipitation can vary widely in semi-arid environments (Loik et al., 2004), the relatively consistent and predictable redistribution of snow across the landscape may provide an important subsidy to plants currently established in drift zones. Drift zones subsidized by redistributed precipitation may act as zones of localized hydrological storage that benefits both productive aspen and mountain big sagebrush communities which are in turn, important areas of habitat refugia. Upland aspen stands provide critical habitat to many avian and ungulate species (DeByle, 1985, Griffis-Kyle and Beier, 2003) and maintain high rates of biodiversity (Kuhn et al., 2011). Future aspen

mortality may alter understory species diversity and ecosystem function (Anderegg et al., 2012a). Similarly, neighboring pockets of productive mountain big sagebrush communities can act as critical habitat for threatened species such as sage grouse (Connelly et al., 2000, Davies and Bates, 2010). Understanding how climate induced shifts in precipitation phase may impact drift zone vegetation will have important implications for the management of vulnerable habitat refugia and sensitive species into the 21st century.

Mesic aspen and mountain big sagebrush communities may also play an important role in larger, landscape scale carbon fluxes where precipitation timing and soil moisture are dominant controls on ecosystem carbon sequestration (Gilmanov et al., 2006, Kwon et al., 2008, Svejcar et al., 2008). Further understanding is needed to determine how individual species or vegetation with specific traits may respond to simultaneous changes in precipitation phase, growing season length, and increasing atmospheric CO₂ concentrations. Currently, the impacts of an increasingly uniform precipitation on carbon cycling in sagebrush steppe ecosystems remain uncertain. Warming temperatures may reduce the ability of certain species to maintain historic levels of productivity while simultaneously creating conditions that benefit co-occurring species with differing traits. Future climatic shifts favoring certain traits or plant functional types may ultimately facilitate shifts in species composition.

We use a biogeochemical process model to understand how changes in climate and precipitation phase will likely impact vegetation productivity and carbon fluxes for three wide-ranging sagebrush steppe species and plant functional types. This study focuses on two key questions:

- 1) How does net primary productivity (NPP) for different plant functional types shift with warming temperatures and co-occurring decreases in precipitation redistribution that are projected to continue to occur in the near future?

- 2) Will net ecosystem productivity (NEP) for different plant functional types increase or decrease with changes in growing season length and precipitation redistribution?

Across all species and growth forms, we predict increased vegetation productivity with warmer spring conditions and increased synchrony with precipitation. However, the impacts of severe drought later in the growing season may disproportionately affect species with longer growing seasons and/or differing responses to drought severity. We determine

how growing season length and the redistribution of precipitation influence the productivity of aspen, mountain big sagebrush, and C3 grasses under both historical and projected mid-21st century climatic conditions. Finally, we assess how warming temperatures and shifts in precipitation influence fluxes of carbon between the atmosphere and biosphere and discuss the implications that potential shifts in species composition may have on ecosystem carbon dynamics.

4.2 Methods

Historical data sets encompassing a wide range of meteorological conditions provide a unique opportunity to simulate the non-linear processes and interactions between vegetation and climate. To determine the effects of shifting precipitation regimes on drift zone vegetation, we adjusted both historical precipitation and meteorological data to represent increased effective precipitation resulting from the redistribution of snow and warmer, mid-21st century climatic conditions. Phenology, net primary productivity (NPP), and net ecosystem productivity (NEP) were simulated across historical and projected climate scenarios spanning 13-20 years to determine the response of three species currently established in sagebrush steppe drift zones to changing climate conditions.

4.2.1. Site location and description

Simulations were run at three sites within the Reynolds Creek Experimental Watershed and (RCEW) and Critical Zone Observatory located in southwestern, Idaho, USA. Since its designation as an experimental watershed, the United States Department of Agriculture (USDA) has amassed an extensive record of hydrometeorological conditions (Slaughter et al., 2001). Within the watershed, temperatures have increased approximately 2°C over the past 40 years resulting in a large decrease in the proportion of total precipitation falling as snow vs rain (snow:rain) at low and middle elevations (Nayak et al., 2010). Increases in the elevation of the rain/snow transition zone are predicted to continue as temperatures increase (Klos et al., 2014). Across the watershed, soil moisture availability is a key driver of vegetation distribution (Finzel et al., 2015). At mid to high elevations, increasingly mesic conditions facilitate the establishment of mountain big sagebrush, trembling aspen (*Populus tremuloides*, referred to as aspen), C3 grasses (e.g. *Festuca idahoensis*, *Calamagrostis rubescens*) in riparian areas, wet meadows, and along wind-

sheltered slopes where preferential deposition and/or the redistribution of snow forms large snow deposits.

The three sites for this study were previously described in Soderquist et al. (in review) and span the current rain/snow transition zone where precipitation phase is sensitive to temperature changes. Sheep Creek (SC) and Johnston Draw (JDW) are located at middle elevations (~1800m). The highest elevation site, Reynolds Mountain East (RME) is located at the southern end of the watershed (~2100m). Each site consists of a single upland aspen stand surrounded by sagebrush steppe vegetation located on leeward slopes below a single snowdrift that provides melt water into the spring. Measured, uniform precipitation varies by site, with SC and RME being the driest and wettest sites, respectively (Table 4.1). The aeolian soils at each site are at least 1m in depth.

4.2.2. Historical and mid-century climate

4.2.2.1. Historical climate

Daily values of maximum air temperature (T_{\max}), minimum air temperature (T_{\min}), daily precipitation (cm), and average daytime vapor pressure deficit (VPD) used to run Biome-BGC MuSo (Hidy et al., 2016, described below) were compiled from measurements of air temperature, precipitation, and relative humidity (RH) obtained from climate stations neighboring each site (Soderquist et al., in review). Additional meteorological parameters including incoming solar radiation (W m^{-2}), average daytime air temperature (T_{daytime}), and daylight length (s) were simulated using the mountain microclimate model MtClim (v 4.3, Thornton, 2000). Historical datasets spanned 1996-2015 (20 years) at Sheep Creek and Reynolds Mountain East, and 2003-2015 (13 years) at Johnston Draw. Unlike Sheep Creek and Reynolds Mountain East, simulation periods were shorter at Johnston Draw where historical meteorological records were not available for a full 20 years.

4.2.2.2. Future climate

To represent climate conditions predicted for the mid 21st century, projected changes in temperature and RH were applied to historical climate datasets. Downscaled (4 km grid cells) monthly T_{\max} and T_{\min} and annual RH for both historic (1985-2005) and mid-century conditions (2046-2065) were obtained from a 20 model mean of CMIP5 general circulation models (Taylor et al., 2012) using the Multivariate Adaptive Constructed Analogs (MACA) downscaling method (Abatzoglou and Brown, 2012). Mid-century climate projections were

based on a continued high CO₂ emissions scenario (RCP 8.5). Increases in monthly T_{max} and T_{min} and shifts in annual RH at each site were determined by the difference between downscaled historical conditions and projected mid-21st century conditions. Average monthly T_{max} and T_{min} increases and changes in average annual RH were then applied to measured daily temperatures and VPD calculations for the years 1996-2015 at RME and SC and 2003-2015 at JDW. Annual CO₂ concentration (ppm) for both historical and mid-century climate followed RCP 8.5 (Meinshausen et al., 2011).

4.2.2.3. Redistribution of frozen precipitation

As described in Soderquist et al. (in review), the redistribution of snow is represented through the application of drift factors to measured precipitation data at each site. Briefly, simulations of daily snow water equivalent (SWE) from the spatially-distributed mass- and energy-balance snow model, iSnobal (Marks et al., 1999) simulations that included an empirical snow redistribution algorithm (Winstral et al., 2013) conducted at or nearby each site (Reba et al., 2011), were used along with precipitation measurements to estimate drift factors using the equation:

$$DF = \frac{\text{Peak simulated SWE (mm)}}{\text{Total measured uniform snow (mm) across drift accumulation period}} \quad (1)$$

Where peak simulated SWE is the seasonal maximum SWE extracted from a point in the center of each iSnobal simulated drift and the drift accumulation period is defined as the period from initial drift formation to peak SWE simulated by iSnobal. At each site, for both historical and mid-21st century simulations, average drift factors were applied to frozen precipitation based on both daytime and nighttime temperature thresholds (Table 4.1).

4.2.3. Vegetation simulations

Currently, aspen is the dominant vegetation type at all three simulation locations. However, we simulated ecosystem processes for two other vegetation types at these same locations to assess the suitability of each site for several different species and plant functional types. Mountain big sagebrush and C3 grasses were chosen because 1) their diversity in phenology and physiological traits and 2) their close proximity to aspen stands which might facilitate species replacement following aspen mortality or increased vulnerability. Incorporating plants with a wide range of ecophysiological traits may provide key insights into the ways drift zone communities may respond to changes in temperature and precipitation phase.

Aspen, mountain big sagebrush, and C3 grass productivity was simulated using the recently developed Biome-BGC MuSo (short for multilayer soil module, v. 4.0, Hidy et al., 2016). Biome-BGC MuSo is a point-based biogeochemical process model similar to the most recent version of Biome-BGC (v. 4.2, Thornton, 2002) in that it uses daily inputs of climate and site data along with ecophysiological parameters to simulate above and below ground fluxes of carbon, nitrogen, and water for a single plant functional type. While the original suite of Biome-BGC models were originally developed from Forest-BGC (Running and Hunt, 1993) to simulate forest ecosystem processes, Biome-BGC MuSo was adapted to simulate grassland ecosystems where phenology and management practices were not as accurately simulated using the original Biome-BGC framework (Hidy et al., 2012). In Biome-BGC MuSo, both phenology and soil hydrology have been updated to represent multiple soil layers, root distributions throughout the vertical soil profile, improved soil temperature calculations, and phenological constraints that limit plant productivity including drought-induced senescence and mortality.

For this study, timing of growing season onset and offset for aspen was simulated using the original Biome-BGC subroutine where leaf flush and senescence are triggered by soil temperatures estimated from an 11-day running average of daily air temperatures (White et al., 1997). In Biome-BGC MuSo, photosynthesis can be additionally limited by the presence of snowpack. For aspen simulations, snowpack presence did not limit photosynthesis, since stands at each site are tall in stature and located just below drifts. However, snowpack, regardless of whether it is uniform or redistributed, can impact the phenology of shorter statured plants. For mountain big sagebrush and C3 grasses we limited photosynthesis when the snowpack exceeded 20 and 5 kg m⁻², respectively (Table S1, Appendix 3). Snowpack thresholds were increased for mountain big sagebrush relative to C3 grasses due to increased plant height. However, since canopy interception of snow is not considered in Biome-BGC MuSo, we conservatively estimated the limiting effects of snowpack on mountain big sagebrush and C3 grasses. By assuming the phenology of shorter statured species can be limited by snowpack presence, our simulations are more representative of vegetation growing in the area occupied by the drift as opposed to vegetation growing downslope from drifts where snow accumulation tends to be more uniform.

The simulation approach for C3 grass phenology is different from that used for aspen simulations and uses Biome-BGC MuSo's heat sum growing season index (HSGSI). The HSGSI is an extension of the phenological model developed by Jolly et al., (2005) that combines minimum air temperatures, VPD, daylight length, and a 10-day heat sum into a single metric governing the length of the growing season. Like aspen, a photoperiod threshold of 10.9 hours is used when initiating leaf flush and senescence of grasses, although temperatures and VPD could also induce grass senescence. While these improvements are only several of many that have been incorporated into Biome-BGC MuSo, they are particularly important for simulations of vegetation in snow-dominated ecosystems where plant function is strongly coupled to water availability. We refer readers to Hidy et al., 2016 for a full description of all modifications made to phenological and hydrological sub-routines.

4.2.4. Species parameterization

Parameterization of Biome-BGC MuSo requires specific ecophysiological data describing morphological and physiological traits of an individual species or plant functional type. For this study, certain parameters such as foliar and root C:N and specific leaf area (SLA) were measured to give site and species specific parameter values. Other values were found in previously published studies or the growing number of plant trait databases (e.g., the TRY plant trait database, Kattge et al., 2011).

4.2.5. Measured parameters

Aspen has been previously parameterized at each site for simulations using Biome-BGC MuSo (see Soderquist et al., in review). For this study, mountain big sagebrush and C3 grasses were parameterized using a similar approach. C3 grasses are the dominant grass plant functional type in the interior Pacific Northwest (Teeri and Stowe, 1976). C3 grasses are also the dominant grass type in mid and high elevation drift zone plant communities where the winter dominated precipitation regimes and cooler temperatures of the RCEW preclude the widespread establishment of C4 grasses (Paruelo and Lauenroth, 1996).

During the summer of 2014, six plots at each site were established in the sagebrush steppe neighboring each aspen stand. On opposite sides of each aspen stand, plots (2.5-m radius) located at stand edge, 10m, and 30m from the stand, extended laterally along the hillslope, paralleling the drift zone. At each plot, sunlit leaves and fine root samples were

collected from at least two mature mountain big sagebrush plants and the four most abundant grass species. Cheatgrass (*Bromus tectorum*) was excluded from this study due to its winter annual growth cycle which differs from the perennial growth cycles of many C3 grasses growing in drift zones. Leaf and root samples were gently rinsed to remove debris, dried at 70 °C for 48 hours, and C:N of leaves and roots were analyzed (Washington State University, Stable Isotope Core Laboratory, Pullman, WA). For mountain big sagebrush, specific leaf area (SLA) was measured using photos of freshly sampled leaves within the image processing software ImageJ (Schneider et al., 2012, available online: <http://rsb.info.nih.gov/ij/index.html>). Leaf area and carbon content of foliage samples was used to calculate mountain big sagebrush SLA at each site. For C3 grasses, literature values of SLA were used since variations in SLA do not significantly impact Biome-BGC NPP simulations (White et al., 2000).

Across sites, differences between average values of C:N_{root}, C:N_{leaf}, and SLA (only C:N_{root}, C:N_{leaf} for C3 grasses) were determined using a one-way ANOVA. Measured C:N values for leaves and roots were not significantly different for mountain big sagebrush (all p-values >0.05, $\alpha=0.05$, Table S1, Appendix 3), however SLA (for aspen), and C:N of leaves and roots for aspen and C3 grasses were significantly different across sites (all p-values < 0.05, $\alpha=0.05$, Table S1, Appendix 3). If site means were significantly different, measured site specific values were used to parameterize Biome-BGC MuSo. Additionally, co-varying parameters, such as percent leaf nitrogen as Rubisco (PLNR) were allowed to vary by site.

4.2.6. Literature derived parameters

The increasing detail and additional modules incorporated into Biome-BGC MuSo has resulted in an increase in the number of ecophysiological parameters needed to describe a specific species. Parameters that weren't measured in the field were obtained from published literature and were selected to closely match a specific species or plant functional type growing in a similar region or climate (Table S1, Appendix 3).

4.2.7. Site conditions

Site specific parameters such as soil texture and maximum rooting depth were measured and estimated, respectively. Soil textures measured at several depths extending at least one meter at each site were used to parameterize simulations of aspen, mountain big

sagebrush, and C3 grasses. For this study, maximum rooting depth was assumed to be 1.5 m for aspen (Berndt and Gibbons, 1958, Sucoff, 1982), 1.5 m for mountain big sagebrush (based on soil moisture profile measurements and water balance calculations from Flerchinger and Seyfried, 2014), and 0.7 m for C3 grasses (Hidy et al., 2016). However, due to a restrictive layer observed at SC, rooting depth of aspen and mountain big sagebrush was restricted to 1.15 m. These parameterizations are site specific, and we note that there is likely considerable variability in rooting depths depending on stand age, soil type, and precipitation timing across a species range.

4.2.8. Assessing climate change impacts plant and ecosystem productivity

For this study, we focus on phenological shifts as a key component of fluxes of ecosystem and vegetation carbon in response to changes in snowpack and drought severity. Simulations for each species provide daily and annual output of vegetation NPP, NEP, and growing season length. Simulation results for aspen have been previously reported and are discussed in greater detail in Soderquist et al. (in review).

4.3 Results

4.3.1. Changes in temperature and precipitation

Average annual temperatures projected for mid-21st century (2046-2065, RCP 8.5) were 3.2°C (SD=0.4) degrees warmer than historical (1985-2005) downscaled temperatures (Table 4.1). Average annual relative humidity slightly is predicted to decrease by 3% across the same period. Predicted increases in monthly temperatures resulted in large decreases in the proportion of winter precipitation falling as snow (Figure 4.1) leading to reductions in redistributed snow water held in drifts and drift residence time (Figure 4.2).

Under historical conditions, mid elevation sites (SC and JDW) were located within the snow/rain transition zone in the RCEW. During the winter months, approximately 60% of precipitation occurred when daily temperatures were below 0°C. Precipitation phase at these sites is particularly sensitive to fluctuations in temperature, resulting in a wide range of variability in the proportion of annual precipitation falling as snow (snow:rain) across historical conditions (Figure 4.1a, c). Under historical simulations, RME received upwards of 80% of winter precipitation below freezing temperatures with less variability relative to mid-elevation sites (Figure 4.1b).

Under mid-21st century conditions, all sites experienced decreases in the proportion of precipitation falling as snow. As expected, warmer, mid-elevation sites (JDW and SC) had the lowest snow:rain ratio relative to the cooler, high elevation site (RME, Figure 4.1). After temperature increases were applied, the snow:rain ratio was reduced by approximately 20 percent at all sites during winter months. However, at RME the average proportion of precipitation occurring when daily temperatures were below 0°C remained around 50% for mid-21st century projected temperatures (Figure 4.1b).

Across the RCEW, drifts vary in size depending on topographic complexity, temperature, incoming precipitation, and position relative to the local wind field. Subsequently, drift factors applied to measured precipitation falling below freezing temperatures varied by site. For example, SC was the site with the largest drift (and drift factor) of all sites despite being the driest mid-elevation site (Table 4.1). Variable drift factors at each site led to differences in historical effective precipitation where, despite being a drier site (e.g. lower uniform precipitation, Table 4.1), effective precipitation held in the drift at SC was similar to the that of RME, a cooler, wet site located below a smaller drift (Figure 4.2a, b). JDW was the warmest site and has historically been located under a relatively small drift, resulting in a drift containing approximately 50% of the snow water simulated at RME and SC. Decreases in annual snow:rain with warming led to reductions in snow water stored in drifts. Under mid-21st century conditions, the total snow water held in snow drifts was greatly reduced at all sites and drift duration was reduced by as much as 1-2 months depending on incoming precipitation and winter temperatures (Figure 4.2). Reductions in snow water held in drifts led to decreases in total effective precipitation at each site. Subsequent decreases in average annual effective precipitation under mid-21st century conditions were 6%, 14%, and 27% at RME, JDW, and SC, respectively.

4.3.2. Phenological shifts

Warming temperatures and decreased snow residence time led to earlier bud break and canopy development for all species. For aspen, the onset of spring NPP for mid-21st century conditions occurred an average of 14 days earlier across all sites (Table 4.2). C3 grasses experienced longer and more variable increases in growing season length with the largest average advances in spring NPP observed at SC (30 ± 18 days), RME (25 ± 17 days), and JDW (22 ± 17 days), respectively. Mid-21st century growing seasons were also increased

for mountain big sagebrush where photosynthesis can take place year-round (Gilmanov et al., 2004) if temperature, incoming radiation, and snow cover aren't limiting factors. Changes in growing season length for mountain big sagebrush are slightly harder to quantify since growth is limited by an increasingly transitory snowpack. However, the number of days where mountain big sagebrush maintained positive rates of NPP increased an average of 70 days across all sites under mid-21st century conditions (Table 4.2). The increase in the number of days with positive NPP was similar to the number of days of snow pack absence indicating that snow cover is a primary factor determining growing season length for mountain big sagebrush that inhabit drift zones.

4.3.3. Model performance

Simulations of historical aspen LAI, phenology, and soil moisture use have previously been compared to field measurements and indicate that these critical processes are reasonably represented by Biome-BGC MuSo (Soderquist et al., in review ^{a,b}). Site-specific field measurements were not available for mountain big sagebrush or C3 grasses. However, historical simulations of mountain big sagebrush LAI averaged across all sites ($1.1 \text{ m}^2 \text{ m}^{-2}$) are comparable to previous measurements made in the RCEW (Clark and Seyfried, 2001, Flerchinger and Cooley, 2000) and similar, mature mountain big sagebrush communities (Cleary et al., 2009). Maximum LAI for C3 grasses averaged across sites was slightly higher than mountain big sagebrush ($1.34 \text{ m}^2 \text{ m}^{-2}$) and followed seasonal peaks and declines similar to those previously documented across middle and high elevations in the RCEW (Seyfried, 2003).

4.3.4. Cumulative and annual net primary production (NPP)

4.3.4.1. Aspen

Under historical conditions, average annual NPP across the simulation period was 421 and 482 $\text{g C m}^{-2} \text{ yr}^{-1}$ at SC and JDW, respectively. At both mid-elevation sites, reductions in snow residence and increased temperatures resulted in decreased aspen NPP under mid-21st century conditions (Figure 4.3, top and bottom panels). Although both mid-elevation sites experienced reduced aspen NPP, decreases in aspen NPP showed the greatest variability at SC. Under future conditions, NPP rates decreased 15% to 357 $\text{g C m}^{-2} \text{ yr}^{-1}$ at SC and 12% to 425 $\text{g C m}^{-2} \text{ yr}^{-1}$ at JDW. At RME, historical annual NPP averaged 400 $\text{g C m}^{-2} \text{ yr}^{-1}$, and increased by 4.5% to 418 $\text{g C m}^{-2} \text{ yr}^{-1}$ on average for the mid-21st century

(Figure 4.3 middle panel, Table 4.2). Cumulative NPP across both climate scenarios was much higher compared to mountain big sagebrush or C3 grasses (Figure 4.4).

4.3.4.2. Mountain big sagebrush

Relative to aspen or C3 grasses, mid-21st century mountain big sagebrush NPP experienced the largest increases from historical simulations. Average historical NPP rates were 87, 118, and 135 g C m⁻² yr⁻¹ at SC, RME, and JDW, respectively. Under warmer conditions with reduced snowpack, mountain big sagebrush NPP was higher across the simulation period with the largest increases observed at warmer mid-elevation sites (Figure 4.3, Table 4.2). Average mid-21st century mountain big sagebrush NPP values were increased across sites an average of 24% (SD=4.1) to 109, 141, and 172 g C m⁻² yr⁻¹ at SC, RME, and JDW, respectively (Table 4.2). Under historical conditions, cumulative NPP of sage was the lowest of all species (Figure 4.4). However, increased mountain big sagebrush NPP rates led to total carbon accumulation levels comparable to those of C3 grasses under mid-century conditions at all sites except SC.

4.3.4.3. C3 grasses

C3 grasses generally had higher historical NPP rates relative to mountain big sagebrush, with mid-elevation sites being the most productive (Figure 4.3, Table 4.2). Historical grass NPP averaged 144, 131, and 165 g C m⁻² yr⁻¹ at SC, RME, and JDW respectively. Under warmer temperatures, shifts in annual C3 grass NPP were lower, with increases averaging approximately 6% across all sites (Table 4.2). As with annual NPP, cumulative NPP across the simulation period remained similar under historical and mid-21st century conditions (Figure 4.4).

4.3.5. Daily NPP

While all species are able capitalize on more favorable spring temperatures under mid-21st century conditions (Figure 4.5), they differed in their response across the remainder of the growing and shoulder seasons. To describe these shifts, we highlight simulations for 2014/2064 at SC, a year with below average measured precipitation (314 mm) and above average annual temperatures (7.9°C historical, 11.0°C mid-21st century). During this simulation year, NPP of aspen and C3 grasses was reduced at mid-elevation sites. However, changes in annual mountain big sagebrush NPP are less prominent (Figure 4.3).

4.3.5.1. *Aspen*

For aspen, earlier leaf flush under warmer conditions led to increased synchrony with incoming spring precipitation and wetter conditions that were historically limited by cold temperatures. Compared to historical simulations, mid-21st century spring leaf flush for aspen occurred an average of 14 days earlier (Figure 4.5, top panel, Table 4.2). Temperature increases typically led to both earlier and increased rates of spring NPP for mid- 21st century simulation years (Figure 4.5, top panel). In 2014 specifically, aspen maintained consistent rates of NPP across the growing season. However, in 2064, aspen NPP continued to increase until late June. At this point evaporative demand became limiting resulting in a sharp drop in daily NPP with stomatal closure. Due to increasing drought conditions resulting from high VPDs, late summer NPP was reduced for the remainder of the 2064 growing season (Figure 4.6). Under both climate scenarios, a decrease in day-length controls final leaf senescence (occurring in late October). By 2064, increased spring NPP played an increasing role in balancing reduced NPP rates that occur during the driest periods of the summer. During particularly warm mid-21st century years (e.g. 2064,2065), increased spring NPP was less than summer NPP reductions which resulted in overall decreases in annual NPP (Figure 4.3).

4.3.5.2. *Mountain big sage*

While daily mountain big sagebrush NPP rates are much lower than aspen, decreased snowpack and increased temperatures resulted in average daily NPP remaining positive later into the spring and fall shoulder seasons (Figure 4.5, middle panel). Compared to 2014, reductions in snowpack and warmer spring conditions led to earlier positive NPP during 2064 (late February to mid- April). Later in the growing season, when evaporative demand was high and precipitation less frequent, mid-summer NPP rates remained positive but fell below historical levels due to increased growth respiration rates (Figure S1, Appendix 3). In the fall (approximately late October through November), mountain big sagebrush NPP increased slightly since it does not undergo complete leaf senescence and both warmer temperatures and decreased snowpack facilitated continued growth into the late fall/early winter.

4.3.5.3. C3 grasses

Compared to aspen and mountain big sagebrush, average periods of peak productivity are shorter for C3 grasses (Figure 4.5). Under historical conditions, spring growth is primarily snowpack-limited leading to delayed spring NPP (Figure 4.6, bottom panel). While daily NPP during 2014 was slower to reach maximum rates, periods of increasing productivity extended longer into the summer compared to mid-century simulations. During 2064, warming temperatures and reduced snowpack resulted in the onset of positive NPP approximately 40 days earlier than historical conditions. Although these early season NPP rates were low, they contributed to an earlier peak in maximum daily NPP (late May) compared to historical conditions (late June). Increased evaporative demand by mid-century led to a sharp decline in productivity that failed to recover across the remainder of the growing season (Figure 4.6). Despite large phenological shifts, total annual NPP rates often remained similar for C3 grasses under historical and mid-21st century climates (Figure 4.3).

4.3.6. Net ecosystem productivity (NEP)

4.3.6.1. Aspen

Average aspen NEP across the entire historical simulation period was positive for RME and JDW (Table 4.2). SC maintained a slightly negative average historical NEP primarily driven by several cool years with prolonged snowpack that were strong carbon sources (i.e. 2008-2011). However, many mid-21st century simulation years experienced slightly reduced NEP rates compared to historical conditions (not shown). Although average aspen NPP decreased at both mid-elevation sites under projected temperature increases, average NEP increased at SC and remained relatively unchanged at JDW under mid-21st century conditions (Table 4.2). RME experienced decreased average NEP with warming. At SC specifically, where average mid-21st century NEP increased the most, shifts in projected NEP were occasionally buffered by a combination of decreased summer maintenance respiration rates resulting from decreased LAI and reduced heterotrophic respiration rates across the growing season (Figure S1, Appendix 3). While trends in annual NEP varied by site, the proportion of simulation years with positive NEP rates remained high, indicating that, despite decreased annual NPP, aspen stands continue to be carbon sinks under warmer temperatures (Figure 4.7).

4.3.6.2. *Mountain big sage*

Unlike aspen, historical NEP rates for mountain big sagebrush were consistently positive across sites, averaging $18.1 \text{ g C m}^{-2} \text{ yr}^{-1}$ (Table 4.2). Although NEP rates tended to be lower than those of aspen, the proportion of historical simulation years with positive NEP rates remained high (Figure 4.7). Under mid-21st century conditions, increased spring gross primary production generally compensated for higher total ecosystem respiration rates (primarily driven by increased growth respiration) during the growing season (Figure S2, Appendix 3). By the mid-21st century, all sites experienced slight increases in average annual NEP (an average of $9 \text{ g C m}^{-2} \text{ yr}^{-1}$ across sites) along with a continued increase in the proportion of years with positive NEP.

4.3.6.3. *C3 grasses*

Annual NEP rates for C3 grasses were the closest to carbon neutral and frequently alternated between acting as a source or sink during historical and mid-21st century simulations (Table 4.2, Figure 4.7). Across sites, average NEP rates were generally insensitive to projected temperature increases and snowpack reductions. However, relative to mid-elevation sites, RME experienced the largest increase in the proportion of years with positive NEP rates under mid-21st century conditions. Although average NEP rates remained relatively consistent between climate scenarios (Table 4.2), the ability of C3 grasses to act as carbon sinks was the weakest across all sites and species (Figure 4.7).

4.4 Discussion

While future decreases in precipitation falling as snow are predicted with increasing confidence (Klos et al., 2014), the impacts of shifts in snow:rain on soil moisture availability and vegetation productivity are less certain. In this study, we have integrated future shifts in both precipitation phase, conditions limiting vegetation growth (i.e. temperature, incoming radiation, VPD, soil moisture), and plant traits to effectively predict climate change impacts on semi-arid sagebrush steppe plant communities growing in areas affected by the redistribution of snow. We show that shifts in precipitation phase and climate influence plant phenology and productivity for several prominent rangeland species and that the response of vegetation can vary by species and across sites in relatively close proximity.

4.4.1. Model assumptions and limitations

For this study, photosynthesis of lower-statured mountain big sagebrush and C3 grasses was limited by snowpack presence, and projected phenological shifts were representative of vegetation growing within the area of drift formation. However, productive plant communities that may benefit from snowmelt are frequently located downslope from drift zones where precipitation is more uniform. For mountain big sagebrush and C3 grasses specifically, our assumption of snow limitations on photosynthesis may: 1) result in decreased sagebrush NPP during the winter and spring compared to sagebrush growing immediately below snowdrifts where snowpack presence can be more transitory, and 2) prolong the onset of spring leaf flush of grasses relative to those located immediately downslope from the drift. Therefore, the phenological shifts of mountain big sagebrush and C3 grasses between historical and mid-21st century simulations presented here may be larger than those experienced by plants growing downslope from drifts where snow distribution is more uniform. Therefore, our simulations of NPP for mountain big sagebrush and C3 grasses are conservative representations of potential drift zone productivity, particularly during historical years with cool temperatures and prolonged snowpack presence.

While decreases in NPP for a given species suggest increasing vulnerability, mortality mechanisms such as disturbance (Briske et al., 2005) or hydraulic failure are either not considered in this study, or not incorporated into the Biome-BGC MuSo framework (e.g. loss of hydraulic conductivity). Mortality resulting from loss of hydraulic function may be particularly important for species like aspen, where hydraulic vulnerability has contributed to widespread decline in aspen forests across the intermountain United States and Canada (Anderegg et al., 2013, Worrall et al., 2013). Since hydraulic vulnerability hasn't been incorporated into Biome-BGC MuSo, we are limited in our ability to fully capture the effects of severe or multi-year drought impacts on the hydraulic function of plants. However, the lack drought-induced leaf senescence and mortality simulated by Biome-BGC MuSo suggests that the species considered in this study (particularly aspen) can continue to minimize hydraulic stress under warming temperatures through reductions in stomatal conductance and continued access to soil moisture stored in deeper layers of the root zone. While mortality resulting from disturbance or hydraulic failure aren't considered in this study, our simulations showing continued positive NPP rates suggest that catastrophic losses

of either aspen, mountain big sagebrush, or C3 grasses via carbon starvation is unlikely by the mid-21st century. However, drought-induced reductions in productivity and whole plant function may ultimately make plants more vulnerable to other mortality mechanisms such as hydraulic failure or biotic attacks (Anderegg et al., 2012b).

4.4.2. Climate change impacts on plant and ecosystem productivity

In winter dominated precipitation regimes, warming temperatures will lead to increasing synchrony between periods of incoming precipitation and vegetation productivity. While less certain than temperature projections, future precipitation projections predict slight increases in annual precipitation across the intermountain west during the 21st century (Abatzoglou and Brown, 2012, Taylor et al., 2012). Future increases in incoming precipitation or shifts in precipitation seasonality may further supplement decreases in soil moisture availability resulting from reductions in redistributed snow. However, based on our assumption that historical precipitation variability and timing will continue into the mid-21st century, each plant functional type in this study experienced increased spring productivity during periods that were previously limited by temperature and/or snow pack.

To maintain current rates of productivity, future increases in spring NPP must be balanced with the limiting effects of longer growing seasons and increasing evaporative demand. Increases in annual NPP with warming were primarily governed by a species' leaf habit and growing season length. Compared to deciduous vegetation, evergreen mountain big sagebrush experienced the largest increase (Figure 4.5, Table 4.2) in growing season days and total annual NPP (Figure 4.3, Table 4.2). Our simulations of NPP for mountain big sagebrush follow trends similar to regional projections of rangeland NPP, which show increases in NPP for high elevation rangelands in the intermountain west exceeding 25 % by the end of the 21st century (Reeves et al., 2014). While simulated NPP rates for mountain big sagebrush were often lower than those of aspen or C3 grasses, warmer spring temperatures and prolonged access to available soil moisture allowed mountain big sagebrush to maintain positive NPP rates across larger portions of the fall, winter, and spring when deciduous species remained dormant (Figure 4.5).

Even in the absence of redistributed snow, drift zones with high total precipitation and increased soil moisture storage may become increasingly important areas of refugia for mountain big sagebrush. Carbon assimilation in sagebrush communities is particularly

responsive to the timing of precipitation and winter temperatures (Svejcar et al., 2008). Provided that future spring precipitation sufficiently recharges soil water, prolonged access to spring soil moisture that is no longer limited by snowpack presence or cold temperatures may contribute to increased mountain big sagebrush NPP (Kwon et al., 2008). Germino and Reinhart (2014) found that sagebrush growing on deep soils experience increased growth and canopy cover with more frequent winter soil irrigation and increased spring soil moisture availability. Similarly, Schlaepfer et al. (2012) found that precipitation timing, as opposed to phase (e.g. rain or snow) was more important to ecosystem water balance of sagebrush environments. Although high elevation big sagebrush ecosystems are projected to expand at high elevations, decreases are also predicted to occur across lower elevations with warmer temperatures (Schlaepfer et al., 2011). Our simulations suggest that, if total precipitation and soil storage capacity are sufficient, mountain big sagebrush growing in drift zones appear to benefit from warming temperatures regardless of precipitation phase.

Although simulations indicate that each species can continue to maintain positive NEP rates under mid-century conditions, the magnitude of potential carbon sequestration varies by plant functional type. For aspen specifically, increased average NEP at SC under mid-21st century conditions was driven by significant increases in NEP during several years that were historically cooler than average. However, most simulation years typically experienced slightly reduced NEP rates under warmer conditions. Future shifts in species composition within drift zone communities could have significant impacts on site productivity and CO₂ exchange between the atmosphere and biosphere. For example, although aspen was the most sensitive species to reductions in redistributed precipitation, annual NPP and total carbon accumulation remained larger than that of mountain big sagebrush or C3 grasses (Figures 4.3, 4.4). Increased aspen mortality followed by replacement by either mountain big sagebrush or C3 grasses could lead to significantly reduced site NPP and potentially weaken the strength of the carbon sink, particularly if grasses become the dominant vegetation type.

The ability of an individual species to remain productive under a wide range of conditions provides some insight into the ways vegetation communities may shift under a changing climate (Weltzin et al., 2003, Huxman et al., 2004). Within the RCEW, mid-21st century simulations suggest that favorable growing conditions will decrease for aspen at

mid-elevations, increase for mountain big sagebrush at both mid and high elevations, and remain relatively unchanged for C3 grasses (Figures 4.3, 4.4). Increased shrub cover and decreased herbaceous biodiversity following aspen mortality has previously been documented (Anderegg et al., 2012) and indicates that biophysical and microclimate conditions created by aspen stands can be important drivers of plant community structure. In the case of upland drift zones, reduced aspen productivity may lead to future displacement by increasingly productive mountain big sagebrush or more phenologically plastic species like C3 grasses or deciduous shrubs like mountain snowberry (*Symphoricarpus oreophilus*). Climate change induced shifts in plant community structure may have additional, farther reaching impacts on wildlife habitat connectivity since upland aspen stands are typically small biological hotspots relative to the surrounding low-statured vegetation (Stohlgren et al., 1997).

5.1 Conclusions

In complex terrain with snow-dominated precipitation regimes, areas of productive sagebrush steppe vegetation can be closely associated with the redistribution of snow. In drift zones, plant communities can be highly productive relative to exposed ridgelines and slopes where effective precipitation is reduced by snow scour and/or preferential deposition. In many of these regions, winter precipitation will likely become increasingly rain dominated as temperatures increase, leading to a more homogenous distribution of precipitation across the landscape. We show, first, that decreases in frozen winter precipitation and increased evaporative demand during the summer will differentially impact species currently inhabiting drift zones based on variations in leaf habit, growing season length, and sensitivity to increased vapor pressure deficits. Under warming temperatures and reduced snowpack, species that maintain leaf area year-round (e.g. mountain big sagebrush) are projected to experience the largest increases in growing season length and productivity relative to deciduous species. Although deciduous species like aspen and C3 grasses can shift the timing of growth to better align with incoming spring precipitation, increases in spring productivity are less able to buffer carbon losses resulting from increased evaporative demand later in the growing season. Second, while all species considered in this study largely maintain positive NEP rates under significant warming and precipitation changes, future climate conditions favoring specific plant functional types or traits may facilitate

shifts in the magnitude of carbon assimilation and/or species composition. As sagebrush steppe ecosystems continue to face increasing pressure from shifting climate regimes, monitoring drift zone vegetation may become increasingly important when assessing and managing rangelands for carbon sequestration and/or critical wildlife habitat.

Acknowledgments

We thank the Reynolds Creek Critical Zone Observatory staff for assistance in the field and Zoltan Barcza and Dora Hidy for assistance when running simulations. Financial support for this research was provided by the Department of the Interior Northwest Climate Science Center (NW CSC) through a cooperative agreement no. G14AP00153 from the United States Geological Survey (USGS).

References:

- Abatzoglou, J. T., & Brown, T. J. 2012. A comparison of statistical downscaling methods suited for wildfire applications. *International Journal of Climatology*. 32: 772–780.
- Ahlström, A., Raupach, M.R., Schurgers, G., Smith, B., Arneeth, A., Jung, M., Reichstein, M., Canadell, J.G., Friedlingstein, P., Jain, A.K. and Kato, E., 2015. The dominant role of semi-arid ecosystems in the trend and variability of the land CO₂ sink. *Science*. 348: 895-899.
- Anderegg, W.R., Anderegg, L.D., Sherman, C. and Karp, D.S., 2012a. Effects of Widespread Drought-Induced Aspen Mortality on Understory Plants. *Conservation Biology*. 26: 1082-1090.
- Anderegg, W.R., Berry, J.A. and Field, C.B., 2012b. Linking definitions, mechanisms, and modeling of drought-induced tree death. *Trends in plant science*. 17: 693-700.
- Anderegg, W. R. L., Plavcová, L., Anderegg, L. D. L., Hacke, U. G., Berry, J. a, & Field, C. B. 2013. Drought's legacy: multiyear hydraulic deterioration underlies widespread aspen forest die-off and portends increased future risk. *Global Change Biology*. 19: 1188–96.
- Berndt, H.W. and Gibbons, R.D. 1958. Root distribution of some native trees and understory plants growing on three sites within ponderosa pine watersheds in Colorado. Rocky Mountain Forest and Range Experiment Station.
- Briske, D.D., Fuhlendorf, S.D. and Smeins, F.E., 2005. State-and-transition models, thresholds, and rangeland health: a synthesis of ecological concepts and perspectives. *Rangeland Ecology & Management*. 58: 1-10.
- Burke, I.C., Reiners, W.A. and Olson, R.K., 1989. Topographic control of vegetation in a mountain big sagebrush steppe. *Plant Ecology*. 84: 77-86.
- Clark, P.E. and Seyfried, M.S., 2001. Point sampling for leaf area index in sagebrush steppe communities. *Journal of Range Management*. 589-594.
- Cleary, M.B., Pendall, E. and Ewers, B.E., 2010. Aboveground and belowground carbon pools after fire in mountain big sagebrush steppe. *Rangeland Ecology & Management*. 63: 187-196.
- Connelly, J.W., Schroeder, M.A., Sands, A.R. and Braun, C.E., 2000. Guidelines to manage sage grouse populations and their habitats. *Wildlife Society Bulletin*. 967-985.
- Davies, K.W. and Bates, J.D., 2010. Vegetation characteristics of mountain and Wyoming big sagebrush plant communities in the northern Great Basin. *Rangeland Ecology & Management*. 63: 461-466.

- DeByle, N.,B. 1985. Wildlife. In: DeByle, N.,V, Winokur, R.,P (eds) Aspen: ecology and management in the western United States. General Technical Report RM-119. USDA Forest Service, Rocky Mountain Forest and Range Experiment Station, Fort Collins. 135–152.
- Finzel, J.A., Seyfried, M.S., Weltz, M.A., & Launchbaugh, K.L. 2015. Simulation of long-term soil water dynamics at Reynolds Creek, Idaho: implications for rangeland productivity. *Ecohydrology*. 9: 673-687.
- Flerchinger, G.N. and Cooley, K.R., 2000. A ten-year water balance of a mountainous semi-arid watershed. *Journal of Hydrology*. 237: 86-99.
- Flerchinger, G.N. and Seyfried, M.S., 2014. Comparison of methods for estimating evapotranspiration in a small rangeland catchment. *Vadose Zone Journal*. 13(4).
- Germino, M.J. and Reinhardt, K., 2014. Desert shrub responses to experimental modification of precipitation seasonality and soil depth: relationship to the two-layer hypothesis and ecohydrological niche. *Journal of Ecology*. 102: 989-997.
- Gilmanov, T.G., Svejcar, T.J., Johnson, D.A., Angell, R.F., Saliendra, N.Z. and Wylie, B.K., 2006. Long-term dynamics of production, respiration, and net CO₂ exchange in two sagebrush-steppe ecosystems. *Rangeland Ecology & Management*. 59: 585-599.
- Gilmanov, T.G., Johnson, D.A., Saliendra, N.Z., Svejcar, T.J., Angell, R.F. and Clawson, K.L., 2004. Winter CO₂ fluxes above sagebrush-steppe ecosystems in Idaho and Oregon. *Agricultural and Forest Meteorology*. 126: 73-88.
- Griffis-Kyle, K.L. and Beier, P. 2003. Small isolated aspen stands enrich bird communities in southwestern ponderosa pine forests. *Biological Conservation*. 100: 375-385.
- Hidy, D., Barcza, Z., Marjanovic, H., Sever, M.Z.O., Dobor, L., Gelybó, G., Fodor, N., Pintér, K., Churkina, G., Running, S. and Thornton, P., 2016. Terrestrial ecosystem process model Biome-BGCMuSo v4. 0: summary of improvements and new modeling possibilities. *Geoscientific Model Development*. 9: 4405-4437.
- Hidy, D., Barcza, Z., Haszpra, L., Churkina, G., Pintér, K. and Nagy, Z., 2012. Development of the Biome-BGC model for simulation of managed herbaceous ecosystems. *Ecological Modelling*. 226: 99-119.
- Hiemstra, C.A., Liston, G.E. and Reiners, W.A., 2002. Snow redistribution by wind and interactions with vegetation at upper treeline in the Medicine Bow Mountains, Wyoming, USA. *Arctic, Antarctic, and Alpine Research*. 262-273.
- Huxman, T.E., Snyder, K.A., Tissue, D., Leffler, A.J., Ogle, K., Pockman, W.T., Sandquist, D.R., Potts, D.L. and Schwinning, S., 2004. Precipitation pulses and carbon fluxes in semiarid and arid ecosystems. *Oecologia*. 141: 254-268.

- Jolly, W.M., Nemani, R. and Running, S.W., 2005. A generalized, bioclimatic index to predict foliar phenology in response to climate. *Global Change Biology*. 11: 619-632.
- Kattge, J., Diaz, S., Lavorel, S., Prentice, I.C., Leadley, P., Bönisch, G., Garnier, E., Westoby, M., Reich, P.B., Wright, I.J. and Cornelissen, J.H.C., 2011. TRY—a global database of plant traits. *Global change biology*. 17: 2905-2935.
- Kapnick, S. and Hall, A., 2012. Causes of recent changes in western North American snowpack. *Climate Dynamics*. 38: 1885-1899.
- Keyser, A.R., Kimball, J.S., Nemani, R.R., and Running, S.W. 2000. Simulating the effects of climate change on the carbon balance of high-latitude forests. *Global Change Biology*. 6: 185-195.
- Klos, P. Z., Link, T.E., & Abatzoglou, J.T. 2014. Extent of the rain-snow transition zone in the western U.S. under historic and projected climate. *Geophysical Research Letters*. 41: 4560-4568.
- Knowles, N., Dettinger, M.D. and Cayan, D.R., 2006. Trends in snowfall versus rainfall in the western United States. *Journal of Climate*. 19: 4545-4559.
- Kuhn, T.J., Safford, H.D., Jones, B.E. and Tate, K.W. 2011. Aspen (*Populus tremuloides*) stands and their contribution to plant diversity in a semiarid coniferous landscape. *Plant Ecology*. 212: 1451-1463.
- Kwon, H., Pendall, E., Ewers, B.E., Cleary, M. and Naithani, K., 2008. Spring drought regulates summer net ecosystem CO₂ exchange in a sagebrush-steppe ecosystem. *Agricultural and Forest Meteorology*. 148: 381-391.
- Lauenroth, W.K., Schlaepfer, D.R. and Bradford, J.B., 2014. Ecohydrology of dry regions: storage versus pulse soil water dynamics. *Ecosystems*. 17: 1469-1479.
- Lehning, M., Löwe, H., Ryser, M. and Raderschall, N., 2008. Inhomogeneous precipitation distribution and snow transport in steep terrain. *Water Resources Research*. 44.
- Loik, M.E., Breshears, D.D., Lauenroth, W.K. and Belnap, J., 2004. A multi-scale perspective of water pulses in dryland ecosystems: climatology and ecohydrology of the western USA. *Oecologia*. 141: 269-281.
- Marks, D., Domingo, J., Susong, D., Link, T., & Garen, D. 1999. A spatially distributed energy balance snowmelt model for application in mountain basins. *Hydrological Processes*. 13: 1935-1959.

- Marks, D. and Winstral, A., 2001. Comparison of snow deposition, the snow cover energy balance, and snowmelt at two sites in a semiarid mountain basin. *Journal of Hydrometeorology*. 2: 213-227.
- Meinshausen, M., Smith, S. J., Calvin, K., Daniel, J. S., Kainuma, M. L. T., Lamarque, J. F., ... & Thomson, A. G. J. M. V. 2011. The RCP greenhouse gas concentrations and their extensions from 1765 to 2300. *Climatic change*. 109: 213-241.
- Nayak, A., Marks, D., Chandler, D.G., Seyfried, M., 2010. Long-Term Snow, Climate, and Streamflow Trends at the Reynolds Creek Experimental Watershed, Owyhee Mountains, Idaho, United States. *Water Resources Research*. 46: 1-15.
- Newman, B.D., Wilcox, B.P., Archer, S.R., Breshears, D.D., Dahm, C.N., Duffy, C.J., McDowell, N.G., Phillips, F.M., Scanlon, B.R. and Vivoni, E.R., 2006. Ecohydrology of water-limited environments: A scientific vision. *Water Resources Research*. 42(6).
- Paruelo, J.M. and Lauenroth, W.K., 1996. Relative abundance of plant functional types in grasslands and shrublands of North America. *Ecological Applications*. 6: 1212-1224.
- Poulter, B., Frank, D., Ciais, P., Myneni, R.B., Andela, N., Bi, J., Broquet, G., Canadell, J.G., Chevallier, F., Liu, Y.Y. and Running, S.W., 2014. Contribution of semi-arid ecosystems to interannual variability of the global carbon cycle. *Nature*. 509: 600-603.
- Reba, M., Marks, D., Winstral, A., Link, A., Kumar, M. 2011. Sensitivity of the snowcover energetics in a mountain basin to variations in climate. *Hydrological Processes*. 25: 3312-3321.
- Reeves, M.C., Moreno, A.L., Bagne, K.E. and Running, S.W., 2014. Estimating climate change effects on net primary production of rangelands in the United States. *Climatic Change*. 126: 429-442.
- Schlaepfer, D.R., Lauenroth, W.K. and Bradford, J.B., 2012. Effects of ecohydrological variables on current and future ranges, local suitability patterns, and model accuracy in big sagebrush. *Ecography*. 35: 374-384.
- Schneider, C.A., Rasband, W.S., Eliceiri, K.W. 2012. NIH Image to ImageJ: 25 years of image analysis. *Nature Methods*. 9: 671-675.
- Seyfried, M.S. 2003. Incorporation of remote sensing data in an upscaled soil water model. p. 309–346. In Y. Pachepsky et al. (ed.) *Scaling methods in soil physics*. CRC Press, New York.

- Seyfried, M. S., Grant, L. E., Marks, D., Winstral, A., & Mcnamara, J. 2009. Simulated soil water storage effects on streamflow generation in a mountainous snowmelt environment, Idaho, USA. *Vadose Zone*. 10: 858–873.
- Shaw, M.R. and Harte, J., 2001. Control of litter decomposition in a subalpine meadow–sagebrush steppe ecotone under climate change. *Ecological Applications*. 11: 1206–1223.
- Shepperd, W.D., Rogers, P.C., Burton, D., Bartos, D.L., 2006. Ecology, biodiversity, management, and restoration of aspen in the Sierra Nevada, General Technical Report RMRS-GTR-178. Rocky Mountain Research Station, USDA Forest Service, Fort Collins, Colorado, 122 p.
- Slaughter, C. W., Marks, D., Flerchinger, G. N., Van Vactor, S. S., & Burgess, M. 2001. Thirty-five years of research data collection at the Reynolds Creek Experimental Watershed, Idaho, United States. *Water Resources Research*. 37: 2819–2823.
- Stohlgren, T.J., Chong, G.W., Kalkhan, M.A. and Schell, L.D., 1997. Multiscale sampling of plant diversity: effects of minimum mapping unit size. *Ecological Applications*. 7: 1064–1074.
- Strukelj, M., Brais, S., Quideau, S. A., Angers, V. A., Kebli, H., Drapeau, P., & Oh, S. W. 2013. Chemical transformations in downed logs and snags of mixed boreal species during decomposition. *Canadian Journal of Forest Research*. 43: 785–798.
- Sucoff, E. 1982. Water relations of the aspens. *University of Minnesota Agricultural Experiment Station*. St. Paul, (Technical Bulletin 338), p.4.
- Svejcar, T., Angell, R., Bradford, J.A., Dugas, W., Emmerich, W., Frank, A.B., Gilmanov, T., Haferkamp, M., Johnson, D.A., Mayeux, H. and Mielnick, P., 2008. Carbon fluxes on North American rangelands. *Rangeland Ecology & Management*. 61: 465–474.
- Taylor, K. E., Stouffer, R. J., & Meehl, G. A. 2012. An overview of CMIP5 and the experiment design. *Bulletin of the American Meteorological Society*. 93: 485–498.
- Teeri, J.A. and Stowe, L.G., 1976. Climatic patterns and the distribution of C 4 grasses in North America. *Oecologia*. 23: 1–12.
- Thornton, P. E., Hasenauer, H., & White, M. A. 2000. Simultaneous estimation of daily solar radiation and humidity from observed temperature and precipitation: an application over complex terrain in Austria. *Agricultural and Forest Meteorology*. 104: 255–271.

- Thornton, P.E., Law, B.E., Gholz, H.L., Clark, K.L., Falge, E., Ellsworth, D.S., Goldstein, A.H., Monson, R.K., Hollinger, D., Falk, M. and Chen, J., 2002. Modeling and measuring the effects of disturbance history and climate on carbon and water budgets in evergreen needleleaf forests. *Agricultural and forest meteorology*. 113: 185-222.
- Tucker, C.L., Tamang, S., Pendall, E. and Ogle, K., 2016. Shallow snowpack inhibits soil respiration in sagebrush steppe through multiple biotic and abiotic mechanisms. *Ecosphere*. 7(5).
- Weltzin, J.F., Loik, M.E., Schwinning, S., Williams, D.G., Fay, P.A., Haddad, B.M., Harte, J., Huxman, T.E., Knapp, A.K., Lin, G. and Pockman, W.T., 2003. Assessing the response of terrestrial ecosystems to potential changes in precipitation. *Bioscience*. 53: 941-952.
- West NE. 1983. Temperate Deserts and Semi-Deserts. Elsevier: Amsterdam.
- White, M.A., Thornton, P.E. and Running, S.W., 1997. A continental phenology model for monitoring vegetation responses to interannual climatic variability. *Global biogeochemical cycles*. 11: 217-234.
- White, M. A., Thornton, P. E., Running, S. W., & Nemani, R. R. 2000. Parameterization and Sensitivity Analysis of the BIOME-BGC Terrestrial Ecosystem Model: Net Primary Production Controls. *Earth Interactions*. 4: 1-85.
- Winstral, A., Marks, D., & Gurney, R. 2013. Simulating wind-affected snow accumulations at catchment to basin scales. *Advances in Water Resources*. 55: 64-79.
- Worrall, J. J., Rehfeldt, G. E., Hamann, A., Hogg, E. H., Marchetti, S. B., Michaelian, M., & Gray, L. K. 2013. Recent declines of *Populus tremuloides* in North America linked to climate. *Forest Ecology and Management*. 299: 35-51.

Tables:

Table 4.1. Site description and climate at Sheep creek (SC), Reynolds Mountain east (RME), and Johnston Draw (JDW) under historic and mid-21st century climate scenarios. Effective precipitation represents increased drift zone precipitation resulting from the redistribution of snow based on drift factors applied to uniform precipitation. Standard deviations are included in parentheses (20 simulation years at SC and RME, 13 simulation years at JDW).

Site	Elevation (m)	Mean annual temp (°C, historical and mid-century)	Uniform precipitation (mm)	Drift factor	Effective precipitation (mm, historical and mid-century)
SC	1817	7.1 (0.7), 10.3 (0.7)	446 (130)	3.98	1030 (412), 757 (321)
RME	2038	5.3 (0.6), 8.5 (0.7)	962 (188)	1.45	1180 (242), 1109 (227)
JDW	1782	7.2 (0.8), 10.4 (0.8)	685 (99)	2.17	944 (134), 810 (99)

Table 4.2. Average shifts in growing season length, net primary productivity (NPP), and net ecosystem productivity (NEP) for aspen, sagebrush, and C3 grasses at Sheep creek (SC), Reynolds Mountain east (RME), and Johnston Draw (JDW) under historic and mid-21st century climate scenarios. Total number of simulation years varies by length of meteorological datasets at each site.

Site	Species	Shift in growing season (# days, SD)	NPP (% change)	Average annual NEP (g C m ⁻² yr ⁻¹ , historic, future)	Proportion of years as C sink (historic, future)	Total number of simulation years
SC	trembling aspen	+13 (6)	-15.3	-1.1, 21.8	0.5, 0.85	20
	mountain big sagebrush	+68 (28)	+25.6	15.7, 20.3	0.85, 0.95	20
RME	C3 grasses	+30 (18)	+5.9	6.0, 7.5	0.6, 0.65	20
	trembling aspen	+14 (8)	+4.5	27.0, 19.5	0.85, 0.85	20
	mountain big sagebrush	+70 (32)	+19.7	20.4, 32.6	0.7, 0.8	20
JDW	C3 grasses	+25 (17)	+6.2	5.1, 6.5	0.35, 0.6	20
	trembling aspen	+15 (6)	-11.9	31.9, 33.1	0.9, 1.0	13
	mountain big sagebrush	+73 (29)	+27.5	18.3, 28.1	0.85, 1.0	13
	C3 grasses	+22 (17)	+0.7	8.2, 8.0	0.54, 0.55	13

Figures:

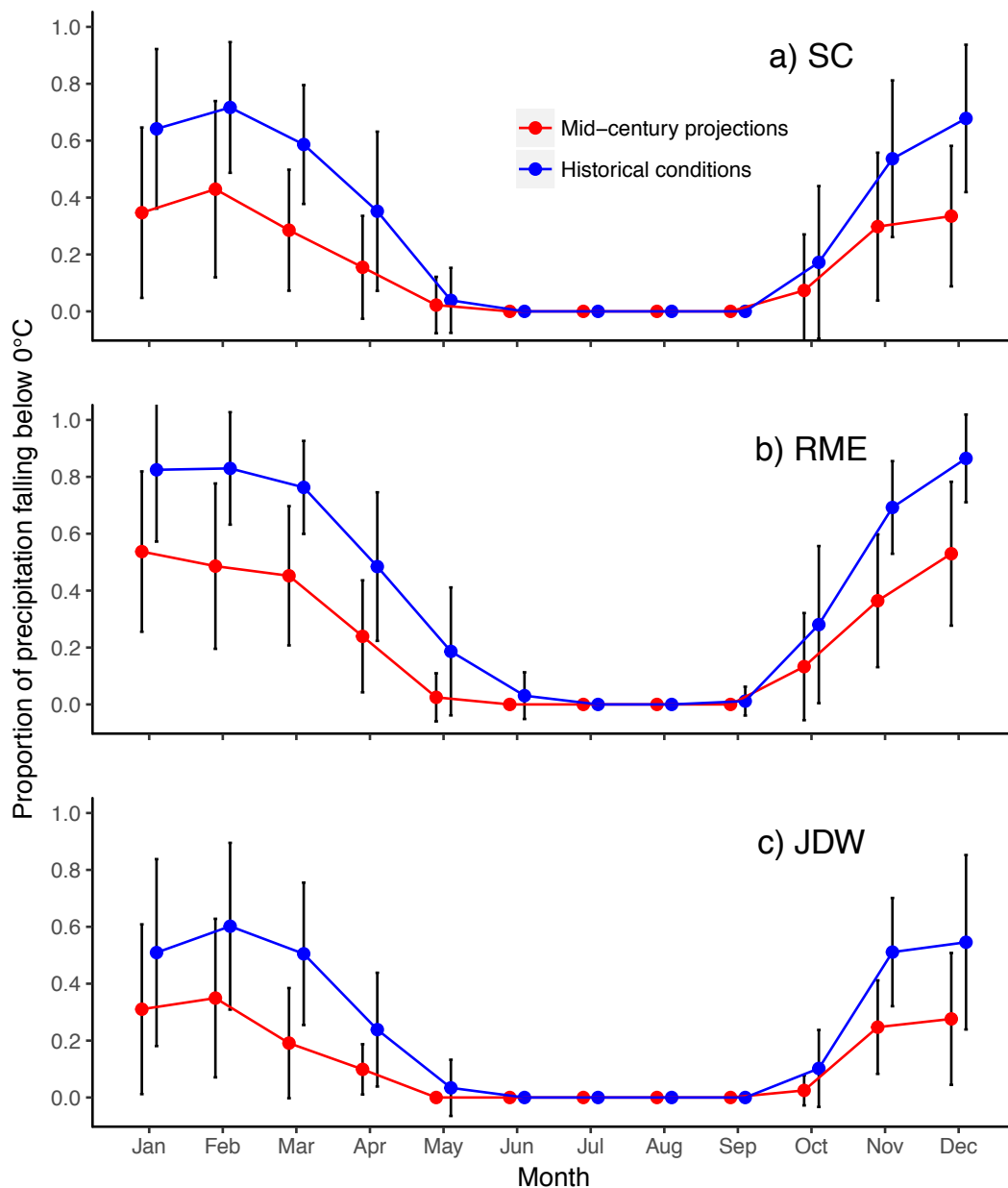


Figure 4.1. Proportion of measured monthly precipitation falling below average daily temperatures of 0°C for historical and mid-21st century conditions. For discussion of shifts in precipitation phase, precipitation occurring below this temperature threshold is assumed to fall as snow. Error bars indicate standard deviations (n= 20 simulation years at SC and RME, n= 13 simulation years at JDW).

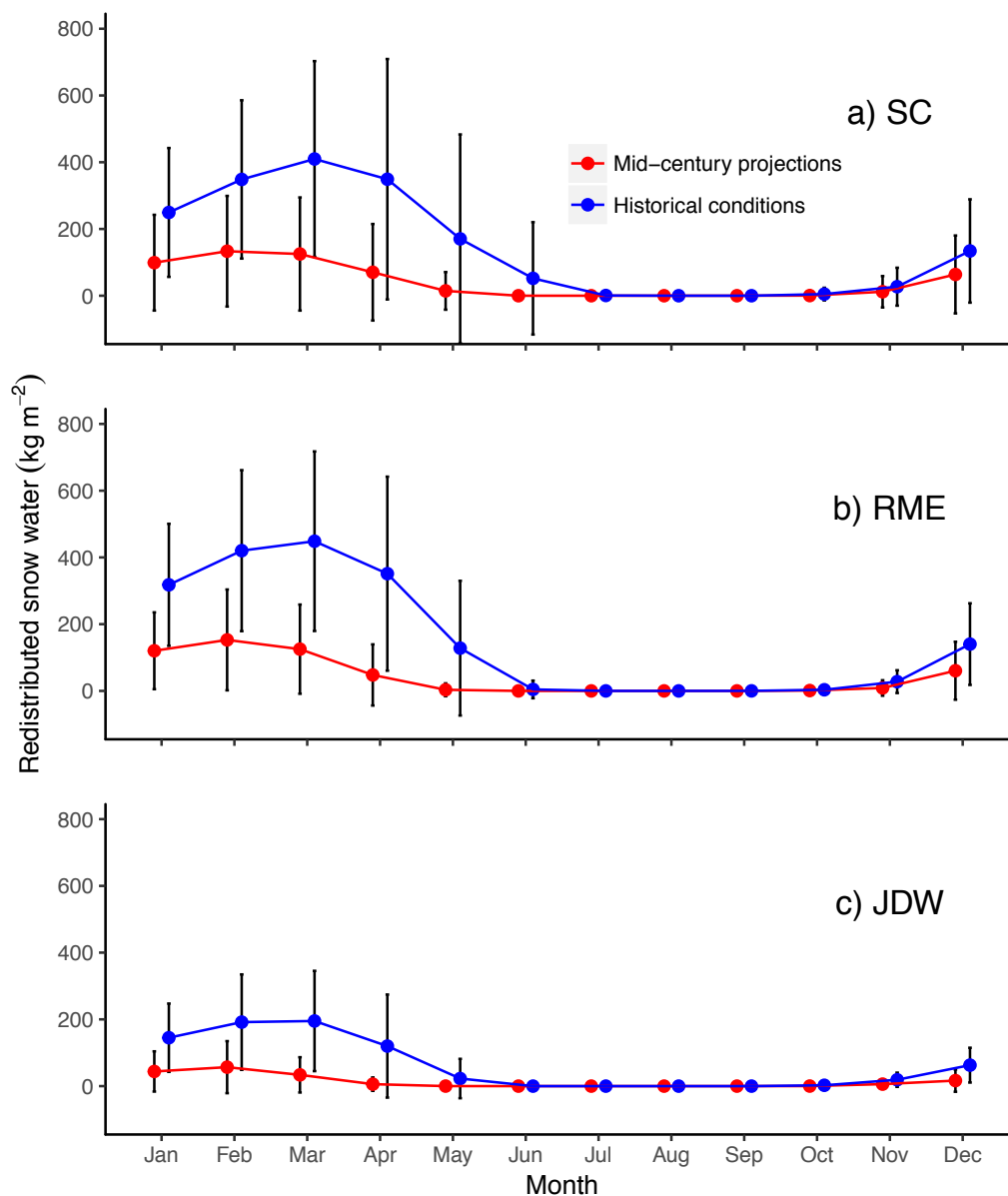


Figure 4.2. Average monthly redistributed snow water held in the drift at each site under historical and mid-21st century conditions. Error bars indicate standard deviations ($n=20$ simulation years at SC and RME, $n=13$ simulation years at JDW). Drift size at each site is a function of topography, temperature, and total precipitation. Variations in calculated drift factors led to similar snow redistribution patterns at the dry mid-elevation site (SC) and wet high-elevation site (RME) while the wetter mid-elevation (JDW) experienced less snow accumulation.

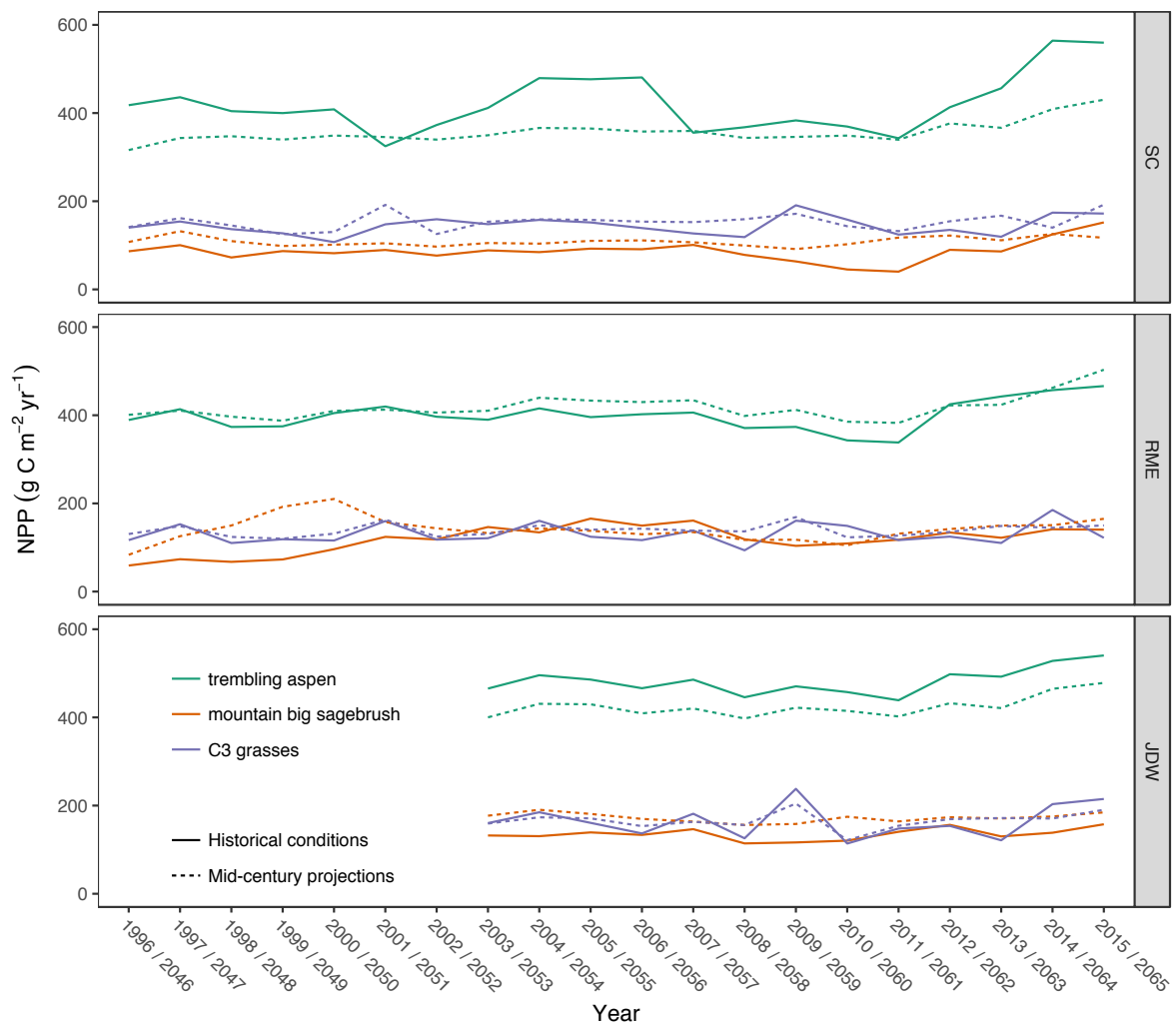


Figure 4.3. Simulated annual NPP rates for each species under historical and mid-21st century conditions. At mid-elevation sites (SC and JDW) aspen experienced decreased NPP under mid-21st century conditions. However, NPP of mountain big sagebrush experienced increased at all sites with warming temperatures. NPP of C3 grasses remained relatively unchanged across historical and mid-21st climate scenarios.

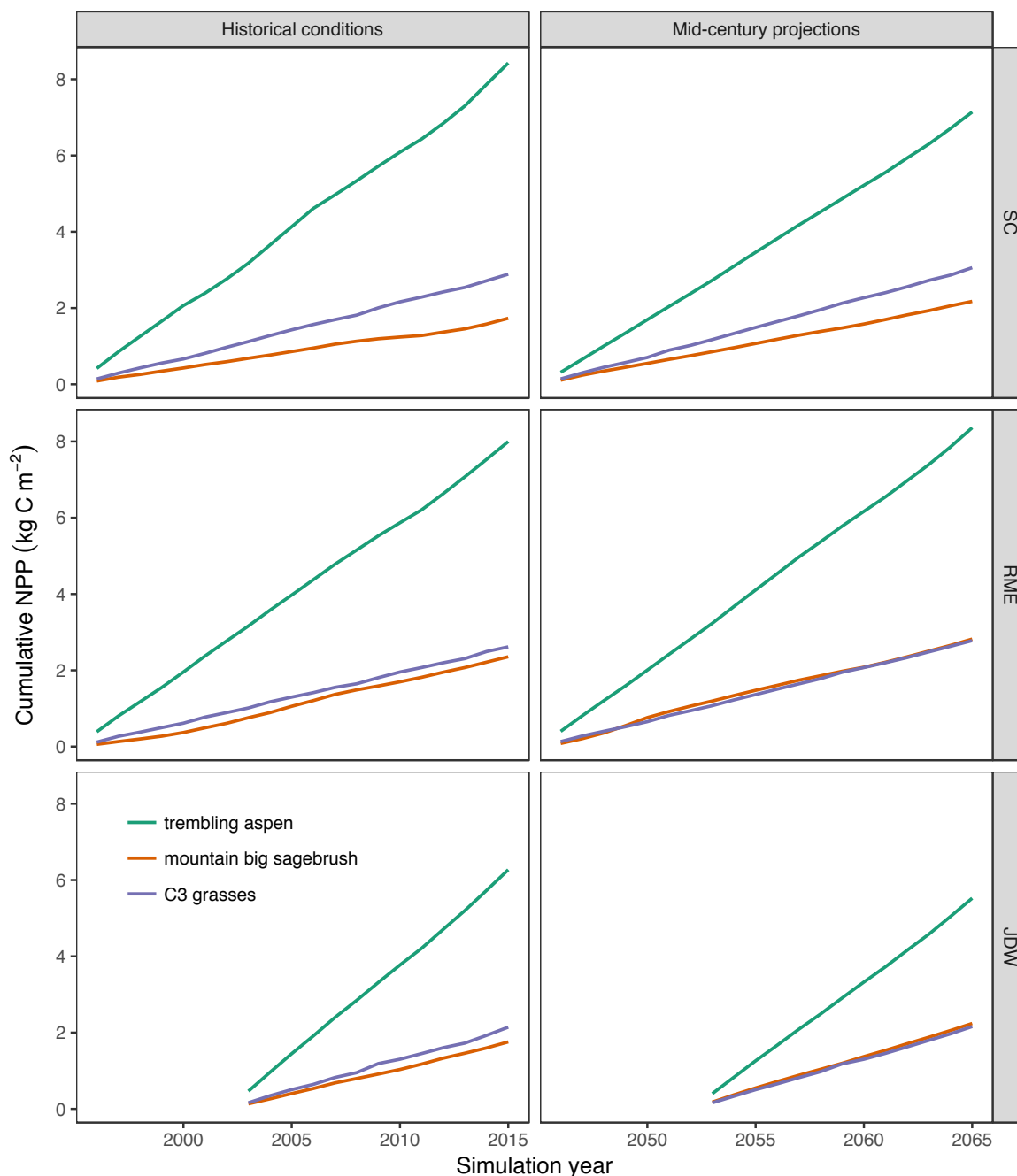


Figure 4.4. Cumulative NPP for aspen, mountain big sagebrush, and C3 grasses at each site under historical (1996-2015) and mid-21st century conditions (2046-2065). Note that simulation periods for JDW are only 13 years compared to those of SC and RME (20 years) resulting in lower cumulative NPP. Under both climate scenarios, aspen accumulated the most carbon relative to mountain big sagebrush or C3 grasses. However, mountain big sagebrush experienced the largest proportional increase in total NPP relative to aspen or C3 grasses with warming.

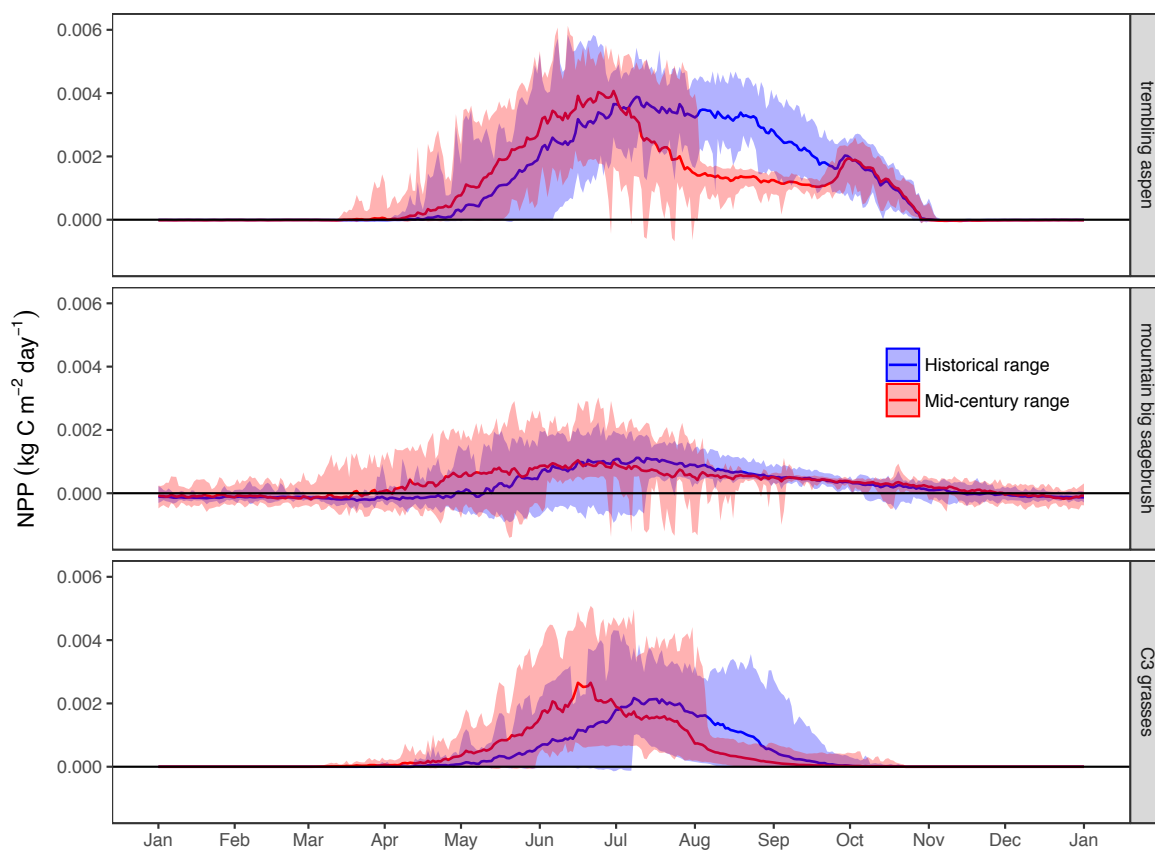


Figure 4.5. Average daily NPP (red and blue lines) for aspen, mountain big sagebrush, and C3 grasses at Sheep Creek (SC) across all simulation years (n=20 at RME and SC, 13 at JDW). Shaded bands indicate maximum and minimum simulation ranges. For shorter statured mountain big sagebrush and C3 grasses, several cool years with prolonged snow drift presence delayed spring growth under historical conditions. Under mid-21st century conditions, increased evaporative demand significantly reduced aspen and C3 grass NPP during the mid/late summer.

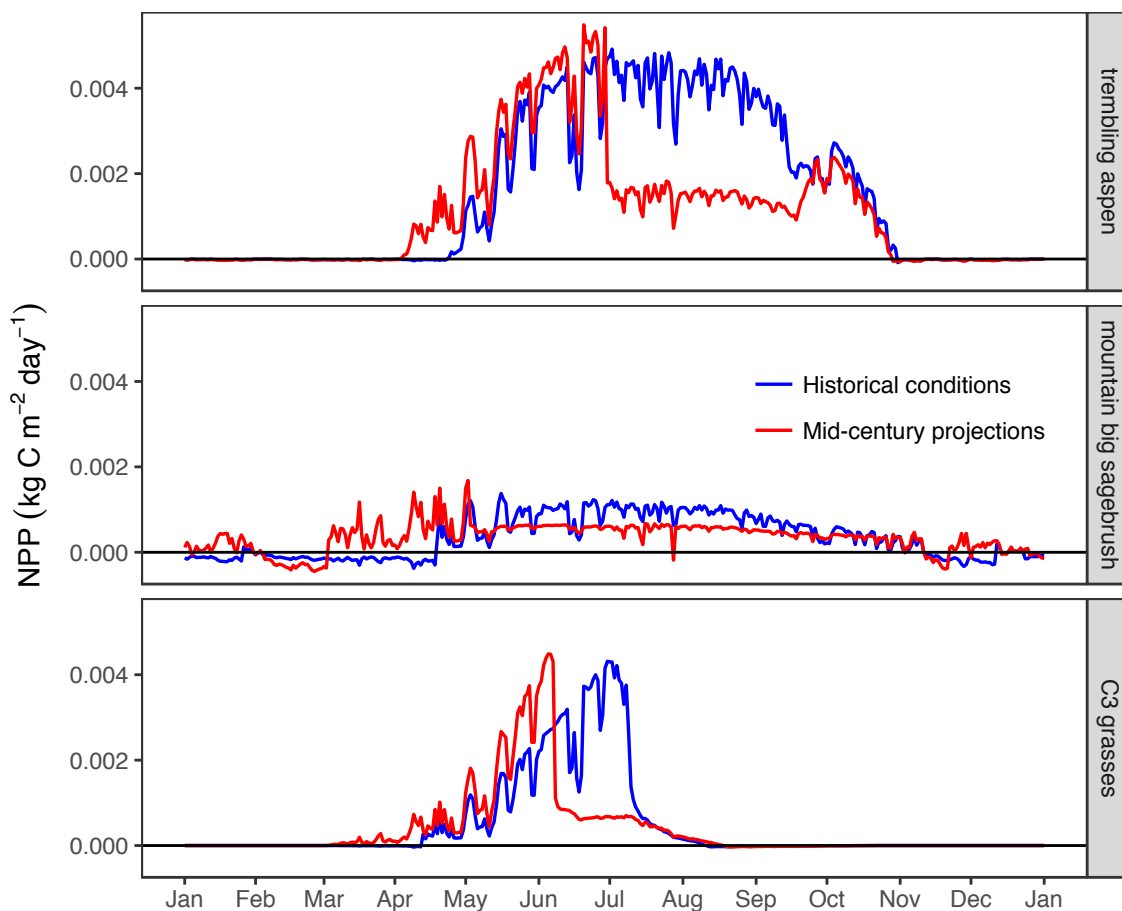


Figure 4.6. Daily NPP for each species at Sheep Creek (SC) during 2014 (blue) and the corresponding mid-21st century year 2064 (red). This simulation year experienced above average temperatures and below average total precipitation. Total annual NPP for aspen and C3 grasses was reduced under warmer and drier conditions, whereas mountain big sagebrush NPP remained similar under both historical and mid-21st century conditions.

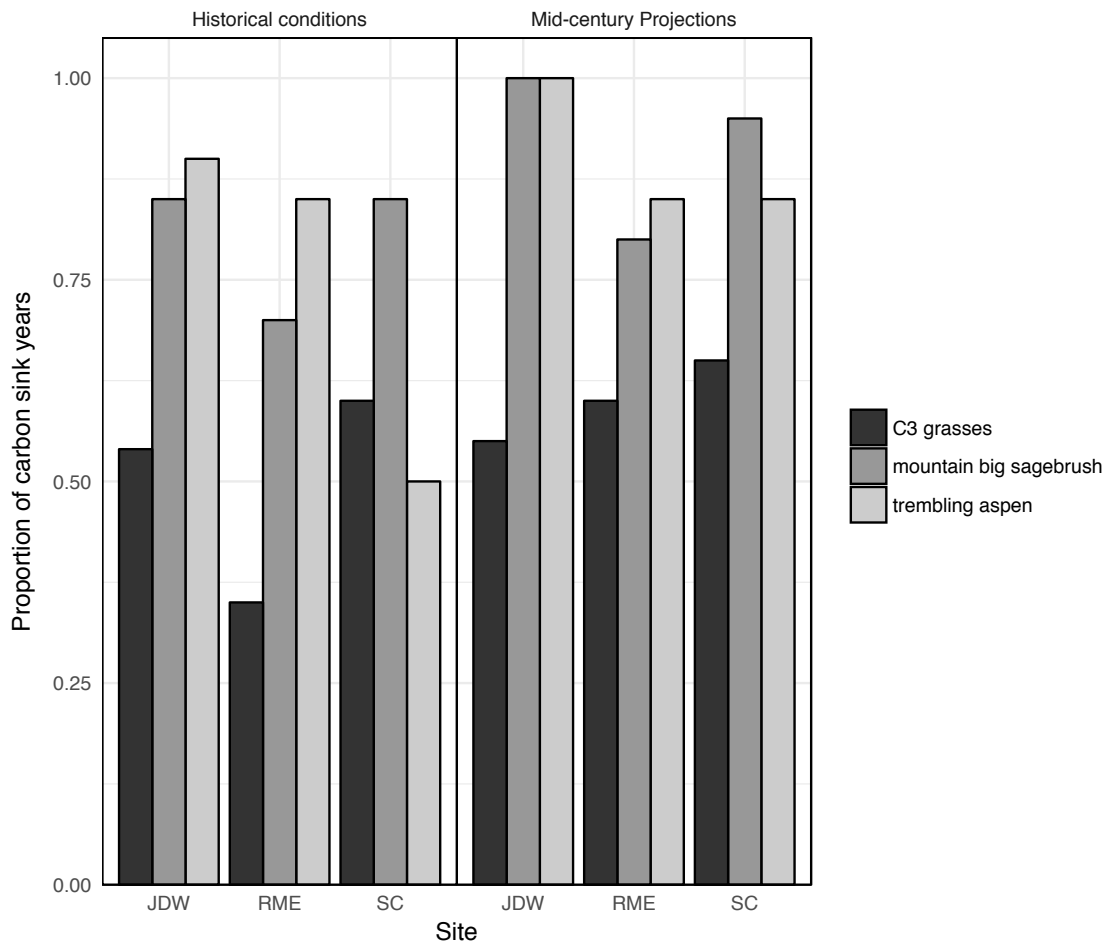


Figure 4.7. Proportion of years with acting as a net carbon sink (i.e. positive rates of net ecosystem production (NEP)) for each species under historical (1996-2015) and mid-21st century conditions (2046-2065). Under warmer and drier conditions, aspen and mountain big sagebrush maintain positive NEP rates across a majority of historical and future simulation years, although the magnitude of NEP for individual years can be reduced relative to historical conditions. Annual NEP of C3 grasses consistently alternated between positive and negative rates under both historical and mid-21st century climate scenarios.

Appendix 1

Supporting information for

Chapter 2: Simulating the Dependence of Aspen (*Populus tremuloides*) on Redistributed Snow in a Semi-Arid Watershed.

Soderquist B. S.¹, Kavanagh K. L.², Link T. E.¹, Seyfried M. S.³, Winstral, A. H.⁴

¹ *Department of Forest, Rangeland, and Fire Sciences, University of Idaho, Moscow, ID, 83844, USA,* ² *Department of Ecosystem Science and Management, Texas A&M University, College Station, TX, 77843-2138, USA,* ³ *USDA Agricultural Research Service, 800 Park Blvd., Plaza IV, Suite 105, Boise, ID, 83712, USA.* ⁴ *Swiss Federal Research Institute for Snow and Avalanche Research WSL, Flühelstrasse 11, 7260 Davos Dorf, Switzerland.*

Table S1. Equations used to calculate measured and simulated root zone soil storage ($S_{rootzone}$, mm) from volumetric water content ($\theta_{(installed\ depth\ (cm))}$, m^3m^{-3}) and layer depths (mm) at Reynolds Mountain east (RME), Johnston Draw (JDW), and Sheep Creek (SC).

Soil moisture data	Equations used to calculate total root zone storage ($S_{rootzone}$, mm) at each site
Measured volumetric water content	$S_{RME,120cm} = \theta_{10} * 200mm + \theta_{30} * 300mm + \theta_{60} * 300mm + \theta_{120} * 400mm$ $S_{JDW,120cm} = \theta_5 * 100mm + \theta_{20} * 250mm + \theta_{50} * 250mm + \theta_{77} * 200mm + \theta_{88} * 400mm$ $S_{SC,110cm} = \theta_{10} * 200mm + \theta_{30} * 300mm + \theta_{70} * 300mm + \theta_{100} * 300mm$
Biome-BGC simulated volumetric water content	$S_{RME,120cm} = \theta_{sim} * 1200mm$ $S_{JDW,120cm} = \theta_{sim} * 1200mm$ $S_{SC,110cm} = \theta_{sim} * 1100mm$

Table S2. Ecophysiological parameters used to parameterize Biome-BGC simulations of aspen at Reynolds Mountain East (RME), Sheep Creek (SC), and Johnston Draw (JDW). Parameter values were either measured in the field, calculated based on field measurements, or obtained from published literature. White et al. (2000) was the primary source for *Populus tremuloides* or deciduous broad leaf forest parameters, an average was taken when multiple values for a single parameter were provided.

Parameter	Unit	RME	JDW	SC	Source
Transfer growth period as fraction of growing season	(prop.)	0.2	0.2	0.2	White et al. 2000
Litterfall as fraction of growing season	(prop.)	0.2	0.2	0.2	White et al. 2000
Annual leaf and fine root turnover fraction	(yr ⁻¹)	1.0	1.0	1.0	Deciduous PFT default
Annual live wood turnover fraction	(yr ⁻¹)	0.7	0.7	0.7	White et al. 2000
Annual whole-plant mortality fraction	(yr ⁻¹)	0.005	0.005	0.005	White et al. 2000
Annual fire mortality fraction	(yr ⁻¹)	0.0	0.0	0.0	Not considered
New fine root C: new leaf C	(ratio)	1.2	1.2	1.2	White et al. 2000
New stem C: new leaf C	(ratio)	2.2	2.2	2.2	White et al. 2000
New live wood C: new total wood C	(ratio)	0.096	0.096	0.096	White et al. 2000
New root C: new stem C	(ratio)	0.152	0.152	0.152	White et al. 2000
Current growth proportion	(prop.)	0.5	0.5	0.5	White et al. 2000
C:N leaves	(kg C kgN ⁻¹)	21.5	18.9	23.2	Measured
C:N leaf litter	(kg C kgN ⁻¹)	65.5	65.5	65.5	Average of White et al. 2000
C:N fine roots	(kg C kgN ⁻¹)	83.3	50.7	92.9	Measured
C:N live wood	(kg C kgN ⁻¹)	50.0	50.0	50.0	White et al. 2000
C:N dead wood	(kg C kgN ⁻¹)	520.0	520.0	520.0	Strukelj et al. 2013
Leaf litter labile proportion	(DIM)	0.356	0.356	0.356	Average of White et al. 2000
Leaf litter cellulose proportion	(DIM)	0.44	0.44	0.44	Average of White et al. 2000
Leaf litter lignin proportion	(DIM)	0.204	0.204	0.204	Average of white et al. 2000
Fine root labile proportion	(DIM)	0.333	0.333	0.333	White et al. 2000
Fine root cellulose proportion	(DIM)	0.444	0.444	0.444	White et al. 2000
Fine root lignin proportion	(DIM)	0.223	0.223	0.223	White et al. 2000
Dead wood cellulose proportion	(DIM)	0.785	0.785	0.785	White et al. 2000
Dead wood ligning proportion	(DIM)	0.215	0.215	0.215	White et al. 2000
Canopy water intercept coeff.	(1 LAI ⁻¹ day ⁻¹)	0.038	0.038	0.038	White et al. 2000
Canopy light extinction coeff.	(DIM)	0.5	0.5	0.5	White et al. 2000
All-sided to projected leaf area ratio	(DIM)	2.0	2.0	2.0	White et al. 2000
Canopy average specific leaf area	(m ² kg C ⁻¹)	17.2	16.4	19.9	Measured
Ratio of shaded SLA: sunlit SLA	(DIM)	2.0	2.0	2.0	White et al. 2000

continued on next page

Table S2 continued

Parameter	Unit	RME	JDW	SC	Source
Fraction of percent leaf N in Rubisco	(DIM)	0.076	0.070	0.070	Calculated by site
Maximum stomatal conductance	(m s^{-1})	0.005	0.005	0.005	Keyser et al. 2000
$V_{c_{\max}}$	($\mu\text{mol CO}_2\text{m}^{-2}\text{s}^{-1}$)	0.95	0.95	0.95	Lenz et al. 2010
Cuticular conductance	(m s^{-1})	0.00001	0.00001	0.00001	White et al. 2000
Boundary layer conductance	(m s^{-1})	0.01	0.01	0.01	White et al. 2000
Leaf water potential: start of conductance reduction	(MPa)	-0.5	-0.5	-0.5	Huang et al 2013
Leaf water potential: complete conductance reduction	(MPa)	-1.4	-1.4	-1.4	Measured
VPD: start of conductance reduction	(Pa)	1000.0	1000.0	1000.0	White et al. 2000
VPD: complete conductance reduction	(Pa)	4200.0	4200.0	4200.0	White et al. 2000

Appendix 2

Supporting information for

Chapter 3: Growing Season Conditions Mediate the Dependence of Aspen on Redistributed Snow Under Climate Change.

Soderquist B. S.¹, Kavanagh K. L.², Link T. E.¹, Seyfried M. S.³, Strand, E. K.¹

¹ *Department of Forest, Rangeland, and Fire Sciences, University of Idaho, Moscow, ID, 83844, USA,* ² *Department of Ecosystem Science and Management, Texas A&M University, College Station, TX, 77843-2138, USA,* ³ *USDA Agricultural Research Service, 800 Park Blvd., Plaza IV, Suite 105, Boise, ID, 83712, USA.*

Table S1. Ecophysiological parameters used to parameterize Biome-BGC MuSo simulations of aspen at Sheep Creek (SC), Reynolds Mountain East (RME), and Johnston Draw (JDW). Parameter values were either measured in the field, adjusted based on field measurements, or obtained from published literature. White et al. (2000) was the primary source for species specific parameters, an average was taken when multiple values for a single parameter were provided.

Parameter name	Aspen parameter values by site (1=SC, 2=RME,3=JDW)	References, parameterization method
Transfer growth period as fraction of growing season	0.2 ^{1,2,3}	White et al., 2000
Litterfal as fraction of growing season	0.2 ^{1,2,3}	White et al., 2000
Base temperature	NA	Not considered
Growing degree day of start of genetically programmed senescence	1 ^{1,2,3}	MuSo default
Annual leaf and fine root turnover fraction	1.0 ^{1,2,3}	White et al., 2000
Annual live wood turnover fraction	0.70 ^{1,2,3}	White et al., 2000
Annual whole-plant mortality fraction	0.02 ^{1,2,3}	Hidy et al., 2016
Annual fire mortality fraction	0.0 ^{1,2,3}	Not considered
New fine root C: new leaf C	1.2 ^{1,2,3}	White et al., 2000
New fruit C: new leaf C	0.0 ^{1,2,3}	Not applicable
New softstem C: new leaf C	0.0 ^{1,2,3}	Not applicable
New woody stem C: new total wood C	2.2 ^{1,2,3}	White et al., 2000
New live wood C: new total wood C	0.096 ^{1,2,3}	White et al., 2000
New coarse root C: new stem C	0.152 ^{1,2,3}	White et al., 2000
Current growth proportion	0.5 ^{1,2,3}	Deciduous broadleaf default
C:N leaves	23.2 ¹ ,21.5 ² ,18.9 ³	measured
C:N leaf litter	65.5 ^{1,2,3}	Average of aspen, White et al., 2000
C:N of fine roots	92.9 ¹ ,83.3 ² ,50.7 ³	measured
C:N of fruit	NA	Not applicable
C:N of softstem	NA	Not applicable
C:N of live wood	50.0 ^{1,2,3}	White et al., 2000
C:N of dead wood	520 ^{1,2,3}	Strukelj et al., 2013
Leaf litter labile proportion	0.356 ^{1,2,3}	Average from White et al., 2000
Leaf litter cellulose proportion	0.44 ^{1,2,3}	Average from White et al., 2000
Fine root litter labile proportion	0.204 ^{1,2,3}	Average from White et al., 2000
Fine root litter cellulose proportion	0.444 ^{1,2,3}	White et al., 2000

Table S1 continued		
Fruit litter labile proportion	NA	Not applicable
Fruit litter cellulose proportion	NA	Not applicable
Softstem litter cellulose proportion	NA	Not applicable
Dead wood cellulose proportion	0.785 ^{1,2,3}	White et al., 2000
Canopy water interception coefficient	0.038 ^{1,2,3}	Average from White et al., 2000.
Canopy light extinction coefficient	0.5 ^{1,2,3}	White et al., 2000
All-sided to projected leaf area ratio	2.0 ^{1,2,3}	White et al., 2000
Canopy average specific leaf area	19.9 ¹ ,17.2 ² ,16.4 ³	Measured
Ratio of shaded specific leaf area:sunlit specific leaf area	2.0 ^{1,2,3}	White et al., 2000
Fraction of leaf N in Rubisco	0.068 ¹ ,0.077 ² ,0.077 ³	Adjusted within calculated range
Fraction of leaf N in Pep carboxylase	NA	Not applicable
Maximum stomatal conductance	0.005 ^{1,2,3}	Keyser et al., 2005
Cuticular conductance	0.00001 ^{1,2,3}	White et al., 2000
Boundary layer conductance	0.01 ^{1,2,3}	White et al., 2000
Relative soil water content limitation 1 (proportion to field capacity value)	0.8 ¹ ,0.6 ² ,0.7 ³	Adjusted by site
Relative soil water content limitation 2 (proportion to saturation capacity value)	1.00 ^{1,2,3}	Default
Vapor pressure deficit: start of conductance reduction	1000 ^{1,2,3}	White et al., 2000
Vapor pressure deficit: complete conductance reduction	4200 ^{1,2,3}	White et al., 2000
Senescence mortality coefficient of aboveground plant material	0.045 ^{1,2,3}	Decreased from default
Senescence mortality coefficient of belowground plant material	0.045 ^{1,2,3}	Decreased from default
Genetically programmed senescence mortality coefficient of leaf	0 ^{1,2,3}	Not considered
Turnover rate of wilted standing biomass to litter	0.1 ^{1,2,3}	MuSo default
Turnover rate of cut-down non-woody biomass to litter	0.1 ^{1,2,3}	MuSo default
N denitrification proportion	0.01 ^{1,2,3}	MuSo default
Bulk N denitrification proportion, wet case	0.0068 ^{1,2,3}	MuSo default

Table S1 continued		
Bulk N denitrification proportion, dry case	0.0003 ^{1,2,3}	MuSo default
Mobile N proportion (leaching)	0.1 ^{1,2,3}	MuSo default
Symbiotic+asymbiotic fixation of N	0.0008 ^{1,2,3}	MuSo default
Ratio of storage and actual pool mortality due to management	0.1 ^{1,2,3}	MuSo default
Critical value of soil stress coefficient	0.467 ¹ ,0.4 ² ,0.4 ³	Adjusted by site
Critical number of stress days	90 ^{1,2,3}	Hidy et al., 2016
Maximum depth of rooting zone (m)	1.15 ¹ ,1.5 ² ,1.5 ³	Estimated in the field ¹ , Sucoff, 1982 ² , Berndt and Gibbons, 1958 ²
Root distribution parameter	1.56 ^{1,2,3}	Calibrated
Growth respiration per unit C grown	0.3 ^{1,2,3}	MuSo default
Maintenance respiration in kgC/day per kg of tissue N	0.218 ^{1,2,3}	MuSo default

Table S2. Equations used to calculate measured and simulated soil storage in the top meter of soil (S_{100}) from volumetric water content ($\theta_{(installed\ depth\ (cm))}$, m^3m^{-3}) and layer depths (mm) at Reynolds Mountain east (RME), Johnston Draw (JDW), and Sheep Creek (SC).

Soil moisture data	Equations used to calculate S_{100} (mm) at each site
Measured volumetric water content	$S_{RME,meas} = \theta_{10} * 100mm + \theta_{30} * 200mm + \theta_{60} * 300mm + \theta_{120} * 400mm$ $S_{JDW,meas} = \theta_5 * 50mm + \theta_{20} * 250mm + \theta_{50} * 250mm + \theta_{77} * 250mm + \theta_{88} * 200mm$ $S_{SC,meas} = \theta_{10} * 100mm + \theta_{30} * 200mm + \theta_{70} * 300mm + \theta_{100} * 400mm$
Biome-BGC MuSo simulated volumetric water content	$S_{RME,sim} = \theta_5 * 100mm + \theta_{20} * 200mm + \theta_{45} * 300mm + \theta_{80} * 400mm$ $S_{JDW,sim} = \theta_5 * 100mm + \theta_{20} * 200mm + \theta_{45} * 300mm + \theta_{80} * 400mm$ $S_{SC,sim} = \theta_5 * 100mm + \theta_{20} * 200mm + \theta_{45} * 300mm + \theta_{80} * 400mm$

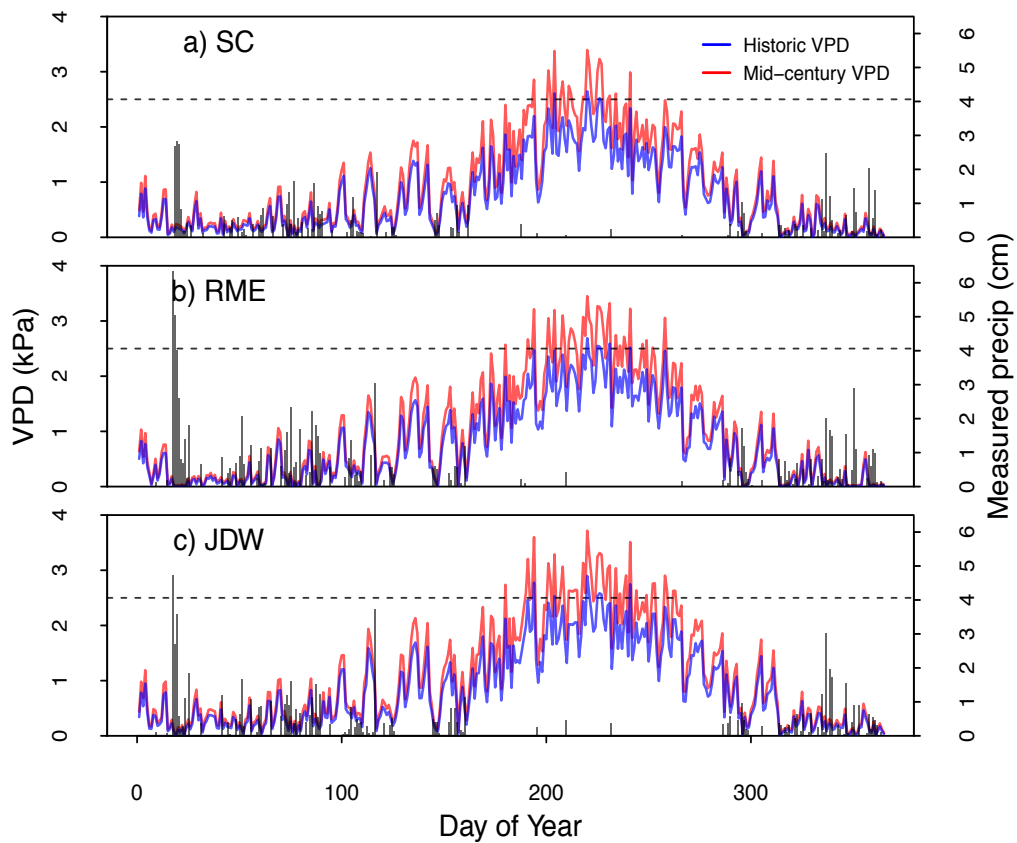


Figure S1. Incoming precipitation and average daytime vapor pressure deficit (VPD) at each site measured during 2012 (blue), and adjusted to represent mid-century conditions (red). This year is characterized by a pronounced summer drought with little precipitation occurring during the growing season.

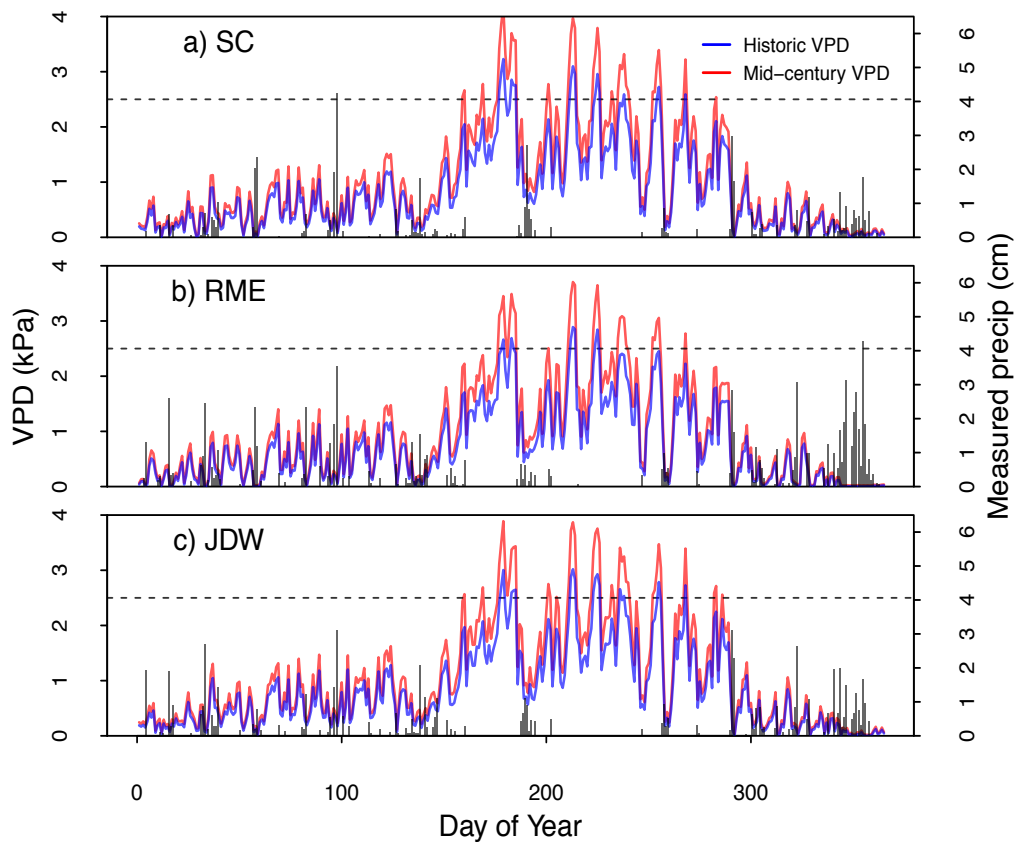


Figure S2. Incoming precipitation and average daytime vapor pressure deficit (VPD) at each site measured during 2015 (blue), and adjusted to represent mid-century conditions (red). This year is the warmest for both historic and mid-century simulations.

Appendix 3

Supporting information for

Chapter 4: Warming Temperatures and Reductions in Redistributed Snow

Differentially Impact the Simulated Productivity of Sagebrush Steppe Vegetation.

Soderquist B. S.¹, Kavanagh K. L.², Strand, E. K.², Link T. E.¹, Seyfried M. S.³

¹ *Department of Forest, Rangeland, and Fire Sciences, University of Idaho, Moscow, ID, 83844, USA,* ² *Department of Ecosystem Science and Management, Texas A&M University, College Station, TX, 77843-2138, USA,* ³ *USDA Agricultural Research Service, 800 Park Blvd., Plaza IV, Suite 105, Boise, ID, 83712, USA.*

Table S1. Ecophysiological parameters used to parameterize Biome-BGC MuSo simulations of aspen, mountain big sagebrush, and C3 grasses at Sheep Creek (SC), Reynolds Mountain East (RME), and Johnston Draw (JDW). Parameter values were either measured in the field, adjusted based on field measurements, or obtained from published literature. Note that snow thresholds limiting photosynthesis are model initialization parameters.

Parameter name	Parameter values by species and site			References or parameterization method (by species symbol)
	aspen* (1=SC, 2=RME,3=JDW)	mountain big sagebrush‡ (1=SC, 2=RME,3=JDW)	C3 grasses† (1=SC, 2=RME,3=JDW)	
Snow limit on photosynthesis (kg m ⁻²)	NA	20.0 ^{1,2,3}	5.0 ^{1,2,3}	Not considered*, approximated‡, Hidy et al. 2016†
Transfer growth period as fraction of growing season	0.2 ^{1,2,3}	0.3 ^{1,2,3}	1.0 ^{1,2,3}	White et al., 2000*‡†
Litterfall as fraction of growing season	0.2 ^{1,2,3}	0.3 ^{1,2,3}	1.0 ^{1,2,3}	White et al., 2000*‡†
Base temperature	NA	NA	3.6 ^{1,2,3}	Not considered*‡, Hidy et al., 2016†
Growing degree day of start of genetically programmed senescence (flag)	1 ^{1,2,3}	1 ^{1,2,3}	0 ^{1,2,3}	MuSo default*‡, using HSGSI†
Annual leaf and fine root turnover fraction	1.0 ^{1,2,3}	0.32 ^{1,2,3}	1.0 ^{1,2,3}	White et al., 2000*‡†
Annual live wood turnover fraction	0.70 ^{1,2,3}	0.70 ^{1,2,3}	NA	White et al., 2000*‡, not applicable†
Annual whole-plant mortality fraction	0.02 ^{1,2,3}	0.06 ^{1,2,3}	0.1 ^{1,2,3}	Hidy et al., 2016*, White et al., 2000*‡†
Annual fire mortality fraction	0.0 ^{1,2,3}	0.0 ^{1,2,3}	0.0 ^{1,2,3}	Not considered*‡†
New fine root C: new leaf C	1.2 ^{1,2,3}	2.75 ^{1,2,3}	1.0 ^{1,2,3}	White et al., 2000*†, calibrated from Reeves et al., 2014‡
New fruit C: new leaf C	0.0 ^{1,2,3}	0.0 ^{1,2,3}	0.0 ^{1,2,3}	Not applicable*‡†
New softstem C: new leaf C	0.0 ^{1,2,3}	0.0 ^{1,2,3}	0.5 ^{1,2,3}	Not applicable*‡, MuSo default†
New woody stem C: new total wood C	2.2 ^{1,2,3}	1.0 ^{1,2,3}	0.0 ^{1,2,3}	White et al., 2000*‡, not applicable†
New live wood C: new total wood C	0.096 ^{1,2,3}	0.05 ^{1,2,3}	0.0 ^{1,2,3}	White et al., 2000*, Reeves et al., 2014‡, not applicable†
New coarse root C: new stem C	0.152 ^{1,2,3}	0.3 ^{1,2,3}	0.0 ^{1,2,3}	White et al., 2000*‡, not applicable†

Current growth proportion	0.5 ^{1,2,3}	0.5 ^{1,2,3}	0.5 ^{1,2,3}	White et al., 2000*‡†
C:N leaves	23.2 ¹ ,21.5 ² ,18.9 ³	23.5 ^{1,2,3} (p>0.05)	26.2 ¹ ,23.6 ² ,39.7 ³	measured*‡†
C:N leaf litter	65.5 ^{1,2,3}	53.0 ^{1,2,3}	49.0 ^{1,2,3}	Average of aspen, White et al., 2000*, Shaw and Hart, 2001‡, White et al., 2000†
C:N of fine roots	92.9 ¹ ,83.3 ² ,50.7 ³	54.6 ^{1,2,3} (p>0.05)	60.3 ¹ ,56.1 ² ,70.1 ³	measured*‡†
C:N of fruit	NA	NA	NA	Not applicable*‡†
C:N of softstem	NA	NA	NA	Not applicable*‡†
C:N of live wood	50.0 ^{1,2,3}	50.0 ^{1,2,3}	NA	White et al., 2000*‡, not applicable†
C:N of dead wood	520 ^{1,2,3}	729 ^{1,2,3}	NA	Strukelj et al., 2013*, White et al., 2000‡, not applicable†
Leaf litter labile proportion	0.356 ^{1,2,3}	0.32 ^{1,2,3}	0.68 ^{1,2,3}	Average or taken from White et al., 2000*‡†
Leaf litter cellulose proportion	0.44 ^{1,2,3}	0.44 ^{1,2,3}	0.23 ^{1,2,3}	Average from White et al., 2000*‡†
Fine root litter labile proportion	0.204 ^{1,2,3}	0.30 ^{1,2,3}	0.34 ^{1,2,3}	Average or taken from White et al., 2000*‡†
Fine root litter cellulose proportion	0.444 ^{1,2,3}	0.45 ^{1,2,3}	0.44 ^{1,2,3}	White et al., 2000*‡†
Fruit litter labile proportion	NA	NA	NA	Not applicable*‡†
Fruit litter cellulose proportion	NA	NA	NA	Not applicable*‡†
Softstem litter cellulose proportion	NA	NA	0.23 ^{1,2,3}	Not applicable*‡, Hidy et al., 2016†
Dead wood cellulose proportion	0.785 ^{1,2,3}	0.71 ^{1,2,3}	NA	White et al., 2000*‡, not applicable†
Canopy water interception coefficient	0.038 ^{1,2,3}	0.045 ^{1,2,3}	0.2 ^{1,2,3}	Average or taken from White et al., 2000. *‡†
Canopy light extinction coefficient	0.5 ^{1,2,3}	0.411 ^{1,2,3}	0.74 ^{1,2,3}	White et al., 2000*‡†
All-sided to projected leaf area ratio	2.0 ^{1,2,3}	2.3 ^{1,2,3}	2.0 ^{1,2,3}	White et al., 2000*‡†
Canopy average specific leaf area	19.9 ¹ ,17.2 ² ,16.4 ³	19.1 ^{1,2,3} (p>0.05)	49.0 ^{1,2,3}	Measured*‡, White et al., 2000†
Ratio of shaded specific leaf area:sunlit specific leaf area	2.0 ^{1,2,3}	2.0 ^{1,2,3}	2.0 ^{1,2,3}	White et al., 2000*‡†

Table S1 continued				
Fraction of leaf N in Rubisco	0.068 ¹ ,0.077 ² ,0.077 ³	0.032 ¹ ,0.032 ² ,0.032 ³	0.12 ¹ ,0.10 ² ,0.19 ³	Decreased from White et al., 2000 [‡] , Adjusted within calculated range* [‡] †
Fraction of leaf N in Pep carboxylase	NA	NA	NA	Not applicable* [‡] †
Maximum stomatal conductance	0.005 ^{1,2,3}	0.003 ^{1,2,3}	0.0032 ^{1,2,3}	Keyser et al., 2005*, Turner et al., 2006 [‡] , Hidy et al., 2016 [†]
Cuticular conductance	0.00001 ^{1,2,3}	0.00001 ^{1,2,3}	0.00006 ^{1,2,3}	White et al., 2000* [‡] , Hidy et al., 2016 [†]
Boundary layer conductance	0.01 ^{1,2,3}	0.02 ^{1,2,3}	0.04 ^{1,2,3}	White et al., 2000* [‡] †
Relative soil water content limitation 1 (proportion to field capacity value)	0.8 ¹ ,0.6 ² ,0.7 ³	0.85 ^{1,2,3}	1.00 ^{1,2,3}	Adjusted by site* [‡] , Hidy et al., 2016 [†]
Relative soil water content limitation 2 (proportion to saturation capacity value)	1.00 ^{1,2,3}	1.00 ^{1,2,3}	0.99 ^{1,2,3}	Default* [‡] , Hidy et al., 2016 [†]
Vapor pressure deficit: start of conductance reduction	1000 ^{1,2,3}	930 ^{1,2,3}	1000 ^{1,2,3}	White et al., 2000* [‡] †
Vapor pressure deficit: complete conductance reduction	4200 ^{1,2,3}	4100 ^{1,2,3}	5000 ^{1,2,3}	White et al., 2000* [‡] †
Senescence mortality coefficient of aboveground plant material	0.045 ^{1,2,3}	0.0 ^{1,2,3}	0.05 ^{1,2,3}	Decreased from default* [‡] , Hidy et al., 2016 [†]
Senescence mortality coefficient of belowground plant material	0.045 ^{1,2,3}	0.0 ^{1,2,3}	0.01 ^{1,2,3}	Decreased from default* [‡] , Hidy et al., 2016 [†]
Genetically programmed senescence mortality coefficient of leaf	0 ^{1,2,3}	0 ^{1,2,3}	0 ^{1,2,3}	Not considered* [‡] †
Turnover rate of wilted standing biomass to litter	0.1 ^{1,2,3}	0.1 ^{1,2,3}	0.006 ^{1,2,3}	MuSo default* [‡] †
Turnover rate of cut-down non-woody biomass to litter	NA	NA	NA	Not considered* [‡] †
N denitrification proportion	0.01 ^{1,2,3}	0.01 ^{1,2,3}	0.01 ^{1,2,3}	MuSo default* [‡] †
Bulk N denitrification proportion, wet case	0.0068 ^{1,2,3}	0.0068 ^{1,2,3}	0.0068 ^{1,2,3}	MuSo default* [‡] †
Bulk N denitrification proportion, dry case	0.0003 ^{1,2,3}	0.0003 ^{1,2,3}	0.0003 ^{1,2,3}	MuSo default* [‡] †
Mobile N proportion (leaching)	0.1 ^{1,2,3}	0.1 ^{1,2,3}	0.1 ^{1,2,3}	MuSo default* [‡] †
Symbiotic+asymbiotic fixation of N	0.0008 ^{1,2,3}	0.0008 ^{1,2,3}	0.0007 ^{1,2,3}	MuSo default* [‡] , Hidy et al., 2016 [†]

Table S1 continued				
Ratio of storage and actual pool mortality due to management	0.1 ^{1,2,3}	0.1 ^{1,2,3}	0.1 ^{1,2,3}	MuSo default* [‡] †
Critical value of soil stress coefficient	0.467 ¹ ,0.4 ² ,0.4 ³	0.5 ^{1,2,3}	0.54 ^{1,2,3}	Adjusted by site* [‡] , Hidy et al., 2016†
Critical number of stress days	90 ^{1,2,3}	90 ^{1,2,3}	60 ^{1,2,3}	Hidy et al., 2016* [‡] †
Maximum depth of rooting zone (m)	1.15 ¹ ,1.5 ² ,1.5 ³	1.15 ¹ ,1.5 ² ,1.5 ³	0.70 ^{1,2,3}	Sucoff, 1982, Berndt and Gibbons, 1958*, Flerchinger and Seyfried, 2014 [‡] , Hidy et al., 2016†
Root distribution parameter	1.56 ^{1,2,3}	1.5 ^{1,2,3}	1.85 ^{1,2,3}	Calibrated* [‡] , Hidy et al., 2016†
Growth respiration per unit C grown	0.3 ^{1,2,3}	0.3 ^{1,2,3}	0.3 ^{1,2,3}	MuSo default* [‡] †
Maintenance respiration in kgC/day per kg of tissue N	0.218 ^{1,2,3}	0.3 ^{1,2,3}	0.218 ^{1,2,3}	MuSo default* [‡] , increased based on Hidy et al., 2016 [‡]

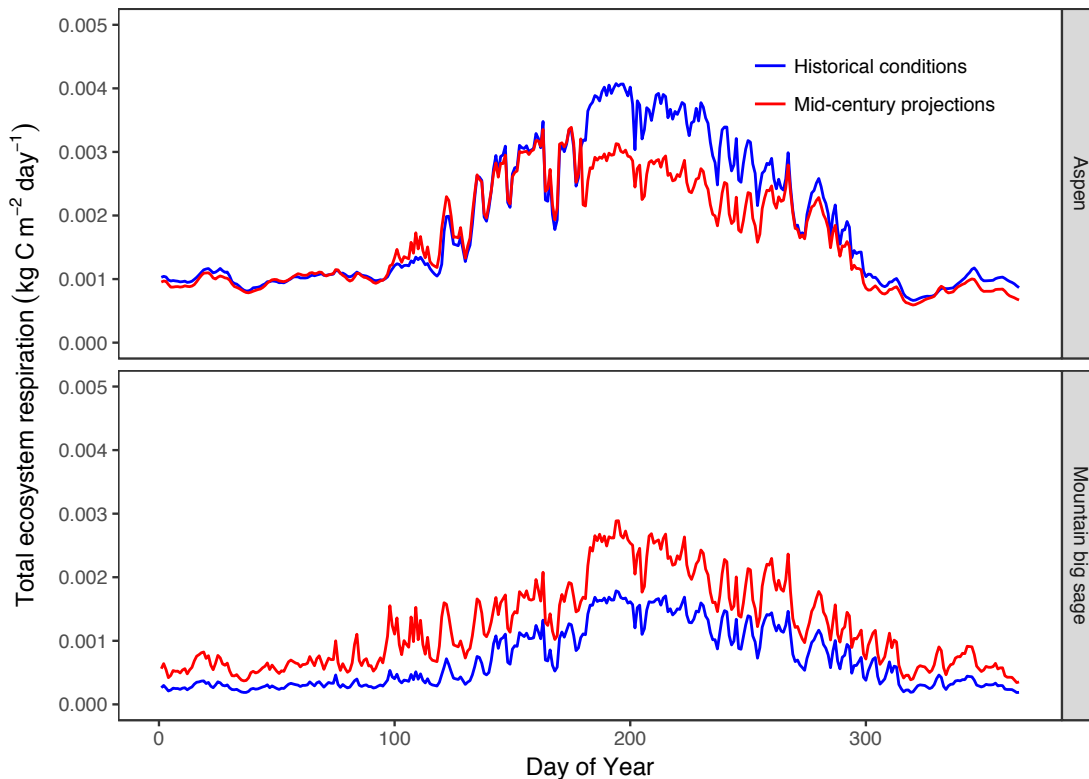


Figure S1. Total ecosystem respiration (TER, autotrophic + heterotrophic) for aspen and mountain big sagebrush at Sheep Creek during 2014 and its associated mid-21st century 2064. Decreases in aspen TER during the 2064 growing season are primarily due to decreased maintenance respiration rates resulting from decreased LAI and reduced heterotrophic respiration. 2064 TER is increased for sage primarily by increased growth respiration rates.